Final Report: Part I

on

Contract DA-33-009-eng-405
Project 8-23-02-003

R.N. Lassettre and P.M. Harris
August 1, 1953

Report No. 9
Final Report: Part I
RF Project 443

REPORT

By

THE OHIO STATE UNIVERSITY
RESEARCH FOUNDATION
COLUMBUS 10, OHIO

Cooperator: ENGINEER RESEARCH AND DEVELOPMENT LABORATORIES, Fort Belvoir, Virginia
Contract DA-44-009eng-405
Project 8-23-02-003

Investigation of: PHOTOEMISSIVE SURFACES

Subject of Report: Part I of Final Report. The Silver Oxidation Step in the Preparation of Infrared-Sensitive Ag-O-Cs Photocathodes.

Submitted by: Donald Tuomi, Walter J. Haubauch, Edwin N. Lassettre, and Preston M. Harris.

Date: Aug. 1, 1953

FOREWORD

The following report constitutes Part 1 of the final report of an investigation of infrared sensitive photocathodes covering the period January 1, 1951 to December 31, 1952. This period is that in which experimental work was conducted. During a part of this period Robert O. Leach was employed part time, especially in connection with the work described in Section 4.3.

CONTENTS - PART I

CONTENTS (continued)

Figures

Tables

PHOTOEMISSIVE SURFACES

1. INTRODUCTION

An initial step in the preparation of the infrared-sensitive Ag-O-Cs photocathode involves the oxidation of silver. The present report deals with the oxidation of silver by methods used in photocathode preparation and by related methods which contribute to an understanding of the processes and products which are involved. The silver-oxidation process constitutes, however, only one step in a more general study of the preparation and properties of Ag-O-Cs photocathodes. In order to place the present report in its proper perspective, it seems desirable to describe briefly the over-all objectives of the general investigation and the manner in which the experiments developed. This, together with a discussion of report organisation, constitutes the remainder of the introduction.

Even before the investigation of infrared-sensitive photocathodes was begun two aspects to the problem were recognised. The first of these arises because the chemical constitution and properties of the substances which might be encountered were not well established. For example, an oxidation process in which silver is made the cathode in a glow discharge through oxygen is a somewhat unusual one. There is no assurance that the most common oxide of silver, Ag_2O, will be produced. Other oxides, perhaps not previously known, might well be (and are) formed. Moreover, the chemistry of cesium compounds has not been extensively studied, although several oxides were known to exist. These deficiencies in chemical knowledge required some auxiliary studies on systems in bulk, in contrast to the photocathode investigation which involves thin films. The second aspect to the problem involves the study of the preparation and properties of the photocathode itself. Despite the apparent simplicity of the process it is found in practice that the preparation of infrared-sensitive photocathodes is not easy. Reproducibility may be poor even when rather careful control is apparently exercised at each stage. Spectral sensitivities reported in the literature by different investigators may differ greatly and, even within the same laboratory, large and unpredictable differences are encountered without recognizable reason. Much evidence exists that concealed variables operate which are uncontrolled because the chemical and physical

nature of the basic processes are not understood. In order to remedy this situation a careful step-by-step investigation of the preparation of photocathodes seemed called for. It is also important to identify the solid phases in the cathode and to determine its chemical composition. Such a program has been carried through and has met with a considerable measure of success, especially during the last year of experimental investigation.

The investigation of the preparation, composition and properties of the photocathode is described in two reports. This is the first and deals with the oxidation of silver. The second deals with the development of infrared sensitivity during the addition of cesium and also with the composition of the final cathode.

Another group of two reports deal, respectively, with the crystal structures of two oxides of cesium, Cs_2O and Cs_3O. We wish to acknowledge here a grant from the University Committee for Allocation of Research Foundation Grants which enabled Dr. Khi-Ruey Tsai to carry out a portion of the work reported by him on oxides of cesium. In the case of both oxides the structures have been established and the atomic positions determined with considerable accuracy. Much useful information concerning their preparation and chemical properties has also been collected.

The nature of the reports in the two groups is quite different. Crystal structure determination lends itself to brevity of reporting while the photocathode investigation, because of its complexity, does not. It seems essential to report the experimental investigations on photocathodes in considerable detail. Moreover, general conclusions usually can not be trusted unless (1) reproducibility is established and (2) all of the established facts can be fitted into the general framework. Item (2) involves reconsideration of a number of early experiments which were described in progress reports but which were not well understood at the time and which were sometimes interpreted incorrectly. This leads to a detailed and bulky report. The alternative, which involves abstracting a few of the more significant results with a few illustrative examples, was considered and rejected as being much less satisfactory. In order, however, to avoid becoming lost in a mass of detail it seems desirable, in the introduction, to summarize a few

of the important results and to discuss the chronology of the experimental work. This serves as an introduction to the present report (Part I) and to the next report (Part II). These two reports are, in fact, closely related. Both deal with the preparation and properties of photocathodes. Emphasis is on silver oxidation in, Part I, and on the chemical and physical changes accompanying cesium addition in Part II.

1.1 Chronological Development of Experimental Work

The oxidation of silver was one of the first steps to be studied in the present program. The products of oxidation of silver wires by means of ozone and also by radiofrequency (rf) glow discharge were investigated by x-ray and electron diffraction. It was established that both Ag_2O and another oxide were formed in two layers, Ag_2O being adjacent to silver and the other oxide being in the outer layer. In the absence of detailed information concerning the structure and composition of the second oxide, it has been designated as the Ψ phase oxide. Preferred crystal orientation in evaporated silver films was also studied and was found to be absent when silver was deposited on glass but was present when silver was deposited on a rocksalt substrate. On oxidation no preferred orientation in the oxide was found in either case. These results have been discussed in another report[1]. It was also established by x-ray studies that cesium formed no alloy with silver, nor was it soluble to any significant extent in solid silver. Moreover, an x-ray study of the products obtained on adding cesium to Ag_2O showed that at temperatures below 65°C a protective film of a higher cesium oxide, perhaps Cs_2O_3, formed which prevented further reduction of Ag_2O. At higher temperatures the reaction rate increased and lower oxides were formed, apparently tending toward the phase equilibrium to be expected for the cesium-to-oxygen atomic ratio of the sample. The final reduction product of Ag_2O was metallic silver. No evidence was found for any compound which involved silver as well as cesium and oxygen, although a solid solution of a small amount of silver in Cs_2O or other cesium oxides could not be excluded.

At the beginning of the present contract, therefore, it was the general conclusion that the silver oxides

functioned chiefly as a source of oxygen which combined with cesium as the latter was added. Since preferred orientation was destroyed on oxidation and since oxygen was removed from silver by combination with cesium, there was no obvious reason why the silver-oxidation should excercise much influence on the finished photocathode as long as enough oxygen was taken up. On the basis of this tentative (and false) hypothesis, attention was therefore turned toward the next objective, namely, the determination of cathode composition and the identification of solid phases in the finished cathode.

Several photocathodes were prepared in order to develop the technique. Both semitransparent cathodes and "massive" silver cathodes (using silver sheet as the base) were prepared. In these experiments there was a noticeable tendency for the massive cathodes to have much higher infrared sensitivity than the semitransparent cathodes. It became clear that we could not rely on the instructions which appeared in the literature for the preparation of infrared-sensitive cathodes. Some rather crude exploratory experiments on the effect of excess cesium on massive cathodes were therefore conducted in order to provide the basis for further development of the technique. A search for the source of trouble in semitransparent cathodes was also begun. One difficulty which was encountered lay in oxidizing a thin silver film of initial white light transmission of 50% to 90% transmission. Hence for the second time attention was turned to the study of the silver oxidation. It was thought that the relative proportions of Ag_2O and Ψ phase mentioned previously, might constitute an uncontrolled variable. Detection of these two solids in a thin film such as that encountered in a semitransparent cathode is, however, a difficult undertaking. The use of x-ray diffraction did not, at first, seem hopeful since even long exposures to x-rays incident perpendicular to the film gave only a few weak lines mostly due to silver. The weakness of the x-ray lines arises because of the very small quantity of material in the x-ray beam. The feasibility of x-ray methods was only established when it became evident that even in a semitransparent cathode a considerable total quantity of oxide was formed although the amount per unit area was small. If large enough crystals were formed, then by scraping material from a large area and loading it into a thin-walled capillary, an ideal powder sample could be obtained for x-ray diffraction. This offered many advantages over either

electron diffraction or grazing incidence x-ray diffraction. The x-ray study of oxidized silver films by this method has been very successful and has constituted the proving ground for this method, which was later used with good success in studying the finished photocathode.

In the x-ray diffraction investigation, silver films of graded thickness were studied in order to obtain the effect of varying thickness within the same film. Oxidation by ozone, rf glow discharge, and dc glow discharge were all studied. Films oxidized to 90% transmission in ozone were found to contain residual silver in considerable proportion while a film oxidized extensively in an rf discharge was found to contain no residual silver and to have less than 90% transmission. This suggested that light transmission goes through a maximum as oxidation proceeds and this was established in several experiments with a dc glow discharge. Semitransparent photocathodes still proved inferior to massive cathodes, however, even with a better controlled oxidation.

It was decided at this point that the cesium addition step required better control, so a study of the development of thermionic emission and photoelectric sensitivity of massive cathode tubes was undertaken using fine capillaries to control the rate of addition of cesium and a system of light filters to follow the photosensitivities during cesium addition at 190°C. This system was perfected to such a degree that both the amount of cesium and oxygen present could be accurately measured, and much valuable information was obtained concerning the effect of process variables and also considerable information concerning the mechanism of reaction. One interesting conclusion is that the reaction of cesium with silver oxide in the photocathode is slow. Even with the finest capillary which was used the reaction with the cathode was the rate determining step. The results strongly suggest a diffusion controlled solid state reaction. This in turn implies that crystals occur in the cathode whose sizes are sufficient to permit the accumulation of an intermediate layer of such thickness that diffusion through the layer is slow compared to the rate of addition of cesium. This agrees well with x-ray diffraction studies on both the oxidized silver films and on the finished cathode. The results of this study are described in the second report. (Part II of this series).

At the same time, in order not to further delay the composition study it was decided to carry out the investigation using a radioactive cesium tracer on a massive cathode, prepared, however, by evaporating a thick silver film on glass. As this study developed it became desirable also to limit cesium flow by a fine capillary, and to follow the development of photosensitivity with light filters. Much additional information was obtained in this way. In fact, the two lines of investigation complemented each other in a highly satisfactory way. In the meantime, quantitative means for the measurement of oxygen deposited in glow discharge oxidation of silver had to be developed and tested. Moreover, the rate of decomposition of the oxide at the temperature of cesium addition (190°C) had to be studied. Hence for the third time the oxidation of silver was studied. The thermal decomposition of silver oxide was also studied. The amount of oxide formed by the passage of a given quantity of charge in the glow discharge was obtained and also the decomposition rate of the oxide was measured at various temperatures. The objective of these experiments was practical. The purpose was to control the extent of oxidation and to verify that the extent of thermal decomposition was negligible, i.e. that oxygen remained on the cathode during cesium addition at 190°C. No serious attempt was made to investigate the mechanism of either the glow discharge oxidation or the thermal decomposition. Nevertheless, the results may be of some practical interest to others and hence are presented in Section 3 of this report.

During the course of the cesium tracer experiments a phenomenon was encountered which throws considerable light on the difficulties experienced in the preparation of infrared-sensitive semitransparent cathodes. Using an evaporated silver film of several thousand Angstroms thickness, four photocathodes were prepared in order to develop the technique. The last of these developed infrared sensitivity after heating, so the tracer experiments were started. The next ten tubes were of very poor quality, comparable with or worse than the semitransparent photocathodes. Every variation conceivable at the time was tried in order to correct this defect but without effect until the thickness of the evaporated silver film was increased. The infrared sensitivity immediately rose to that for a good massive cathode tube and remained there for all the remaining tubes (ten or more). Thickness, however, is not the

significant variable because a silver film even thinner than the original and evaporated at a very low rate gave a very good infrared-sensitive cathode comparable with a massive cathode. This cathode was semitransparent when completed, although with a considerably thicker film than the normal semitransparent cathode. This constitutes a clear-cut case in which the condition of the silver base determines the subsequent development of the cathode to such a degree that none of the intermediate variations could significantly alter the final product. For this reason alone the set of experiments described is very useful. In addition, however, the composition of the photocathode was determined, the ratio of the number of cesium atoms to the number of oxygen atoms being about 1.6 - 1.8 for good infrared-sensitive cathodes. The experiments are described in Part II.

Finally, an x-ray investigation of the finished photocathode revealed, for infrared-sensitive photocathodes, only Cs_2O and silver. Some other constituent, either silver oxide or a higher cesium oxide, must be present in order to account for the radio tracer experiments, but the proportion is too small to be detected in the x-ray experiments. This work, together with the radioactive cesium tracer work, is described in Part II.

The final chemical picture of the photocathode is as follows. The most infrared-sensitive photocathodes contain Cs_2O which is very probably the source of photoelectrons. The cathodes also contain another oxide, perhaps Cs_2O_3, in intimate contact with Cs_2O. The second oxide also has an important function which will be discussed in Part II. These conclusions concerning cathode composition are supported by additional data which are also discussed in Part II.

1.2 Organization of Report on Silver Oxidation

From the above description of the manner in which the research developed it is evident that the silver oxidation process has been studied on three different occasions. In each case the objectives were different and different apparatus was used. This complicates to some degree the problem of organizing a report on the subject. To avoid confusion it seems worthwhile to indicate in more detail the manner in which the report is organized.

To eliminate repetition in the description of

apparatus the experimental techniques are described together in Section 2 and reference to this section is made thereafter in the following text.

After a considerable number of trials the dc glow discharge was adopted as the oxidation procedure for the preparation of tubes having both semitransparent and massive cathodes. The reasons for this selection together with a description of control methods and results on the rate of oxidation and of thermal decomposition of oxide are given in Section 3.

The results of an x-ray diffraction study of oxidation products are given in Section 4. In this study attention was not confined to the glow discharge oxidation. Instead, a variety of oxidation methods, including ozone oxidation, were studied. This was necessary in order to investigate the number of solid phases present in the oxidation products. New solid phases, not previously obtained, have been found. Some useful qualitative results pertaining to particle sizes and optical properties have also been obtained.

In Section 4.5 a brief summary is given of the effect of silver evaporation and oxidation on photocathode properties. This point is discussed in more detail in Part II.

Section 5 contains an appraisal of the present status of the problem and suggestions for further work. Conclusive evidence that the silver evaporation process has a decisive effect on the finished cathode was obtained rather late in the experimental investigation. As the result, some gaps in our study of silver oxidation were indicated which there was no time to fill. These are pointed out in Section 5.

2. EXPERIMENTAL METHODS

In this section the details relating to the experimental equipment and procedures used to study the oxidation of the silver are discussed. The organization of the section is based upon the order involved in performing the experiments. The topics considered are as follows: (1) tube design, (2) vacuum systems, (3) oxidation methods, (4) preparation of silver surfaces, (5) oxide decomposition, and (6) x-ray diffraction characterization. This organization was adopted in order to avoid unnecessary duplication in the description of the experimental results presented in subsequent

sections. A detailed discussion of the micro Pirani gauges used to measure the pressure changes during oxidation is given in Appendix 1.

2.1 Design of Tubes

In the course of the oxidation studies three distinct tube designs have been used. The tubes were, for the most part, not designed specifically for studies of the oxidation process, but rather for the investigation of the preparation of different types of photocathodes. For this reason, it is convenient to describe the tubes by the following names: massive silver cathode, radioactive tracer cathode, and evaporated silver wedge cathodes.

The massive silver cathode tube corresponds to the simplest design possible for the preparation of the infrared-sensitive Ag-O-Cs photocathode. The design of this tube is shown in Fig. 1A. The cathode surface is formed by mounting a silver sheet approximately 4x5 cm in a tantalum wire frame which is spot-welded to a nickel lead-in wire. The silver used was 0.010-inch thick "fine quality" silver sheet from the Handy and Harmon Co. New York, N.Y. This tube design was used for the investigation of the general characteristic of the glow discharge oxidation of massive silver. In addition, a similar tube design was used to investigate the relationship between the tube gross composition and the photoelectric and thermionic emission.

The thick evaporated silver cathode tube design was utilized in the radioactive cesium tracer studies of the gross composition of the photosurface. This tube design is shown in Fig. 1B. The cathode consists of a thick silver film evaporated on a definite area of a 3/4-inch diameter microscope cover glass. The cover glass holder for the silver evaporation is so designed that a narrow silver tongue extenting to the edge of the glass disc is formed during the evaporation. This tongue is used to make electrical contact with the tantalum clips in which the cover glass is mounted. The area covered by silver in the evaporation process is 2.84 cm^2 and is accurately reproducible since the same template is used in each case to define the area. Since it was very important that the oxygen during the oxidation be deposited quantitatively on the silver cathode, tantalum was used in the construction of the auxiliary elements of this tube. This tube design was used to investigate the rate of the decomposition of the oxidized silver at 190°C. A similar tube in which the

A. Massive Silver Cathode

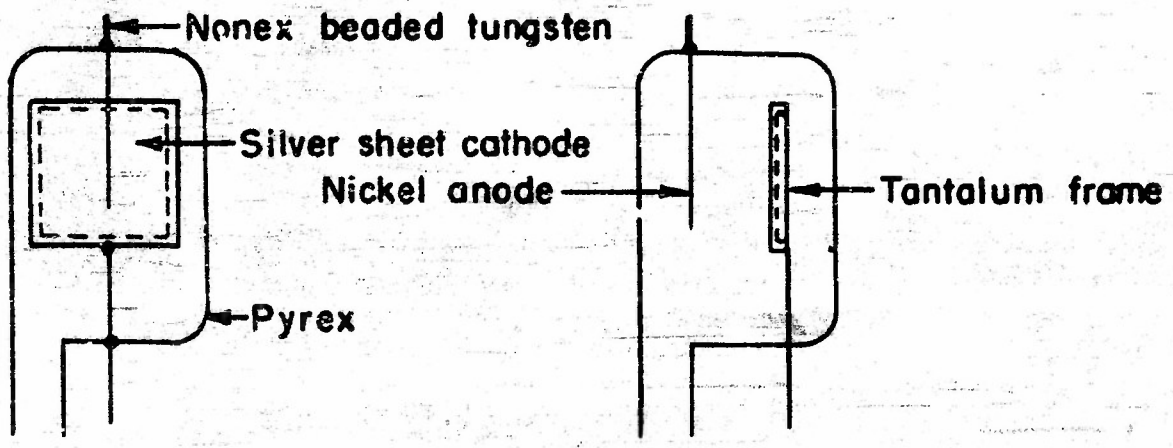

B. Thick Evaporated Silver Cathode

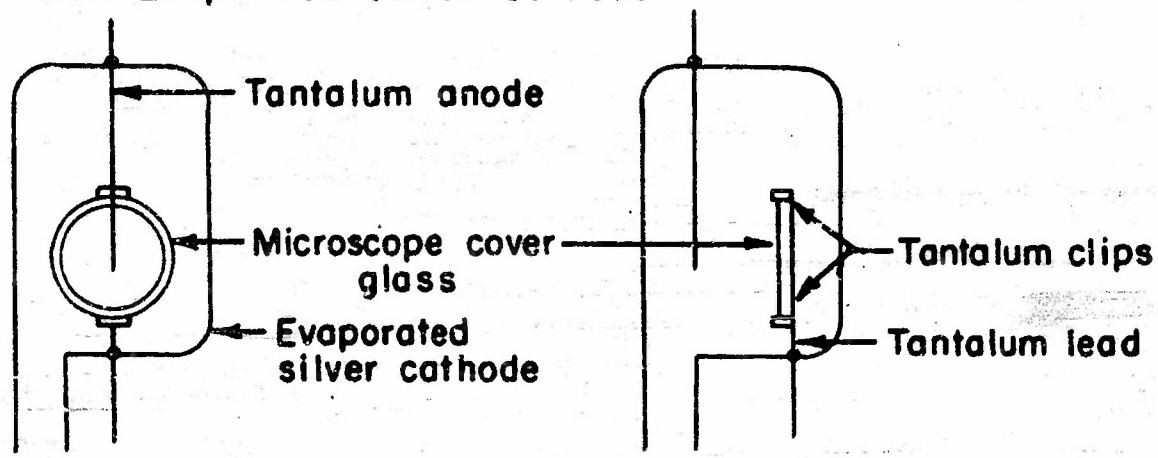

C. Evaporated Silver Wedge Cathode

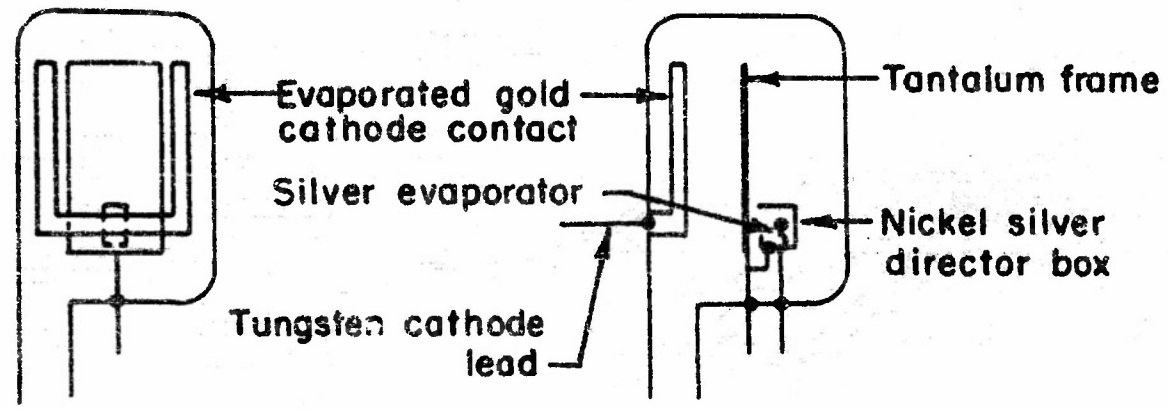

FIGURE 1. Tubes Used in Silver Oxidation Study

cathode surface was replaced by a massive silver disc was used to investigate the rate of oxidation in the glow discharge and the decomposition of the oxide (formed in the glow discharge) at 190°C and higher temperatures.

The evaporated silver wedge cathode tube design has been utilized in the investigation of the surface formed in the controlled glow discharge oxidation of thin silver films. This tube design is shown in Fig. 1C. The silver surface is formed by the high-vacuum evaporation of a silver film of graded thickness (wedge) on the front interior surface of the tube envelope. As shown in Fig. 1C the silver evaporator consists of a silver bead fused to a tantalum wire and mounted in a nickel box which difines the shape and extent of the silver film. The film thickness decreases as the distance from the bead increases. Electrical contact with the evaporated silver is obtained by the overlapping of the silver deposit onto an evaporated gold "U" which makes electrical contact with a tungsten lead-in wire sealed through the pyrex tube wall. The anode is formed by a tantalum wire block "O" which is spot-welded to the front lead-in wire for the silver evaporator unit. The drawing of Fig. 1C is schematic and is not to scale. A scale drawing of the tube is given in the second report of this series.

2.2 Vacuum Systems

Experiments relating to the oxidation process have been performed using two different vacuum systems. I was designed for the preparation of massive silver and semitransparent cathode phototubes, whereas vacuum system II was designed for the investigation of the photocathode gross composition using radioactive cesium. The components and characteristics of the two systems are described in this Section.

Schematic drawings of the two vacuum systems are shown in Fig. 2. In system I a D.P.I. GF25W triple-stage oil-diffusion pump is connected through a large bore stopcock to a manifold with a total volume of 1.0 liter, whereas in system II a two-stage mercury-diffusion pump is connected, through a triple-effect liquid air trap and a large-bore stopcock, to a manifold with a total volume of 0.230 liter. The pressures below 6×10^{-4} mm Hg were measured using a D.P.I. VG1A ionisation gauge. In system I the pressure range

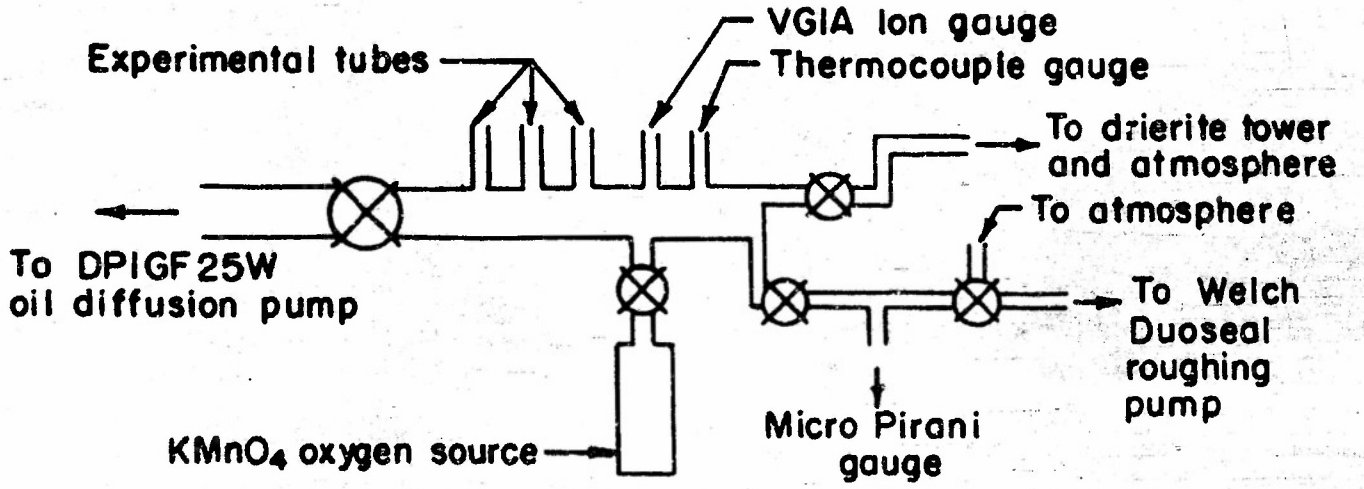

Vacuum System I

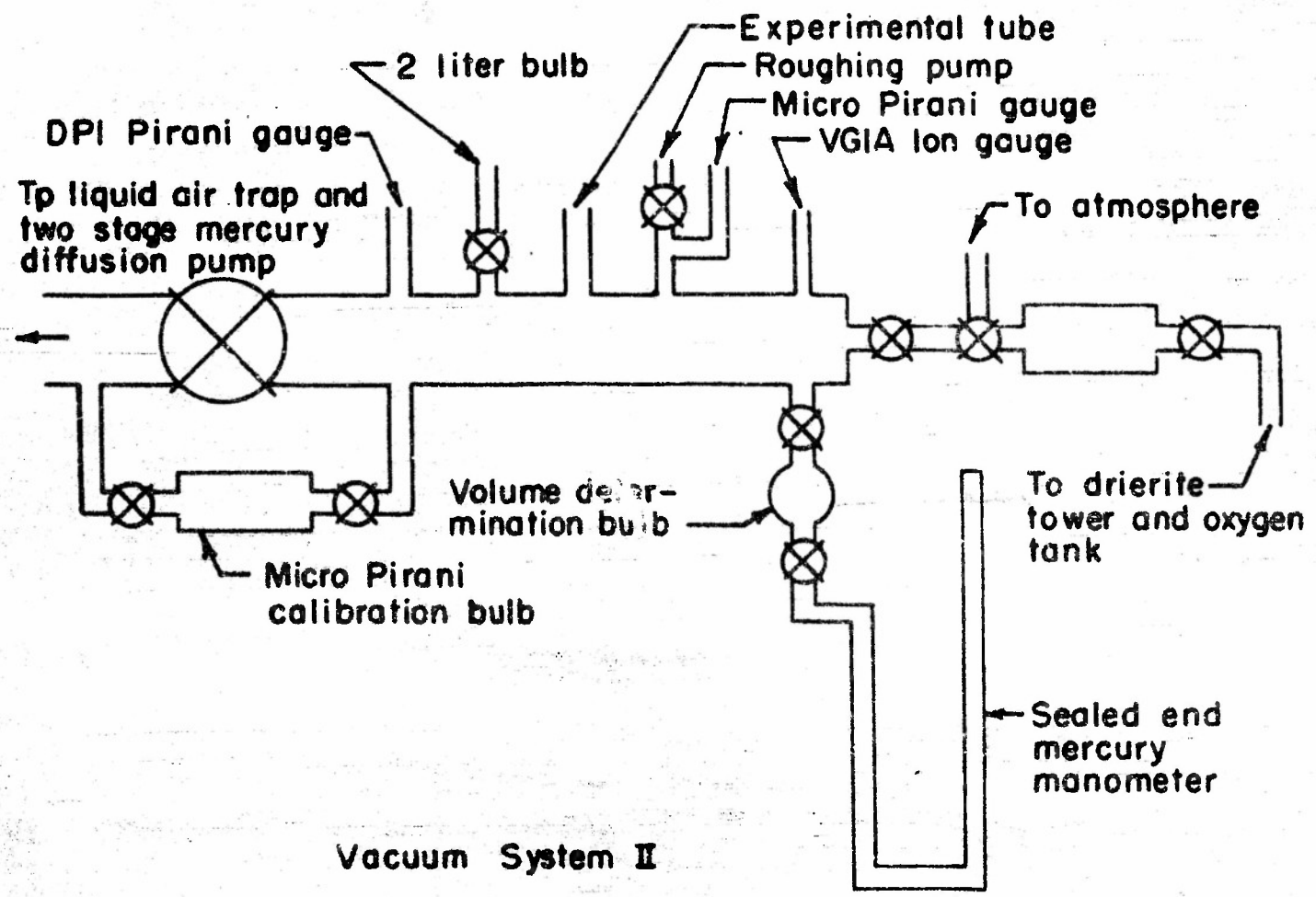

Vacuum System II

FIGURE 2

1-400 microns was measured with a Cenco thermocouple gauge unit, but for system II a calibrated D.P.I. Pirani gauge was used.

The oxygen pressures (1.0 to 0.4 mm Hg) during the oxidation step were measured using micro Pirani gauge tubes designed by Dr. Sam. Naiditch while employed by The Ohio State University Research Foundation. For System I the micro Pirani gauge circuit involved the use of an unbalanced bridge circuit, the actual pressure change during oxidation being determined from the change in the deflection of a galvanometer connected across the bridge. With this gauge it was possible to measure the pressure in the range from 0.5 to 0.8 mm Hg to an accuracy of ±4 microns. In system II it was necessary for the quantitative study of the composition of the cathode to obtain a more precise determination of the oxygen pressure. The micro Pirani gauge circuit for this system involved the use of a balanced Wheatstone bridge circuit, the actual pressure change during oxidation being determined by the change in resistance required to rebalance the bridge. In actual use, this gauge was recalibrated each time that a set of oxygen pressure measurements was performed. For the pressure range 0.6 to 0.9 mm Hg this gauge had sensitivity of 1.7 cm galvanometer deflection per micron. However, because of various factors the actual accuracy was ±1 micron.

A detailed discussion of the two micro Pirani gauges is presented in Appendix I to this report.

In the preparation of transparent cathode tubes on system I the transmission characteristics of the evaporated silver films were measured using a phototube with an S-4 surface and a GE-82-6CP light bulb operated at 6 volts. The current from the photocell was measured by means of a No.3402 HH Rubicon galvanometer with a sensitivity of 0.006 $\mu a/mm$ and an Aryton shunt.

To outgas the experimental tubes which were sealed to the vacuum system a three-inch diameter quartz tube resistance furnace was used. The tubes were outgassed at 400-450°C for at least two hours or until the pressure was less than 5×10^{-6} mm Hg as measured with the VG1A gauge. In general, the final pressure after outgassing was less than 10^{-6} mm Hg.

For system I the oxygen for the silver oxidation was obtained by heating $KMnO_4$ pellets in a side tube as

shown in Fig. 2. In system II commercial tank oxygen, passed through a Drierite drying column, was used. This choice of oxygen source involved a problem of convenience in performing the experiments. During the preparation of each tube on system II the total volume of the system was determined by a gas expansion method in addition to the recalibration of the micro Pirani gauge, and it was more convenient to use tank oxygen. It has also been established experimentally that the same oxide phases are formed during oxidation with the oxygen from the two different sources.

In the course of the radioactive tracer experiments an auxiliary vacuum system was constructed for the oxidation and heat treatment of the thick evaporated silver cathodes prior to mounting in a tube envelope. This system consisted of a manifold connected through a large-bore stopcock to a liquid-air trap and a single-stage mercury-diffusion pump. The female end of a 32-mm standard tape joint with a long central cathode wire sealed into the base was attached to the manifold by a 15-mm bore side tube. The male end of the joint was extended with a piece of 32-mm tubing and a tungsten anode wire mounted close to the wall. The lengths of the tungsten wires were so chosen that a thick evaporated silverfilm cathode could be mounted on the cathode lead-in wire, the male tube portion placed in position, and the cathode oxidized in a glow discharge. The distance from the silver cathode to the standard taper joint was sufficiently long so that the joint was not appreciably heated during the heat treatment of the cathode. The oxygen for the oxidation was obtained by heating $KMnO_4$ pellets. An Octoil-S manometer was used to measure the pressure for the oxidation operation. This system was used only for the pretreatment of silver sheet on film before the final oxidation in vacuum system II. Repeated oxidation and thermal decomposition of the oxide made it easy to perform the final oxidation uniformly.

2.3 Oxidation Methods

In the experimental investigation of the oxidation process oxide surfaces have been formed by (1) the "ozonized" oxygen oxidation of silver wires and evaporated silver wedges, (2) the "electrodeless" (rf) glow discharge oxidation of silver wires and thin evaporated silver films, and (3) the dc glow discharge oxidation of massive silver, evaporated silver films,

and evaporated silver wedges. In the remainder of this report the oxidation methods are designated by the following names: O_3, rf, and dc glow discharge oxidations. The equipment and procedures for these different oxidations are described in the following paragraphs.

For the O_3 oxidation the apparatus shown in Fig. 3 was used. In this system commercial cylinder oxygen was passed through a series of P_2O_5 drying tubes, through a silent discharge ozonizer, and then either through a bubbler to add water to the gas or directly to the reaction chamber. The silent discharge type ozonizer was operated with a 15,000-volt neon sign transformer. The ozone oxidations were performed by the insertion of the sample into the reaction chamber, flushing the system with oxygen, and then oxidizing the sample for the desired time with the O_3-O_2 mixture formed in the ozonizer. Samples prepared at elevated temperature were allowed to cool to room temperature in the O_3-O_2 stream prior to removal from the reaction chamber.

A sketch of the apparatus used for the study of the rf oxidation of silver wires is shown in Fig. 3B. In this apparatus the silver wire sample was mounted between the ends of a chromel-alumel thermocouple in the oxidation chamber. By measuring the thermocouple emf it was possible to determine a temperature for the wire sample during the bombardment in the glow discharge. It was established experimentally that for a given oxygen pressure and rf power the emf developed was the same for both silver and platinum junction wires. The rf source was a BC-375-E Signal Corps transmitter. A relative measure of the rf power output was obtained from the plate current meter reading, P, which could be varied from 120 to 220 units. As shown in the figure the oxygen pressure was determined with an Octoil-S manometer. The actual volume of the system was sufficiently large so that there was no significant pressure change during oxidation.

The rf source described above was also used in the rf glow discharge oxidation of thin evaporated silver films. This oxidation was performed by placing over the area to be oxided a tightly fitting cap which was connected to the rf source.

The circuit for the dc glow discharge oxidations described in this report is shown in Fig. 3C. The

A. Ozone Oxidizer

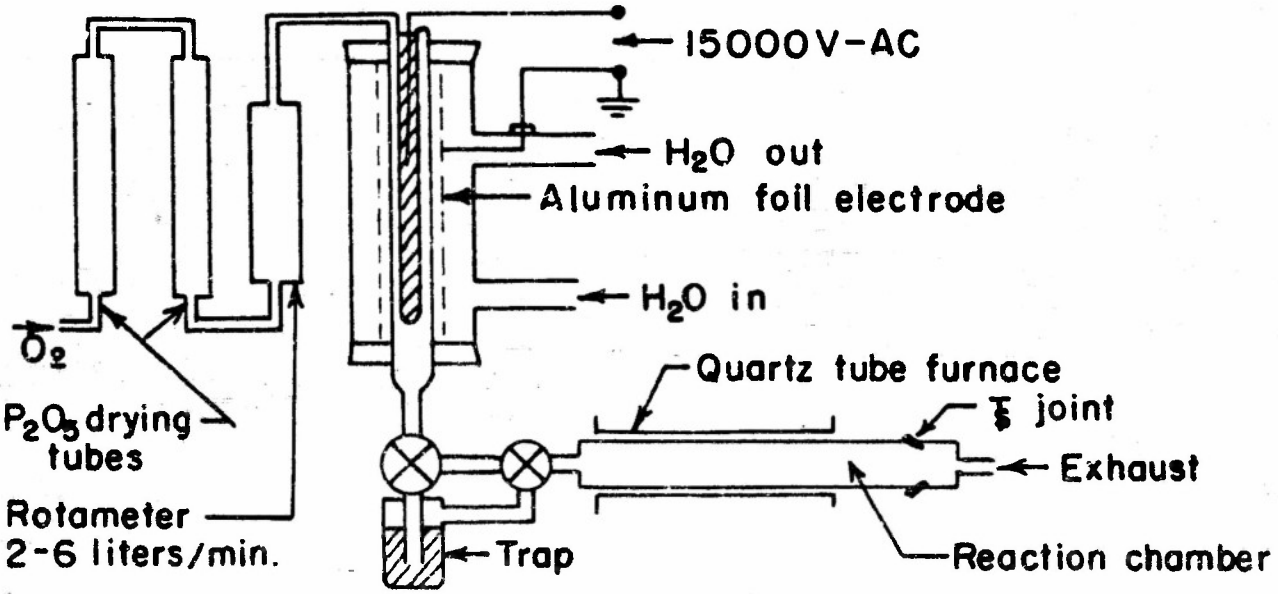

B. Silver Wire R-F Oxidation Apparatus

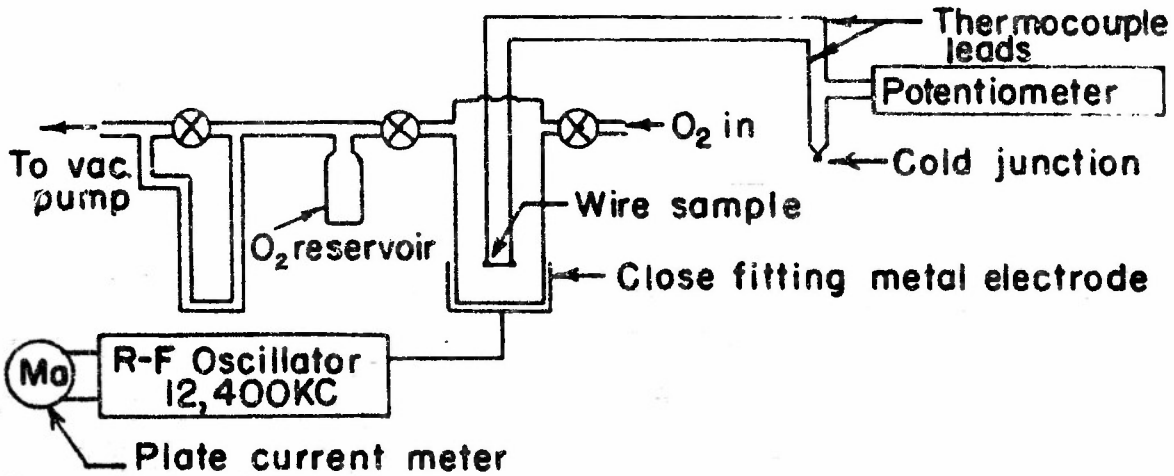

C. High Voltage Glow Discharge Circuit

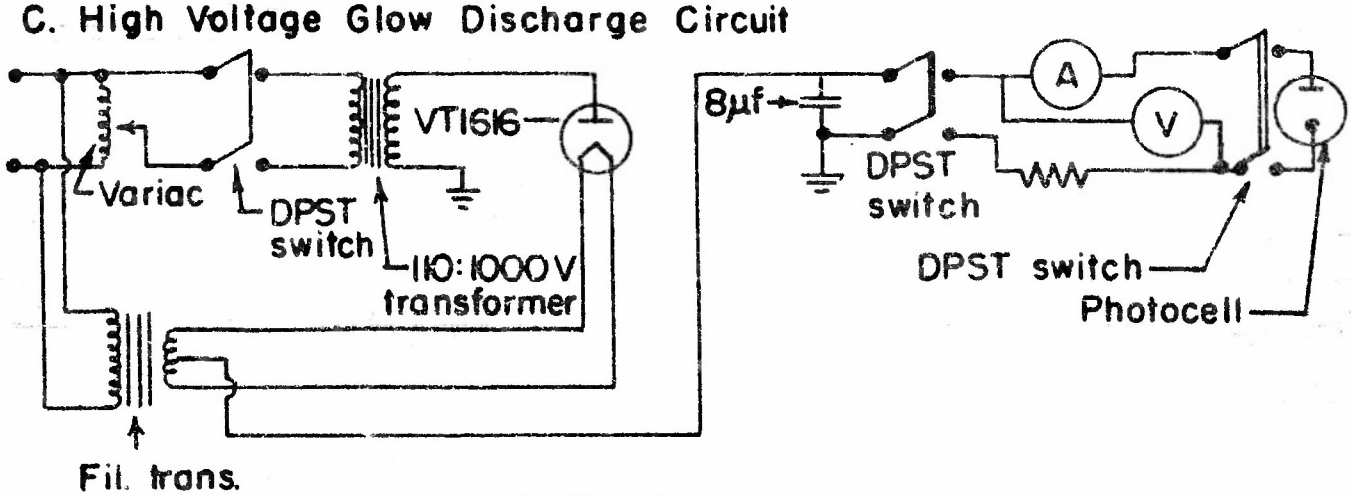

FIGURE 3

high voltage from the nonregulated dc power supply was continuously variable from 100 to 1700 volt. For this particular power supply satisfactory operation was obtained using a 50,000-ohm current limiting resistor in the high-voltage current. The oxidations were performed using the silver film as a cathode in the discharge, and with a voltage drop across the tube of 400 to 550 volts.

2.4 Preparation of Silver Surfaces

The oxidation process has been studied using three different types of silver surfaces namely, massive silver, thick evaporated silver films, and evaporated silver films of graded thickness (wedges). The techniques used to prepare the various surfaces are described below. "Fine Quality" Handy and Harmon Co. silver which was nearly spectroscopically pure has been used throughout the investigations.

The silver sheet used for the preparation of the massive silver cathodes was mounted in the tantalum frame as described in section 2.1. After the mounting, the silver cathode was lightly etched with 6N HNO_3, rinsed thoroughly with distilled water, and then dried at 150°C. (A similar procedure was used to prepare the silver wires for the ozonized rf oxidations.) After mounting in the tube envelope and sealing to the vacuum system, the silver surface was given a preliminary high-voltage glow discharge oxidation in oxygen at 0.7-0.9mm Hg. During this step it was possible to determine whether the oxidation would proceed uniformly over the entire surface. If the oxidation was nonuniform, the surface was oxidized until complete coverage was obtained. The oxide surface was subsequently decomposed by heating to 400-450°C in a vacuum ($p < 1 \times 10^{-5}$ mm Hg). This process was repeated until uniform oxidation of the cathode was obtained. In addition, during this step it was possible to determine the minimum input voltage to the high-voltage transformer required to provide complete coverage of the cathode by the glow discharge[3,4]. It is to be noted that if the voltage across the tube is too high during the oxidation, silver is sputtered off the cathode. After the oxidation process had been studied, oxide was decomposed by heat treatment in a vacuum at 400-450°C until the pressure was less than 5×10^{-6} mm Hg. The clean cathode could then be re-used.

Silver films evaporated onto a glass substrate in a DPI vacuum evaporation unit have been used in the preparation of the thick silver film radioactive Cs tracer tubes, and in the investigation of the ozone oxidation of evaporated silver wedges. The details for the preparation of the two surfaces are described below.

The glass substrate for thick evaporated silver films consisted of a circular microscope coverglass 22 mm in diameter and 0.007 ± 0.001 inch thick. The disc was cleaned by rubbing with a mixture of precipitated chalk and ammonium hydroxide, rinsing with distilled water, and drying with cheesecloth. The disc was then mounted in a stainless steel holder which defined the silver deposition area (2.84 cm^2). The holder was then mounted in the DPI evaporator unit over a tantalum trough containing a piece of massive silver. To evaporate the silver the tantalum trough was electrically heated by passing a high current through it. The DPI evaporator was then evacuated to approximately 100 microns and a glow discharge passed through the bell jar to further clean the surfaces by positive ion bombardment. After evacuation to 10^{-5} mm Hg, the heating current was turned on and the desired amount of silver was evaporated on the glass disc.

After the silver evaporation, the disc was mounted in the tantalum clip support. To avoid sputtering of silver within the tube envelope and to determine the oxidation characteristics of the surface, the cathode was then mounted in the auxiliary vacuum system described in Section 2.2. The surface was then repeatedly oxidized and heat-treated in a vacuum at 400-450°C until uniform oxidation was obtained. After this treatment the clean cathode was mounted in a tube envelope and the tube sealed to the vacuum system. Prior to preparation of the final oxide film the surface was again slightly oxidized to verify that oxidation proceeded uniformly. This oxide film was decomposed during the final outgassing of the tube, thus leaving a clean silver cathode for the subsequent oxidation experiment.

The silver wedges for the ozone oxidation study (Section 4.31) were prepared by the evaporation of silver onto a 1x3-inch microscope slide from a multiple silver bead tantalum wire filament mounted in the DPI evaporator unit. The glass substrate slides

were cleaned with a hot Calgonite solution, followed by a thorough rinsing with distilled water. The slides were individually mounted in a glass container which was loosely covered with a glass plate and then dried in a hot-air oven at 150°C. For the evaporation, the slides were mounted perpendicular to the multiple silver bead tantalum wire evaporator with one end of the slide at a perpendicular distance of one centimeter from the evaporator. During the evacuation of the bell jar to 10^{-5} mm Hg the surfaces were subjected to a glow discharge bombardment. With the evaporation geometry used, it was possible to prepare silver wedges with greater than 50% transmission at the thin end, and an opaque, essentially massive silver surface at the thick end. A similar technique has been used by Sennet and Scott[5] to investigate the structure and optical properties of evaporated silver films.

The geometry of the silver wedge tubes used to investigate the dc glow-discharge oxidation of silver films (Section 4.33) has been described in connection with Fig. 1C. After the tube had been thoroughly outgassed, a silver film was evaporated on the tube wall by heating the silver bead mounted on the tantalum wire with alternating current. The evaporation was controlled so that the thinner portion of the film furthest from the silver bead transmitted 50% of incident white light. The silver-beaded tantalum filaments were prepared in the DPI evaporation unit by the fusion of small pieces of silver wire onto the tantalum wire.

2.5 Oxide Decomposition

Prior to the determination of the cathode gross composition using radioactive cesium[6,7] it was necessary to investigate the thermal decomposition characteristics of the silver oxide formed in the glow discharge. The thermal decomposition studies (Section 3.4) were performed on vacuum system II using both massive silver disc cathodes and thick evaporated silver films. The auxiliary equipment and the experimental procedures are described in this Section.

After mounting the experimental tube on vacuum system II, the total volume of the system was measured by a gas expansion method, and the micro Pirani gauge calibrated by the method described in Appendix I. After outgassing

the tube at 400-450°C, the cathode was oxidized to the desired extent using a dc glow discharge. The amount of oxygen deposited was determined using the measured volume of the system and the observed change in the oxygen pressure.

After the oxidation the system was evacuated to 10^{-5} mm Hg, the manifold diffusion pump stopcock closed, and the room temperature "leak" rate established as being negligible. The oxygen pressure during the decomposition was measured using the DPI Pirani gauge calibrated for the 0-20 micron range with a McLeod gauge and for the 10-170 micron range by a manometer and a gas-expansion method. The actual oxide decomposition was performed using a quartz tube resistance furnace for temperature above 250°C and a Dow Corning dc 550 high-temperature oil bath for temperatures below 250°C.

The observed pressure was corrected to room temperature by the following approximate equation:

Let

V_1 = volume of system minus the volume of the tube
V_2 = volume of immersed tube
T_1 = room temperature
T_2 = bath temperature
P_1 = total pressure at room temperature
P_2 = total pressure with the tube heated;

then

$$P_1 = \frac{P_2}{V_1 + V_2} \left\{ V_1 + V_2 \left(\frac{T_1}{T_2} \right) \right\}.$$

This equation assumes an infinite temperature gradient at the bath surface; however, since the connecting tube volume is small compared to the total volume, the assumption does not introduce any serious error.

2.6 X-Ray Diffraction

Throughout the investigation of the silver oxidation it has been possible to characterize the oxide by means of x-ray diffraction powder photographs. The equipment and procedures used for the x-ray diffraction work are briefly discussed in this section.

During the early phases of the oxidation studies[1] a series of x-ray transmission photographs of unoxidized and oxidized silver films were prepared. In these experiments a flat film cassette camera with a 5-cm sample-to-film distance was used in conjunction with a copper-target x-ray tube and a nickel filter as a source of

copper K_α radiation ($\lambda = 1.5418A$). In these experiments complete diffraction data for the samples could not be readily obtained because of excessive exposure times required for small scattering volume of the oxide films.

A second x-ray diffraction method has been employed during the present contract period (Section 4.3) which has made possible the x-ray characterization of very thin oxide films. This has been accomplished by modifying the sample-preparation techniques. Using a Bausch and Lomb 90X binocular microscope, it has been possible to scrape loose small oxide samples from selected areas of oxidized cathodes and to load these samples into Pyrex capillaries with bores of the order of 0.04 mm. X-ray powder photographs of these samples were prepared in a 57.3-mm diameter Debye-Scherrer powder-diffraction camera with a Straumanis type of film holder and using a nickel-filtered copper radiation. Two procedures were used in the computation of interplanar spacings. In the case of routine photographs of oxide films no correction was applied to the measured film distances for film shrinkage. This corresponds to the assumption that one millimeter on the film was equal two degrees of glancing angle θ. It has been observed, for the camera used, that the camera diameter computed by the Straumanis method very rarely differed from the assumed radius by greater than one part in five hundred. The interplanar spacings for photographs having well-defined back reflection lines were computed using 2θ values corrected for film shrinkage. These values are reported to at least the third decimal place in the subsequent sections of the report. In the computation of the interplanar spacings d/n, extensive use has been made of the tables prepared by Switzer, Axelrod, Lindberg, and Larsen[8].

3. OXIDATION OF SILVER BY MEANS OF THE DIRECT-CURRENT GLOW DISCHARGE. THERMAL DECOMPOSITION OF THE OXIDE.

During the study of the products of oxidation of silver (Section 4) a considerable variety of oxidation processes was studied. Several of these were also used in the preparation of photocathodes. It was finally decided, however, that the dc glow discharge through oxygen was most satisfactory for our purposes and this method was used in the preparation of almost all of

the photocathodes which are described in the second report of this series. It is therefore important to have a clear understanding of the methods of control which have been used, and also some knowledge of the properties of the oxide which is formed. The necessary background is supplied in this section.

3.1 General Characteristics of DC Glow Discharge.

The dc glow discharge was selected as the oxidation method in photocathode preparation chiefly because of convenience in control. Other methods such as rf discharge have, however, also been used. The oxidation process is so complicated that there seemed to be little chance, within a reasonable period of time, of unraveling completely the mechanism of the intermediate stages of oxidation. The problem, therefore, was to find a process (1) which could be controlled easily, (2) which could be adapted to a variety of tube designs and still be operated under conditions which were recognizably similar in each case, and (3) which brought about the oxidation quickly and efficiently. The conditions having been adjusted, the products of oxidation could then be determined by x-ray investigation (see Section 4) so that at least the end result of the oxidation could be established even though the mechanism remained obscure. The dc glow discharge fulfills these requirements rather well. The fact that glow discharges have been previously studied at some length has been of considerable assistance and it seems well to review briefly some of the pertinent facts before passing on to the consideration of specific applications to the present research.

The mechanism of the glow discharge has been studied extensively and several good reviews are available[3,4]. The mechanism has, of course, been studied most extensively for those discharges in which the electrodes are inert, i.e. no chemical reaction with gas occurs during the discharge process. In the oxidation of silver by making a silver sheet or film the cathode in a discharge through oxygen there is, however, a reaction between oxygen and the cathode. The cathode therefore undergoes a progressive change as the discharge is operated and hence the nature of the discharge very probably undergoes a change. The known facts concerning the operation of discharges are expected to apply

accurately, therefore, only in the initial stages of operation before any substantial oxidation has occurred. In order to utilize as fully as possible the known information about glow discharges it is therefore necessary either to adjust conditions with silver cathodes by studying the discharge characteristics in the first fraction of a second, or alternatively to conduct a preliminary study in which the silver cathode is replaced by one of another metal which is chemically inert but which is otherwise expected to behave similarly to silver. The second alternative has been adopted for the purpose of a preliminary study, platinum being chosen for the cathode.

For definiteness we consider a discharge tube of the type of Fig. 1B with a platinum disc as cathode. The glow discharge through oxygen at a pressure in the range 0.5 to 1 mm Hg is produced as follows. The disc is made the cathode in the discharge by attaching it to the negative terminal of a high voltage dc power supply. A straight wire whose length is parallel to the cathode surface is used as anode. The discharge tube is placed in series with a high resistance. As the voltage is gradually raised the tube current remains very small until the breakdown potential is reached. Once breakdown has occurred the tube current rises rapidly so that the major voltage is across the high resistance and the voltage drop across the tube is relatively small. If the high resistance is properly chosen the resulting glow discharge operates immediately after breakdown in the normal discharge region. In this region the voltage drop across the tube is independent of tube current because of the fact that the cathode is not completely covered by the discharge, 3,4. As the power supply voltage is increased the voltage drop across the tube remains constant and the tube current increases until a point is reached at which further increase in current causes an increase in tube voltage. This is the point at which the cathode becomes completely covered by the glow. A convenient test for complete cathode coverage can be made by determining tube voltage as a function of tube current. A graph of voltage vs. current exhibits an abrupt change in slope when complete coverage is reached. The results of two such determinations using a platinum cathode are given in Table I. From the results of experiment A it is evident that at tube currents below 1 milliampere the discharge is in the normal region and at tube currents above 1 ma in the abnormal region. The "normal" potential fall is 355 volts. The flat region from 2.5 to 3.0 ma is interpreted as being due to the cathode glow spreading

TABLE I. TUBE VOLTAGE AS A FUNCTION OF TUBE CURRENT AT TWO PRESSURES

Experiment A*		Experiment B**	
Tube Current (ma)	Tube Voltage (v)	Tube Current (ma)	Tube Voltage (v)
0.4	355	0.5	355
0.6	355	0.6	355
0.8	355	0.8	360
1.0	355	1.0	365
1.5	365	1.5	375
2.0	375	2.0	385
2.5	380	2.5	400
3.0	380	3.0	415
3.5	385	3.5	430
4.0	395	4.0	445
4.5	400	4.5	460
5.0	405	5.0	475
6.0	420	6.0	500
7.0	435	7.0	525
8.0	445	8.0	550
9.0	460	9.0	555
10.0	475	10.0	580
11.0	485	12.0	660
12.0	490		

*Oxygen pressure ≅ 0.8 mm. 85.000 ohm series resistance. Tube fired at 650 volts and tube voltage dropped to 385 (3.1 ma). Power supply voltage then reduced until tube current reached 0.4 ma.

**Oxygen pressure ≅ 0.5 mm. 50.000 ohm series resistance. Tube fired at 600 volts and tube voltage dropped to 425 (3.6 ma). Power supply voltage then reduced until tube current reached 0.5 ma.

Pt Cathode area 3 cm^2 in both cases.

over the reverse side of the cathode. The results of experiment B performed at lower oxygen pressure indicate a "normal" potential fall of 355 volts and complete cathode coverage above 0.6 ma tube current. According to the so-called "similarity principle" the cathode fall in potential is a function of current density divided by the square of the pressure[9,10]. Since most of the tube voltage drop is across the cathode layer the current density which marks the transition between normal and abnormal regions can be computed from the results of others (see ref. 3, page 578) and compared with the observations of Table I. Agreement is fairly good and provides confirmation of the interpretation of the results of Table I.

Having determined the current and voltage which mark the transition from normal to abnormal glow discharge the question now arises as to the most favorable conditions for discharge operation in an oxidation experiment. In order to achieve uniform oxidation of the cathode it is, of course, essential to have the cathode covered by the glow. Oxidations are therefore carried out by operating in the abnormal glow discharge region far enough to insure complete cathode coverage, but not far enough to cause cathode sputtering. A tube voltage about fifty volts above that for normal operation is satisfactory and has been used in most of our experiments. In practice the high resistance in series with the discharge is so selected and the power supply is so adjusted that immediately on throwing a switch the breakdown potential is exceeded and the tube voltage adjusts to 50 volts above normal.

It is useful to have the point of complete coverage as a reference since this can be determined with any tube geometry, and by operating at a voltage exceeding the normal by some fixed amount, such as 50 volts, comparable conditions for oxidation can be obtained in tubes with different dimensions. The experiments described above indicate how discharge conditions are adjusted with a tube of the type of Fig. 1B. In the case of a tube such as that of Fig. 1C for the study of silver films it is not convenient to substitute platinum for silver. Hence the discharge conditions were adjusted by a determination of current versus voltage using a silver cathode. Transition from normal to abnormal glow discharge could still be detected despite the accompanying oxidation of silver, and discharge conditions were fixed in accordance with these results.

These determinations are more approximate than those described above for the tube of Fig. 1B. Nevertheless, it is possible by visual observation to confirm that the cathode is covered by the glow and, since the results of Section 4 show that the oxidation products are rather insensitive to oxidation method, we believe that the method is adequate. With this explanation out of the way we now proceed to discuss the oxidation process using again the tube of Fig. 1B but now with a silver cathode.

It might be thought that uniformity of oxidation on a silver cathode would be favored by the fact that the oxide is a poor conductor. If a thick patch of oxide were to form, then current density through the patch would be reduced, because of the high resistance, while current density in the remaining areas would remain high, thus tending to retard the oxidation rate in the thick area more than in the thin. The oxidation would then be self-regulating to some degree. Once oxidation has been initiated it does indeed tend to proceed uniformly. The above view implies, however, that oxidation is caused by the bombardment of the cathode with positive ions (perhaps O_2^+), and this is certainly an oversimplification as is shown by the following facts and by others to be described later.

In the first stages of oxidation, uniformity is greatly influenced by previous treatment of the cathode. Under certain circumstances the initial oxidation is markedly nonuniform. This has been particularly noticeable with certain evaporated thick silver ($\sim$10,000 A) films. It is found that uniformity is improved in almost all cases by first oxidizing and then decomposing the oxide by heating to temperatures above 275°C. After one or more cycles of this treatment there is a marked improvement in uniformity. This has been used in the oxidation of both silver sheet and thick evaporated silver films with good results. Other investigators have previously remarked about this fact.

Impurities also seem to affect uniformity of oxidation under certain circumstances. During the course of preparing a series of photocathodes on bases made up of silver sheet ("massive cathodes") it was observed that a thin film of white solid formed within the tube while sealing off the end after introducing the cathode element. During the subsequent outgassing at high

temperature the white solid distils into the vacuum manifold. The solid is water soluble and it has been found that rinsing the tube with distilled water just prior to final mounting on the vacuum system, for outgassing and photo tube preparation, results in a silver surface which is consistently oxidized uniformly by the dc glow discharge. In this case a slight impurity seems to markedly affect the uniformity of oxidation.

The initial oxidation of thick evaporated silver films sometimes starts on small areas, almost points, in such a way as to strongly suggest a nucleation process such as is frequently observed in the first formation of a solid phase. Nucleation as an initial step is also compatible with the observation that uniformity of oxidation is affected by impurities. One such case is mentioned above, and such behavior may be of frequent occurrence. These extreme examples of nonuniform oxidation are certainly quite different from anything which might be deduced from the simple conception of a uniform positive ion bombardment of a uniform silver film with a definite fraction of ions combining with silver to produce the oxide. Preparation of the silver cathode is of decisive importance, and unfortunately this is one of the operations which is least well understood in the whole process although, as stated earlier, some effective practical measures can be taken to prepare the cathode for uniform oxidation. The observations quoted above, being qualitative and fragmentary, certainly cannot be considered as proof that a nucleation process is rate determining in the initial stage of silver oxidation. The idea is advanced as a tentative hypothesis, however, not alone on the basis of these observations but also because of a mass of evidence to be discussed later in this report. No conclusive proof of the mechanism is available, so the hypothesis must be considered a tentative one whose chief support comes from the fact that it coordinates to some degree a considerable body of information which would otherwise be completely confusing. The matter is again discussed in Section 4.

From the above discussion it is evident that pre-treatment of the cathode, together with complete cathode coverage by the glow, tends to favor uniformity of oxidation. When, however, we wish to compare oxidations carried out in two tubes with different dimensions and geometrical arrangements, then how can

we be sure, not only that oxidation occurs uniformly in each case, but that conditions within the discharge near each cathode are also the same so that the solid products of oxidation might be expected to be the same? It is obviously impossible to be certain that conditions in different tubes are exactly the same. Nevertheless, some very sensible precautions can be taken in advance. In order to indicate clearly the nature of these precautions it is necessary to discuss further some well-known characteristics of glow discharges[2]. In glow discharges several dark spaces occur near the cathode. One of these, the Crookes dark space, is of great importance to the discharge mechanism. This dark space is followed by a thin luminous layer (the negative glow) and then by another dark space (the Faraday dark space). Beyond the Faraday dark space, in the direction of the anode, there comes the positive column from which the greatest radiation emission occurs. This region makes up the bulk of the discharge and gives the discharge its characteristic visual appearance. If, without change in pressure, the anode is moved away from the cathode the positive column becomes longer and the voltage required to maintain the discharge is slightly increased by an amount equal to the IR drop across the added length of positive column. The discharge is otherwise unchanged. In particular, the thickness of the dark spaces and the negative glow are unchanged. It is further known[3] that the voltage drop across the positive column is much smaller than that across the Crookes dark space. In fact, almost the whole potential drop is across the Crookes dark space. There is also the final fact that in the immediate neighborhood of the cathode the chief current carriers are positive ions[11] of which the bulk probably have a single positive charge. As much as 95% of the current flow may be due to positively charged ions.

We are now in position to inquire into the question of what molecular species may be the active oxidizing agents. Neutral, unexcited, oxygen molecules can be eliminated at once since a large mass of chemical evidence indicates that oxygen does not readily react with metallic silver at room temperature or even at high temperatures. The active agents must then be excited oxygen molecules, their dissociation products (atoms), or positive ions which are continually accelerated to the cathode with considerable kinetic energies. Consider first the positive ions. The average kinetic energy with which these strike the cathode is determined by the acceleration between collisions and this is determined

by the product of field strength by the mean free path. In comparing two different tubes, the mean free paths are equal if the pressures are equal. In order that the field strengths in the vicinity of the cathode be also nearly equal, even with different tube designs, two conditions must be met. First, the cathode-anode distance must considerably exceed the thickness of the dark space. Since this thickness is only a fraction of a millimeter at 1 mm pressure, this condition is easy to satisfy. The second condition is that the potential drop across the Crookes dark space should be the same for the two tubes. Since the largest potential drop is that across the Crookes dark space this will be nearly satisfied if the tube voltages are equal. It would be more accurate to make the current densities equal since from the "Similarity Principle" the cathode fall in potential would then tend to be the same in the two cases[10]. Location of the voltage which divides the normal from the abnormal region and operating at a fixed amount above this voltage accomplishes the same end. It follows that methods are available by which discharge conditions can be so adjusted that even with rather different tube designs positive ions are accelerated to the cathode with nearly equal kinetic energies. Thus the oxidation products which result from positive ion bombardment are expected to be the same.

Oxidation by electrically neutral but excited oxygen molecules involves a similar situation. If we suppose that conditions are adjusted as above so that the cathode fall in potential is the same in two tubes, then the rates of production of excited species near the cathode should also be the same since the same conditions for excitation prevail. The chief differences lie in the different magnitudes of the positive columns. The thickness of the Crookes dark space for an oxygen glow discharge lies between 50 and 100 molecular mean free path lengths[12]. If the positive column in each case is made more than ten times the thickness of the Crookes dark space, then excited species produced in the outermost portion of the positive column could reach the cathode only after undergoing at least 500 collisions. It seems reasonable that the probability of deactivation on collision is sufficiently high so that excited species produced far out in the positive column are deactivated before reacting the cathode. Thus further increase in the cathode-anode distance would have little effect on cathode oxidation since this only increases the positive column. Other short-lived species produced in the positive column would behave similarly.

It thus appears that oxidizing conditions at the cathode, due to positive ions or to short-lived neutral species produced either near the cathode or in the positive column, are not sensitive to changes in cathode-anode distance under the above conditions. For the purposes of the present investigation it was essential to utilize somewhat different tube designs for different experimental purposes, and the above characteristics of the dc glow discharge seemed to make it better suited to our purposes than any other oxidation method. The tubes used were not radically different but some differences proved to be essential. It was not possible to study systematically the effect of every variable in the glow discharge and so the procedure outlined above was adopted. This procedure still has the defect that the portion of oxidation brought about by very long-lived species, produced in the positive column, will differ from one tube design to another. Other oxidation methods which have been considered do, however, have additional disadvantages.

It is clear from the above discussion that although sensible precautions can be taken which insure that conditions in the vicinity of the cathode (within a centimeter, say) are very nearly the same with different tube designs, nevertheless it cannot be proven that the oxidation products are the same except by analysis of the products. The x-ray investigation of Section 4 is, therefore, of particular interest since the oxidation products are directly studied. In subsequent Sections some of the above points are discussed again in connection with the description of pertinent experimental results.

3.2 Tube Element Oxidation

Since, in the photocathode composition studies using a radioactive cesium tracer, it was necessary to have oxygen deposited only on the cathode surface, and not on support wires, etc., a series of tests were performed on the deposition of oxygen on several metals which might serve to support the cathode and other tube elements. Platinum and tantalum were of particular interest. Experiments were not performed using nickel since, in the process of preparing experimental tubes, it had already been observed that nickel wire anodes were appreciably oxidized.

In a series of experimental tubes a silver disc,

a platinum disc, and a tantalum disc were oxidized in a dc glow discharge under similar conditions, and the pressure decrease in the system caused by oxygen deposition determined. In addition an oxidation was performed under similar conditions using a tube with short tantalum electrodes to determine whether an appreciable amount of oxygen could be deposited on the glass. The results of these experiments were as follows:

Substance	Pressure decrease (microns)
Silver	29
Platinum	23
Tantalum	2
Glass	2

It is clear that tantalum is less oxidized than either of the other two metals. As the result of these experiments tantalum has been adopted as the metal from which the anode and cathode supports are formed in experimental phototubes.

3.3 Oxidation of Massive Silver. Oxygen Deposition and Current Efficiency.

It is well known that color changes accompany the oxidation of silver sheet in a glow discharge. As silver is oxidised the surface color passes through the sequence yellow, red, blue for several cycles. The surface color is sometimes used in practice as a means of controlling the extent of oxidation[13,14]. We have found that the number of cycles observed depends on how uniformly the silver base is oxidized. Silver sheets which have been repeatedly corroded by glow discharge oxidation frequently can be made to pass through three and even four cycles of color changes before the final black oxide surface is formed. In the absence of repeated oxidation and thermal decomposition only two cycles are normally observed.

In view of the fact that surface color change is sometimes used as a means of controlling the extent of oxidation it has seemed worthwhile to collect data on the amount of oxygen taken up on oxidation to a given surface color. The amounts of oxygen corresponding to the different colors have been determined in two experiments which are described below. These

experiments also throw some additional light on the mechanism of the oxidation process.

It is found that the oxidation of silver cathodes proceeds rather rapidly. In order, therefore, to obtain reliable pressure measurements, which require considerable time, silver cathodes have been oxidized by switching the power supply on for a short period of time. It is then shut off and the pressure remeasured. This process is then repeated. The results obtained in a series of such measurements are given in Table II. The results of a second set of measurements performed several months later are given in Table III. These experiments were carried out using vacuum system II and the tube of Fig. 1B with a cathode in the form of a disc cut from a silver sheet. The pressure changes were measured with the micro Pirani gauge and are determined with considerable accuracy. Although the actual pressures may be subject to an error of one unit in the second decimal place, the pressure changes are probably reliable to ± 0.0005 mm. This follows because the Pirani is a differential gauge which was calibrated by repeated expansion of a large gas volume into a volume made slightly larger by an attached tube of small volume. Since both volumes can be accurately measured, very small pressure changes can be determined with high precision. The percentage accuracy with which a pressure change can be measured is virtually equal to the percentage accuracy in the initial pressure value. The variables of Tables II and III have the following meanings.

P = oxygen pressure in mm of Hg.

ΔP = change in pressure during the interval in which the discharge is on.

Δt = time interval during which the discharge operated to produce pressure change ΔP.

t = total operation time for discharge, i.e. the sum of previous time increments Δt.

I = tube current (milliamperes) while discharge was on.

ΔM_{O_2} = mass of oxygen, in micrograms, deposited on cathode during time interval Δt. This is calculated from the perfect gas law using the known pressure decrease ΔP together with the volume and the temperature.

M_{O_2} = mass of oxygen on cathode, i.e. the sum of all previous ΔM_{O_2}.

$\Delta M_{O_2}^{+}$ = mass of O_2^{+} ions reaching cathode in time Δt as computed from the tube current and time increment Δt assuming that at the cathode

TABLE II. SURFACE COLOR CHANGE AS A FUNCTION OF EXTENT OF OXIDATION

Surface (Color)	P (mm)	ΔP (mm)	t (sec)	Δt (sec)	I (ma)	m_{O_2} (μg)	Δm_{O_2} (μg)	$m^+_{O_2}$ (μg)	$\Delta m^+_{O_2}$ (μg)	$100\frac{\Delta m_{O_2}}{\Delta m^+_{O_2}}$	$100\frac{m_{O_2}}{m^+_{O_2}}$
	0.551		0								
1st yellow	.543	.008	2.2	2.2	4.1	5.06	5.06	2.99	2.99	169	169
1st red	.536	.007	5.1	2.9	4.1	9.51	4.45	6.93	3.94	113	137
1st blue	.529	.007	9.5	4.4	4.1	14.0	4.45	12.91	5.98	74.3	108
2nd yellow	.510	.019	22.9	13.4	4.0	26.0	12.0	30.7	17.8	67.5	84.6
2nd red	.484	.026	45.9	23.0	3.95	42.3	16.5	60.9	30.2	54.7	69.5
2nd blue	.459	.025	72.8	26.9	3.85	58.3	15.5	95.3	34.4	45.1	61.2
dirty green	.440	.019	100.4	27.6	3.7	70.5	12.0	128.0	32.7	36.7	55.0
red-yellow-green	.434	.006	118.2	17.8	3.75	74.4	3.81	150.2	22.2	17.1	49.6
red yellow	.426	.008	136.2	18.1	3.75	79.4	5.06	172.8	22.6	22.4	45.7
red	.421	.005	155.3	19.0	3.7	82.3	3.16	196.2	23.4	13.5	42.0
red	.415	.006	174.1	18.8	3.65	86.5	3.81	219.0	22.8	16.7	39.5
lighter red	.410	.005	193.3	19.2	3.55	89.4	3.16	241.6	22.6	14.0	36.9
red	.405	.005	214.0	20.7	3.6	92.5	3.16	266.4	24.8	12.7	34.8
red	.400	.005	235.0	21.0	3.55	95.6	3.16	291.2	24.8	12.7	32.8
darker red	.394	.006	259.2	24.2	3.55	99.5	3.81	319.7	28.5	13.3	31.1
dark red	.388	.006	284.3	25.1	3.5	103.0	3.81	348.9	29.2	13.0	29.5
dark red	.382	.006	310.3	26.0	3.5	107.0	3.81	379.1	30.2	12.6	28.2
dark red	.377	.005	334.6	24.3	3.5	110.0	3.16	407.3	28.2	11.2	27.1

TABLE II. (Continued)

Surface (Color)	P (mm)	ΔP (mm)	t (sec)	Δt (sec)	I (ma)	m_{O_2} (μg)	Δm_{O_2} (μg)	$m_{O_2}^+$ (μg)	$\Delta m_{O_2}^+$ (μg)	$100\frac{\Delta m_{O_2}}{\Delta m_{O_2}}$	$100\frac{m_{O_2}}{m_{O_2}^+}$
darker red	.372	.005	361.2	26.6	3.4	114.0	3.16	437.3	30.0	10.5	26.1
darker red	.366	.006	385.6	24.4	3.45	117.0	3.81	465.3	28.0	13.6	25.2
black red	.361	.005	411.7	26.1	3.35	120.0	3.16	494.3	29.0	10.9	24.3
almost gray	.355	.006	438.6	26.9	3.35	124.0	3.81	524.2	29.9	12.7	23.7
gray-black	.347	.008	465.7	27.1	3.3	129.0	5.06	553.9	29.7	17.0	23.3

Volume of system = 0.3676 liter
Temperature 24.8°C
Cathode area ~3 cm^2

TABLE III. SURFACE COLOR CHANGE VS. EXTENT OF OXIDATION

Surface (Color)	P (mm)	ΔP (mm)	t (sec)	Δt (sec)	I (ma)	m_{O_2} (μg)	Δm_{O_2} (μg)	$m^+_{O_2}$ (μg)	$\Delta m^+_{O_2}$ (μg)	$100\frac{\Delta m_{O_2}}{\Delta m^+_{O_2}}$	$100\frac{m_{O_2}}{m^+_{O_2}}$
	.609		0								
1st yellow	.606	.003	2	2	2.5	1.89	1.89	1.66	1.66	114	114
1st red	.599	.007	5.4	3.4	2.8	6.30	4.41	4.82	3.16	140	131
1st blue	.592	.007	9.1	3.7	2.8	10.71	4.41	8.26	3.44	120	130
	.584	.008	14.8	5.7	2.8	15.75	5.04	13.56	5.30	95	116
2nd yellow	.578	.006	20.9	6.1	2.8	19.53	3.78	19.23	5.67	67	102
	.559	.019	37.2	16.3	2.75	31.50	11.97	34.1	14.9	80	92
2nd red	.532	.027	64.7	27.5	2.75	48.51	17.01	59.2	25.1	68	82
	.519	.013	84.5	19.8	2.75	56.70	8.19	77.3	18.1	45	73
	.502	.017	111.8	27.3	2.7	67.41	10.71	101.8	24.5	44	66
	.495	.008	132.3	20.5	2.7	72.45	5.04	120.2	18.4	27	60
2nd blue	.482	.012	158.1	25.8	2.65	80.01	7.56	142.9	22.7	33	56
	.474	.008	183.8	25.7	2.65	85.05	5.04	165.5	22.6	22	51
3rd yellow	.452	.022	231.4	47.6	2.6	98.91	13.86	206.6	41.1	34	48
	.424	.028	291.2	59.8	2.55	116.55	17.64	257.2	50.6	35	45

Volume of system = 0.3722
Temperature 30.0°C
Cathode area ~3 cm^2

all current is carried by positive ions O_2^+.

$M_{O_2}^+$ = sum of previous increments $\Delta M_{O_2}^+$.

$100 \frac{\Delta M_{O_2}}{\Delta M_{O_2}^+}$ = oxidation efficiency, i.e. the ratio of oxygen deposited on cathode to that reaching electrode by conduction in time interval Δt.

$100 \frac{M_{O_2}}{M_{O_2}^+}$ = cumulative oxidation efficiency.

Several rather interesting facts are obtained from these results. In the first place the amount of oxygen per square centimeter at each color is of interest. For convenience these have been compiled in Table IV. The results at comparable colors in the two experiments agree only roughly, as might be expected. The trends with increasing oxidation differ in the two cases. Whether the differences are due to difference in cathode preparation or to gas pressure and current density is not definitely known. In subsequent experiments it has, however, been observed in oxidations to the second yellow that the amounts of oxygen may differ considerably. Cathode color is, therefore, only a very rough means for control of the extent of oxidation. This agrees with the results of others[14].

It has been reported by Tiapkina and Dankov[15] that the oxidation of silver in a glow discharge obeys the parabolic law, i.e. the square of M_{O_2} is a linear function of t. The data of Tables II and III[2] do not accurately obey this law. A graph of M_{O_2} vs. t does, however, give a curve whose shape roughly resembles a parabola. The result is at least approximately that which is expected for a diffusion controlled chemical reaction. The diffusion presumably takes place through the oxide layer, the moving species probably being silver ion since this is the smallest ion involved. Although the data do not prove that the reaction is diffusion controlled, they are at least in rough agreement with this idea. Exact agreement with the simplest theory based on a uniform layer can hardly be expected since it has been shown by metallographic examination that islands of silver remain behind completely surrounded by oxide (see ref. 1). The oxidation of silver wires apparently proceeds by corrosion along grain boundaries (see ref. 1) and hence is irregular. Under these conditions no simple law can be expected to fit the data. Despite the lack of an unambiguous proof it seems very likely that diffusion occurs.

The oxidation efficiency tends to be above 100% in the initial stages of oxidation. If this result is

TABLE IV. AMOUNT OF OXYGEN AT EACH SURFACE COLOR

Color	Initial Pressure 0.609 mm Hg Initial Current Density 0.83 ma/cm^2			Initial Pressure 0.551 mm Hg Initial Current Density 1.37 ma/cm^2		
	t (sec)	mass oxygen (μg/cm^2)	gram atoms oxygen/cm^2 X10^7	t (sec)	mass oxygen (μg/cm^2)	gram atoms oxygen/cm^2 X10^7
1st yellow	2	0.63	0.4	2.2	1.69	1.1
1st red	5.4	2.10	1.3	5.1	3.17	2.0
1st blue	9.1	3.57	2.2	9.5	4.67	2.9
2nd yellow	20.9	6.51	4.1	22.9	8.67	5.4
2nd red	64.7	16.17	10.2	45.9	14.10	8.8
2nd blue	158.1	26.67	16.7	72.8	19.43	12.1

reliable the implication is that the amount of oxygen reaching the cathode by electrical conduction is too small to account for the extent of oxidation in the initial phase of oxidation. The error in time measurements is probably 0.2 second and that in pressure change less than 10%. At the smallest time intervals this introduces an error into the efficiency measurement of about 20%. The efficiency exceeds 100 by more than this amount and, moreover, the same tendency is observed in two sets of measurements so that we are inclined to think that the results are significant although not very accurate. This view is considerably reinforced by the observation that a silver sheet is oxidized in a glow discharge even when it is made the anode. In fact, oxidation occurs even when the silver is not an electrode (see ref. 14). This certainly demonstrates that some species other than O_2^+ contributes to the oxidation process. Since this is just what is required to account for oxidation efficiencies greater than 100% the results of Tables II and III seem quite reasonable.

It is to be noted that oxidation efficiency goes down as the extent of oxidation increases. The final values are, however, considerably different in the two experiments as is evident from Tables II and III. If we compare the amounts of oxidation at equal times, however, we find that they agree at least roughly, even though the tube currents differ considerably. We do not know whether this is generally the case.

3.4 Thermal Decomposition of Oxide

Numerous reports exist in the literature with regard to the thermal decomposition of silver oxides. In the majority of the experiments an approximate decomposition temperature is defined by the low temperature limit for observable decomposition with the oxygen pressure measuring device used. The oxide film formed during the glow discharge oxidation of silver is a polyphase oxide or a single oxide of, probably, trivalent silver (see Section 4). In addition, the oxide particle size is generally small and the surface area probably large. Thus it would be incorrect to assume that the decomposition characteristics of this oxide are the same as for bulk Ag_2O. Moreover, because of the expected effect of particle size on decomposition rate the work of others cannot be assumed to apply under the experimental conditions used here.

Consequently a series of experiments on the thermal decomposition of oxidized silver has been performed using vacuum system II.

In a preliminary series of experiments the oxide film formed on a massive silver disc (tube of Fig. 1B) was completely decomposed at temperatures greater than 300°C. The decomposition was performed by lowering a preheated quartz tube furnace over the evacuated tube mounted on the manifold, and measuring the tube temperature and oxygen pressure as a function of time. The oxygen deposited during oxidation was measured with the micro Pirani gauge, while the oxygen evolved during decomposition was measured with the D.P.I. Pirani gauge.

Three experiments were performed and the results are given in Figs. 5, 6, and 7. It must be emphasized that these data were taken while the tube was heating. Hence the pressure was changing during the first two-thirds of the interval. The graphs of pressure vs. temperature therefore do not give the equilibrium dissociation pressures, but instead give the pressure as a function of the temperature at the instant of measurement. From the data it appears that dissociation pressure becomes appreciable at a temperature of 265°C under the conditions of these experiments. It will be shown later, however, that substantial decomposition occurs below this temperature if enough time is allowed.

The results of the material balance determinations on the same samples as above are given in Table V. Columns four and five give the pressure drop on glow discharge oxidation and the pressure increase on thermal decomposition respectively. The latter pressure is corrected back to room temperature as explained in Section 2.

It seems at first sight that approximately 10% of the oxygen deposited during oxidation was not recovered. From observation of the operational characteristics of the Pirani gauge for pressures greater than 20μ (which must be measured on the millimeter pressure range position) it is extremely probable, however, that the major portion of the observed discrepancy ($\sim$10%) arises from errors in the gauge calibration for the range 20 to 200 microns. Actually, considering the gauge calibraion problem, the discrepancy does not seem serious. This remark applies only to the D.P.I.

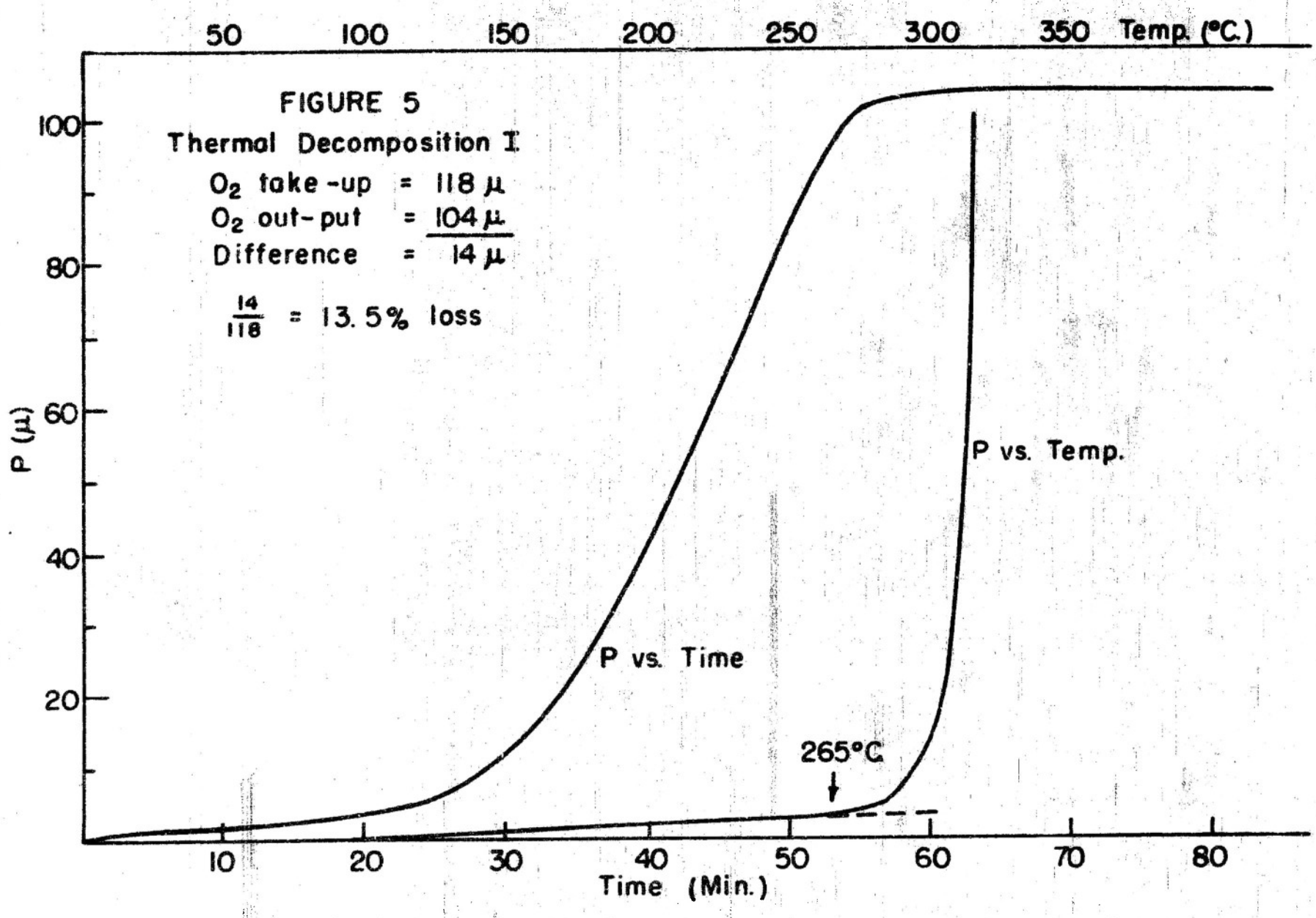
50
100
150
200
250
300
350
Temp. (°C.)
FIGURE 5
Thermal Decomposition I
O2 take-up = 118 μ
O2 out-put = 104 μ
Difference = 14 μ
14/118 = 13.5% loss
100
80
60
40
20
P (μ)
P vs. Temp.
P vs. Time
265°C
10
20
30
40
50
60
70
80
Time (Min.)

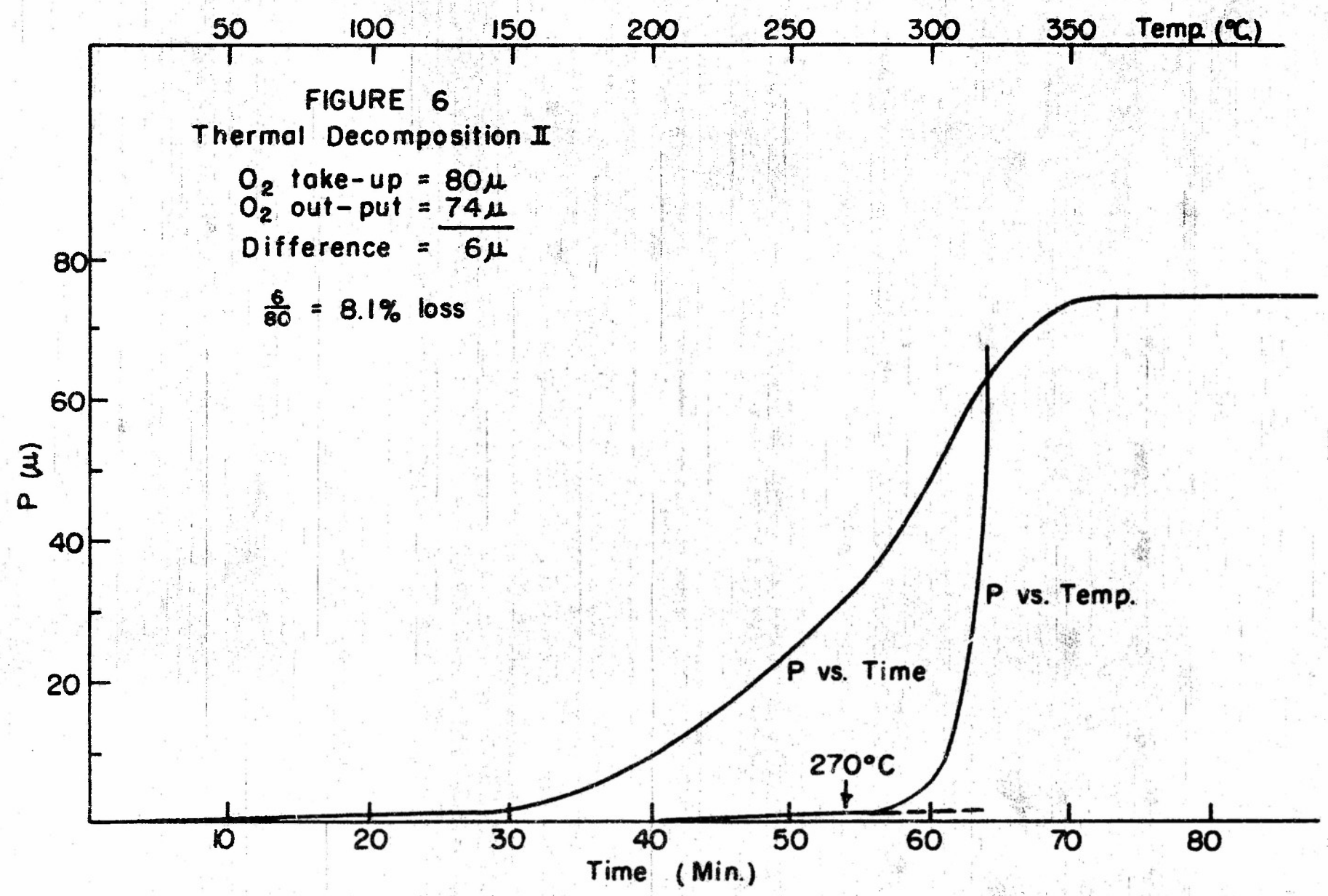
50
100
150
200
250
300
350
Temp. (°C.)
FIGURE 6
Thermal Decomposition II
O_2 take-up = 80μ
O_2 out-put = 74μ
Difference = 6μ
$\frac{6}{80}$ = 8.1% loss
80
60
40
20
P (μ)
P vs. Temp.
P vs. Time
270°C
10
20
30
40
50
60
70
80
Time (Min.)

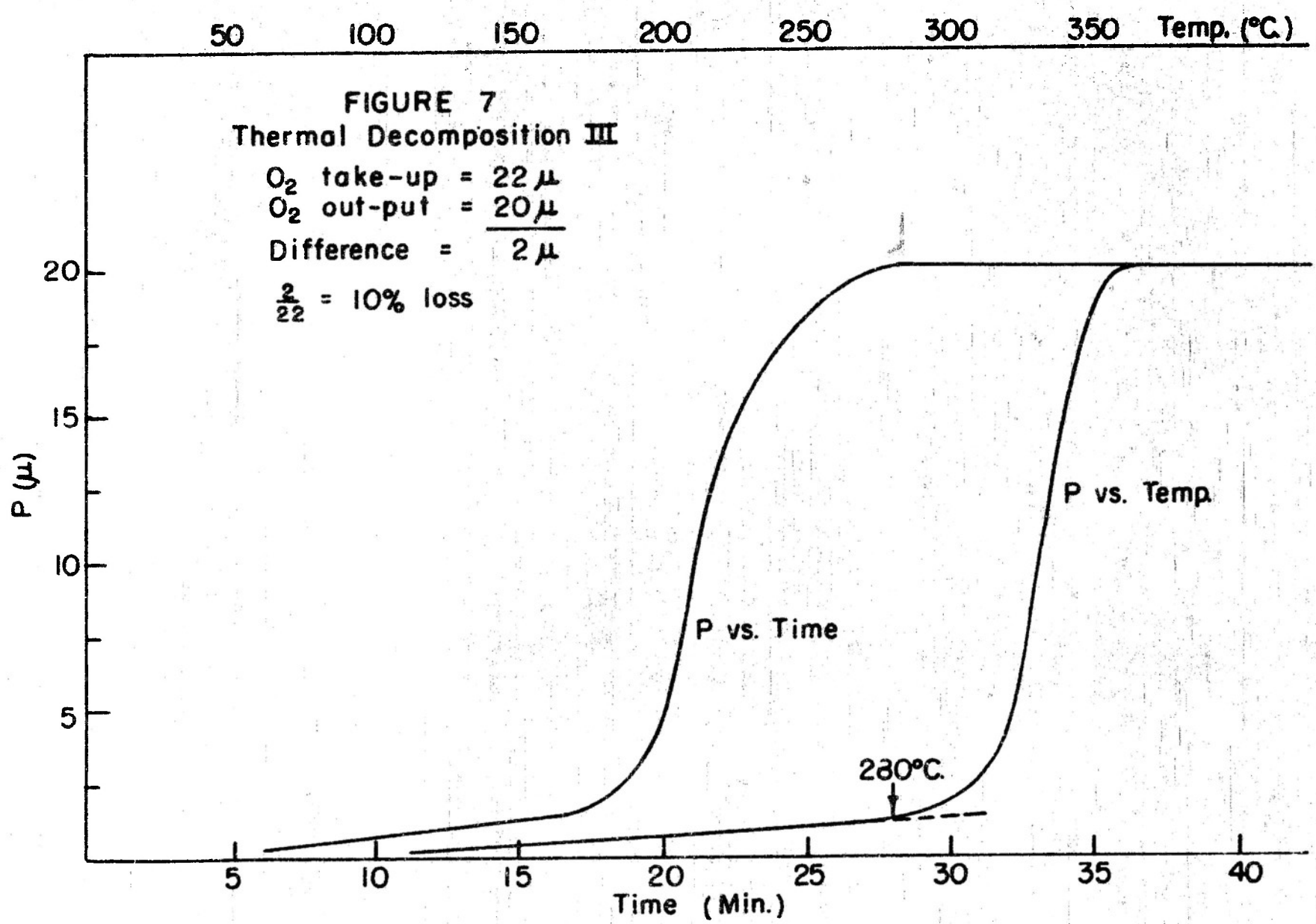
50
100
150
200
250
300
350
Temp. (°C.)
FIGURE 7
Thermal Decomposition III
O_2 take-up = 22 μ
O_2 out-put = 20 μ
Difference = 2 μ
$\frac{2}{22}$ = 10% loss
20
15
10
5
P (μ)
P vs. Temp.
P vs. Time
280°C.
5
10
15
20
25
30
35
40
Time (Min.)

TABLE V. SUMMARY OF RESULTS FOR MATERIAL BALANCE EXPERIMENTS

Experiment No.	Final Tube Temp. °C	Temp., °C, of Initial Rapid O_2 Evolution	Microns Deposited	Microns Evolved	ΔP_2 Microns
I	~310	265	118	104	14
II	>350	270	80	74	6
III	340	280	22	20	2

gauge used to measure pressure during heating. The pressures in column four were determinded using the micro Pirani and are much more accurate.

In a second series of experiments the rate of decomposition of the oxide was measured at 250°, 200°, and 190° C using the massive silver disc tube (Fig. 1B with silver disc cut from sheet silver), at 190° C using a thick evaporated silver film cathode tube (Fig. 1B) such as was used in the radioactive Cs tracer experiments. In these experiments the silver disc was first oxidized at room temperature by means of a dc glow discharge. After oxidation the excess oxygen was pumped out and the tube containing the oxidized silver disc was suddenly immersed in a preheated oil bath. The pressure was then followed as a function of time at constant temperature. The results of the decomposition experiments at 190°C and 200° C are shown in Fig. 8 and at 250° C in Fig. 9. The rate of decomposition at 190° C is quite small. A rapid rise in the pressure, as shown in Fig. 8, occurs during the initial heating of the tube in the oil bath. This initial rise is probably associated with the desorption of a fractional monolayer of oxygen on the tube walls. It appears highly probable, from the data presented later on the development of photoemission and thermionic emission during cesium addition, that the loss of oxygen from the surface by silver oxide decomposition must be very small during the cesium addition to massive silver cathodes. In the case of oxidized thin silver films no experiments have been performed.

3.5 Oxidation of Thin Films.

According to one method for the preparation of semitransparent photocathodes a silver film is evaporated on glass until the white light transmission is reduced to 50%. The film is then oxidized until the transmission increases to 90%. The remaining fabrication steps are then carried out. Since it was of interest to study photocathodes fabricated in this way, light transmission has been used as the means of controlling both the silver film evaporation and the subsequent oxidation.

At the beginning of the project it was assumed that increased oxidation of a silver film was accompanied by increased light transmission. With the oxidation methods then in use, however, oxidized films exhibited less than 90% transmission. More extensive oxidation did not increase

FIGURE 8

Ag_xO_y Decomposition

A. Massive Ag – 25μO_2 – 200°C.

B. Massive Ag – 172μO_2 – 190°C.

C. Evap. thick Ag film – 66μ – 190°C.

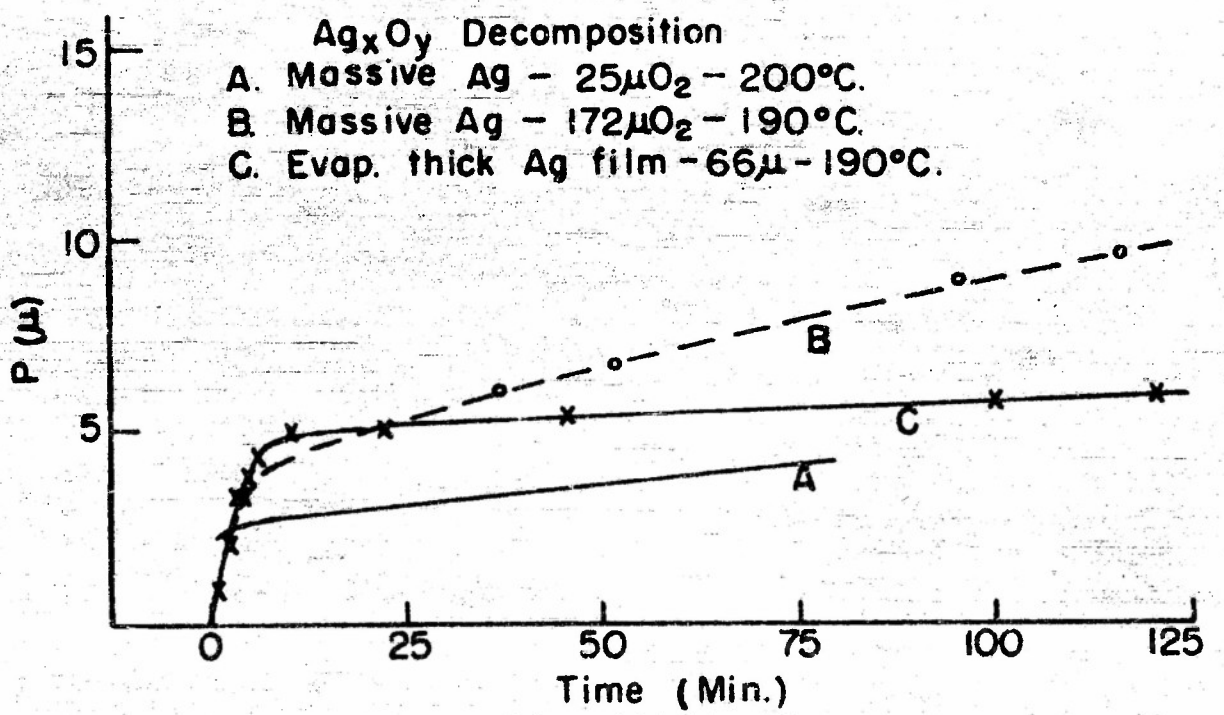

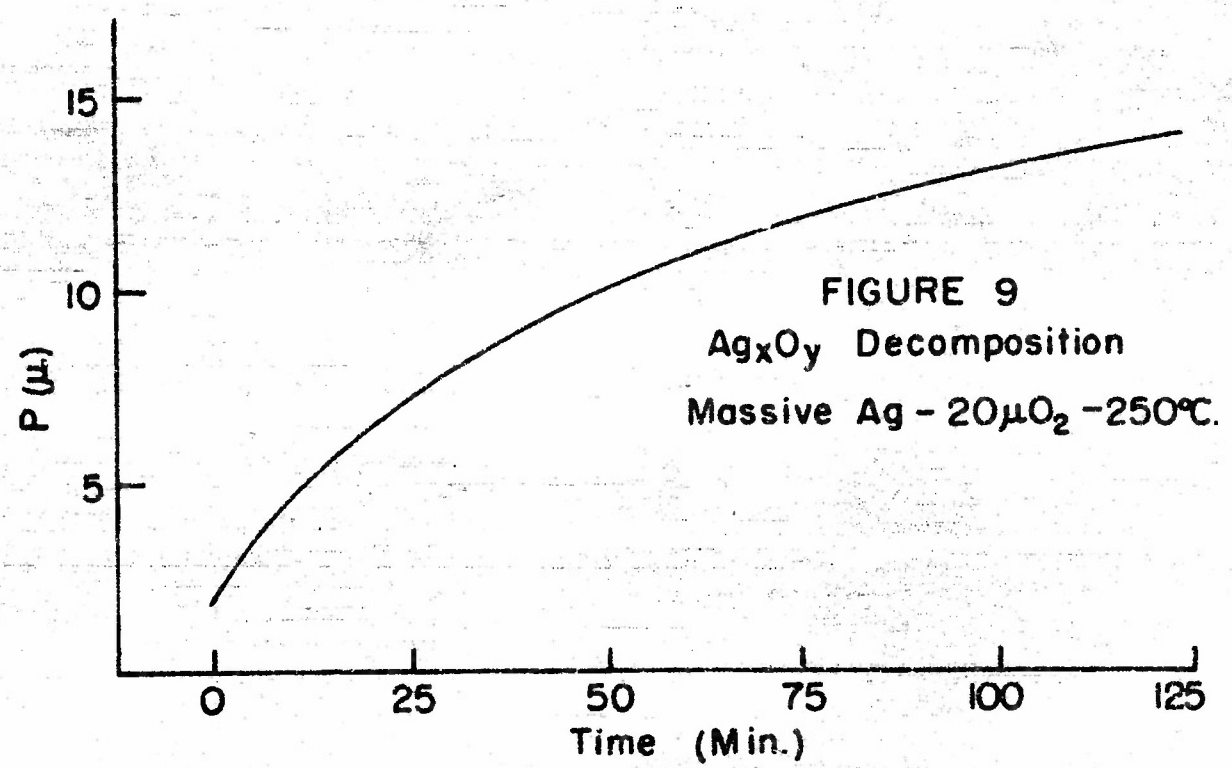

FIGURE 9

Ag_xO_y Decomposition

Massive Ag – 20μO_2 – 250°C.

the transmission. The first clue to an understanding of this observation came during the ozone oxidation of silver films of graded thickness (see Section 4). Certain sections of these films were oxidized to 90% transmission and, moreover, it was found on x-ray examination that the films contained silver so that the oxidation was certainly not complete. On the other hand, films which had been heavily oxidized in an rf discharge contained no silver and had transmissions considerably less than 90%. Thus complete oxidation produced a film of low transmission. This suggested at once that a maximum in transmission is to be expected as oxidation proceeds. This was confirmed by means of investigations using a silver wedge type tube (Fig. 1C) and a dc glow discharge. The results obtained in a typical run are shown in Fig. 4. A maximum transmission is obtained. This experiment is described in more detail in Section 4.33 where the results of an x-ray diffraction investigation are also given. The conditions used in the preparation are given in Table XVII, tube 19-27-15-3. A maximum in transmission is obtained in the oxidation of silver films whether evaporated slowly (300 sec) or rapidly (15 sec). Transmissions were measured with white light and with an S-4 surface as detector. By means of an x-ray study (see Section 4) it has been demonstrated that thin films oxidized by the dc glow discharge contain unoxidized silver. The thermal decomposition of oxidized thin silver films has not been studied.

In the next section it is pointed out that the presence of an unoxidized residue of silver in a thin film indicates that isolated silver grains, not in contact with others, were contained in the original film. In thicker films where grain contact is established the maximum in transmission may not form, although we have not tested this by experiment.

3.6 Silver Film Orientation.

In considering the production of the photocathode it is of interest to know whether crystal orientation of an evaporated silver layer has any effect on crystal orientation in the oxide surface formed. Consequently an x-ray diffraction investigation of the oxide surface formed on oriented and nonoriented silver films was undertaken. This study was performed under a previous contract and the results have already been described in a previous report[16]. A brief summary is given here,

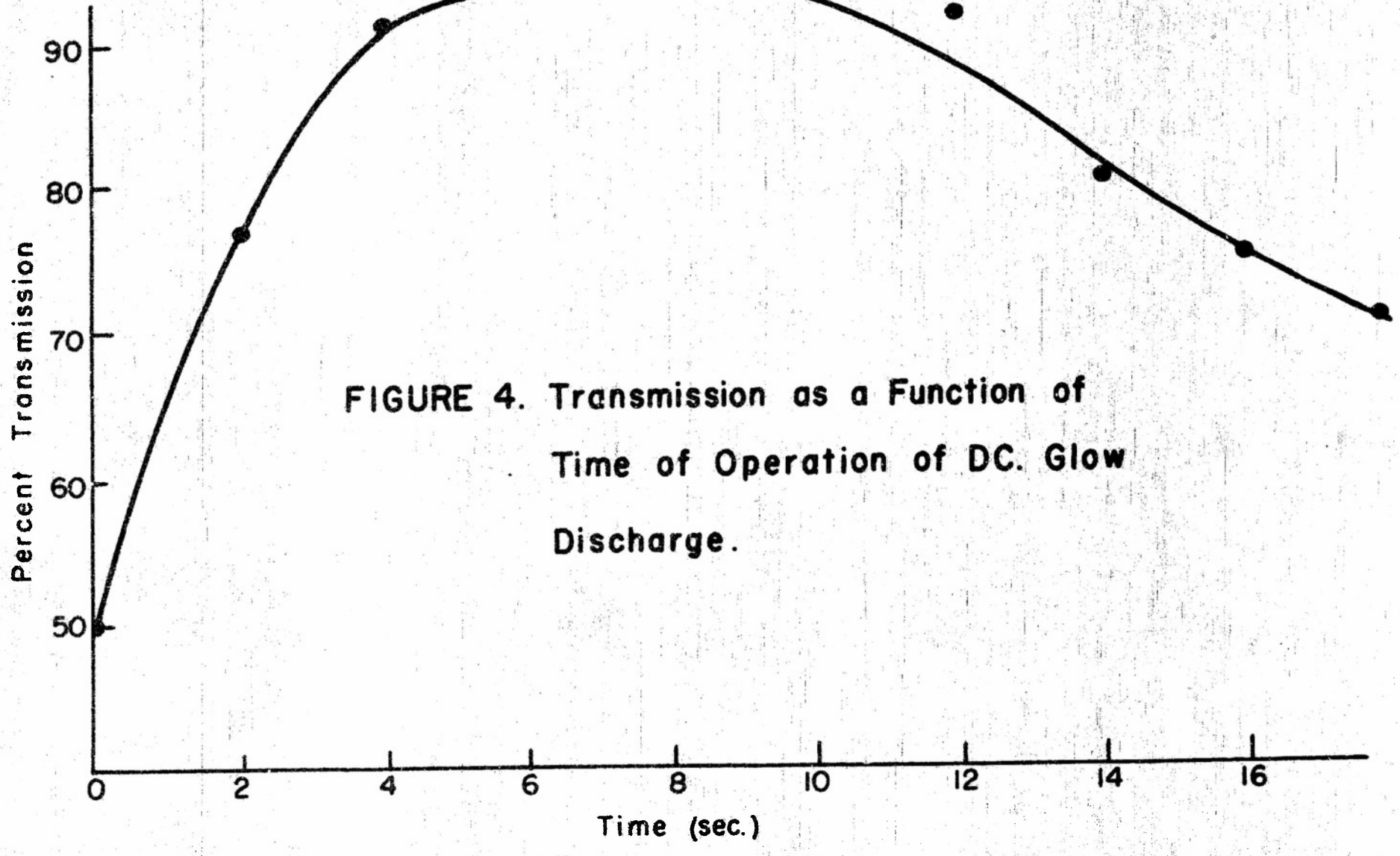

FIGURE 4. Transmission as a Function of Time of Operation of DC. Glow Discharge.

however, for the sake of completeness.

Unoriented and oriented silver films were prepared by the evaporation of silver on glass and rocksalt substrate respectively[16]. The films were partially oxidized in a glow discharge in oxygen at 0.3 - 0.75 mm Hg, and the resultant films were examined by the x-ray diffraction method previously described. The x-ray photographs clearly demonstrated that the oxide film in both cases did not have any preferred orientation.

In the preparation of the Ag-O-Cs photocathode the base silver may be of several types, namely: silver sheet, evaporated or sputtered silver films, and silver films obtained by chemical methods. Photocathodes produced by these various methods of substrate formation are said to possess essentially the same photosensitive characteristics. Thus, since the silver oxide surface formed consists of randomly oriented oxide grains, the conclusion suggested is that the structure of the oxide film with which the cesium reacts should be independent of the structure of the silver base. It is, however, shown later (Section 4.5) that, contrary to the above, the structural characteristics of the substrate may exert a profound effect upon the formation and photoelectric properties of the surface. The above x-ray results show, however, that this influence is not due to preferred crystal orientation.

4. NATURE OF OXIDATION PRODUCTS

In the preceding section the method of oxidizing silver by means of the dc glow discharge has been discussed. The oxidation efficiency, thermal decomposition, and other pertinent facts have been described. Those results tell us very little, however, about the nature of the oxidation products. In order to obtain this information the x-ray study which is described in the present section was undertaken. The principal objective of the study was to obtain x-ray powder diffraction patterns for oxidation products prepared in various ways and to compare the observed patterns with those for the known oxides of silver for the purpose of identifying the solid phases present. The oxidation of massive silver was studied under a previous contract and the results have been described in another report[1]. During the present contract, reasons have arisen for further study of the oxidation of thin silver films. The results of the investigation performed under this

contract are given in Section 4.3. For the sake of completeness a review of the work performed under the previous contract[1] is given in Section 4.2. For comparison purposes the powder diffraction patterns for silver and for the known oxides of silver are given in Section 4.1.

4.1 Powder Diffraction Patterns for Silver and Silver Oxides

In a previous report[1] the interplanar spacings d/n and intensities (I) have been given for Ag, Ag_2O, and AgO respectively. For convenience of comparison these data are reproduced here in Tables VI, VII and VIII. It is worthwhile to note that the formula for the last of these substances was written as Ag_2O_2 in the earlier report[1] and the substance was there referred to as silver peroxide. During the present contract period it was recognized that the substance is probably not a peroxide. This view is strongly indicated by the work of Yost[17] and was further confirmed by a few chemical experiments on a sample of the same material as that used to obtain the x-ray powder pattern of Table VIII. This material dissolved in sulfuric acid to form a brown solution, and this solution was a sufficiently strong oxidizing agent to oxidize manganous salts to permanganate. This behavior is not characteristic of a peroxide, but it agrees very well with the behavior reported for solutions containing divalent silver. It seems highly likely, therefore, that the solid contains divalent silver and hence the symbol AgO more appropriately describes its chemical behavior.

It is a well-established fact[18,19,20,21,22] that monovalent silver ion can be converted to trivalent silver ion in solutions which are treated with sufficiently powerful oxidizing agents. The oxide to be expected with trivalent silver is Ag_2O_3. A reliable x-ray powder diffraction pattern for Ag_2O_3 is, however, not available because of difficulties encountered (by other investigators) in the preparation of pure Ag_2O_3. The methods used for the preparation (anodic oxidation of silver using aqueous solutions of electrolytes containing various silver salts such as nitrates, chlorates and sulfates) always led to a product containing significant amounts of impurity (nitrate,

TABLE VI. INTERPLANAR SPACINGS AND RELATIVE INTENSITIES FOR METALLIC SILVER

hkℓ	d/n	I (rel.)
(111)	2.359	100
(200)	2.044	40
(220)	1.445	40
(311)	1.232	60
(222)	1.180	30
(400)	1.022	10
(331)	0.937	50
(420)	0.914	50
(422)	0.834	60
(333)	0.786	70

TABLE VII. POWDER DIFFRACTION DATA FOR Ag_2O (a.o = 4.720). (Structure: Cubic Cuprite Type)

hkℓ	d/n(A)	I (rel.)
110	2.725	100
200	2.360	60
220	1.669	60
311	1.423	50
222	1.363	20
400	1.180	10
331	1.083	20
420	1.055	10
422	0.9635	10
333	0.9084	10
440	0.8344	5
531	0.7978	2
442	0.7867	5

TABLE VIII. POWDER DIFFRACTION DATA FOR AgO.
(Structure: Unknown)

No.	d/n(A)	I (rel.)	No.	d/n(A)	I (rel.)
1	2.738	100	26	0.9871	10
2	2.592	27	27	0.9796	5
3	2.382	83	28	0.9712	1
4	2.255	33	29	0.9534	4
5	1.730	15	30	0.9407	29
6	1.687	50	31	0.9287	29
7	1.662	17	32	0.9230	10
8	1.611	35	33	0.9103	17
9	1.468	31	34	0.8965	8
10	1.445	58	35	0.8831	21
11	1.421	14	36	0.8724	5
12	1.406	14	37	0.8661	6
13	1.383	58	38	0.8492	23
14	1.347	12	39	0.8379	12
15	1.305	17	40	0.8303	15
16	1.201	23	41	0.8207	31
17	1.139	5	42	0.8138	4
18	1.121	17	43	0.8110	31
19	1.099	31	44	0.8106	13
20	1.085	15	45	0.8035	50
21	1.064	25	46	0.8802	12
22	1.048	12	47	0.7971	14
23	1.040	12	48	0.7951	16
24	1.011	14	49	0.7929	13
25	0.9966	6	50	0.7826	19
			51	0.7806	35
			52	0.7761	23

chlorate or sulfate). A structural investigation of the products obtained by anodic oxidation of silver has been carried out by Braekken[31]. Braekken reported that the product Ag_2O_3(N) prepared by the electrolysis of silver nitrate gave the best single crystals. The crystals, for the most part, have an octahedral form which is not very well developed. From x-ray diffraction studies of the powder and single crystals it was shown that the crystals have a common structure. The photographs could be readily indexed by Braekken on the basis of a face-centered cubic unit cell with a variable lattice constant (depending on the amount of impurity), and which contained 16 molecules of Ag_2O_3. The following lattice constants were found.

Preparation	a_o
Ag_2O_3(N)	9.82 ± 0.03 kx
Ag_2O_3(N)	9.870 ± 0.003 kx
Ag_2O_3(F)	9.911 ± 0.001 kx
Ag_2O_3(Cl)	9.916 ± 0.005 kx
Ag_2O_3(S)	9.896 ± 0.003 kx

Thus actual lattice constant of the oxide depended upon the conditions used in the preparation of the sample. The letters in parenthesis indicate the anion of the electrolyte used in the preparation (N for nitrate, etc.).

Braekken found that the diffraction pattern could also be indexed on the basis of a pseudo-cell with a lattice constant one-half the true value if only the weak reflections were neglected. The smaller cell was shown to be approximately face-centered and contained 4 silver atoms. The arrangement of silver atoms in the pseudo-cell is almost identical to that observed in Ag_2O.

Since oxygen positions could not be derived on the basis of the possible cubic space groups, Braekken suggested that the entire structure is only pseudo cubic, but a good approximation to cubic. It was, however, established that the lattices of the two oxides, Ag_2O and Ag_2O_3, are similar. In addition, since the method of preparation of the oxide resulted only in lattice constant variations, Braekken concluded that only one silver oxide was present in the products from anodic oxidation, namely Ag_2O_3.

The interplanar spacings for the silver oxide,

$Ag_2O_2(N)$, reported by Braekken are presented in Table IX. It is clear from the above discussion that the sample of Table IX is not pure and hence no accurate agreement can be expected between this powder diffraction pattern and those obtained on pure Ag_2O_3. Since, however, the impurities are apparently present in solid solution, it seems possible that the powder patterns of pure Ag_2O_3 and of Table IX differ chiefly because of a difference in lattice constant caused by impurities in solid solution.

4.2 Massive Silver Oxidation

During the course of the present contract no x-ray study of the products resulting from the oxidation of massive silver was made because, as a part of the same project but under a previous contract, a rather complete study had already been carried out. For the sake of completeness in the present report, an account of this work is being included. Almost all of the present Section (4.2) is based on a report of this previous work[1], the only exception being subsection 4.23. While this involves some repetition in the discussion of work which has already been reported, it has the advantage of providing a rather complete account of the present status of the oxidation process.

4.21 Preliminary experiments

Prior to a rather detailed study of the rf oxidation of silver wires, preliminary experiments were performed in which the oxide formed on silver wires by ozone and rf oxidation was characterized by x-ray diffraction powder photographs.

During the ozone oxidation of silver wires it appeared that the oxide film catalyzed the further formation of the oxide. Initially the process of oxidation does not seem to occur (at least visibly). Once a spot becomes oxidized, the oxide grows out from this point in a ring around the wire and proceeds rapidly along the length of the wire. At times the growth of the oxide film would suddenly stop as if the surface were "poisoned" and the layer of oxide would then start growing at another place on the wire. Similar phenomena were observed in the rf oxidation

TABLE IX. INTERPLANAR SPACINGS FOR Ag_2O_3(N)
(Lattice Type: Pseudo Cubic)

hkl	d/n	hkl	d/n
222	2.85	844 }	1.009
400	2.47	557 }	
331	2.33	771 }	0.995
420	2.26	339 }	
422	2.01	666 }	0.963
440	1.79	2,2,10 }	
531	1.71	864	0.919
622	1.49	10,4,0	
444	1.45	10,4,2	.903
551-771	1.39	880	.874
642	1.32	1062	.836
731 }	1.287	884 }	.825
553 }		12,0,0 }	
800	1.235	7,7,7 }	.816
662	1.135	11,5,1 }	
840	1.106	12,2,2	.809
753 }	1.088	11,5,3 }	.795
911 }		975 }	
		12,4,8	.782

of wires.

From the comparison of the x-ray diffraction photographs for the ozone and rf oxidized wires it was evident that the structures of the two oxide films were similar, and that oxide phases other than Ag_2O were present. From the interplanar spacing data which appeared to be definitely associated with Ag_2O, a series of Ag_2O lattice constants for the different samples were derived. The observed Ag_2O lattice constant varied from 4.724 to 4.732 A. compared to Faivre's values of 4.695 A. for pure Ag_2O and 4.736 A. for Ag_2O saturated with silver at 200°C[32]. This result suggests that there is appreciable solid solution of silver in the silver oxide formed in the oxidation of wires.

During attempts at identification of the observed interplanar spacings, it was found that a group of the lines distinct from Ag and Ag_2O could be indexed on the basis of a face-centered cubic unit cell with a_o=4.55 A. This group of lines was given the designation ψ phase. However, considering the number of lines not assignable, it seems certain that this cell choice is only an approximation. In fact it will be shown in Section 4.3 that the ψ phase is a mixture of at least two solid phases.

4.22 Rf oxidation of silver wires.

In the previous technical report the detailed procedure and results of a systematic investigation of the rf oxidation of silver wire were presented[1]. In these experiments silver wires were oxidized in an rf glow discharge using the equipment described in Section 2.3 (Fig. 3B). The experimental results and conclusions are briefly summarized below.

During the glow discharge oxidation of the silver wires the sample was mounted between the ends of a chromel-alumel thermocouple so that an approximate determination of the temperature of the wire in the glow discharge was possible. It was observed that temperature equilibrium during the glwo discharge bombardment was quickly obtained. A total of 24 oxidized wire samples were prepared using three-minute oxidations at four oxygen pressures (0.2, 0.4, 0.6, and 1.0 mm Hg) and three different relative rf power inputs (220, 160, and 120). The temperature

observed during the oxidation ranged from 130° to 285°C. The equilibrium temperature was dependent upon the oxygen pressure and the rf power input.

X-ray powder diffraction photographs were prepared using one set of the samples, while metallographic examinations were made of the second set. Using the diffraction lines which appeared to be definitely associated with Ag_2O, a series of Ag_2O lattice constants were derived using the $\cot\theta\cos^2\theta$ extrapolation method. The average ao for the Ag_2O was 4.736 ± 0.005 A., in good agreement with the value 4.736 A. obtained by Faivre for Ag_2O saturated with Ag at 200°C.

In the x-ray diffraction photographs a series of lines were observed which could not be associated with either Ag_2O or Ag. One group of the extra lines could be indexed as belonging to the Ψ phase discussed in the previous section. A complete list of the interplanar spacings for sample 12 is given in Table X. A comparison of the intensities of the Ψ lines to those of Ag and Ag_2O within the sets of photographs indicated there was no marked intensity variation of the Ψ lines relative to the silver lines. The line intensity ratio for $\Psi(220)$ to Ag_2O (220), however, varied from 0.05 to 0.90, indicating a large variation in relative abundance of Ag_2O compared to the actual phase or phases producing the $\Psi(220)$ line. The variation of the intensity ratio could not be correlated with the sample preparation data.

In order to obtain more extensive x-ray data on the rf oxide an x-ray photograph was prepared of the oxide layer which could be readily brushed off a small coil of silver wire after the oxidation in an rf discharge. The data from the photograph are presented in Table X. In the photograph 41 lines were observed which could not possibly be assigned to Ag_2O or Ag. Of this group of 41 lines only 10 lines could be associated with a cubic Ψ phase. Considering the number of extra lines it is very probable that the Ψ phase indexing of a portion of the stronger "foreign" lines is not particularly significant. It was also established that the extra diffraction lines could not be associated with the presence of AgO.

In a related experiment a sample of pure silver oxide (Ag_2O) was oxidized by oxygen in an rf discharge. The x-ray diffraction pattern of this material so formed

TABLE X. INTERPLANAR SPACINGS FOR RF OXIDIZED WIRE NO. 12 AND RF OXIDE COATING FROM SILVER WIRE.

d/n(A) Sample No. 12	d/n(A) rf Oxide Coat	Assignment	d/n(A) Sample No. 12	d/n(A) rf Oxide Coat	Assignment
3.38	3.39		1.130	1.139	ψ(400)
3.19	3.19			1.124	
3.03	3.03			1.104	
2.89	2.89		1.0795	1.079	Ag_2O(331)
2.698	2.73	Ag_2O(111)		1.067	
2.596	2.62	ψ(111)		1.052	
	2.50		1.035	1.045	ψ(331)
	2.41		1.019	1.032	Ag(400)
2.341	2.35	Ag(111),Ag_2O(200)	1.010	1.015	ψ(420)
2.243	2.27	ψ(200)		0.989	
	2.15			0.977	
2.029	2.04	Ag(200)		0.968	
	1.97			0.948	
	1.86			0.941	
	1.74		0.936	0.937	Ag(331)
	1.705		0.927	0.929	
1.660	1.658	Ag_2O(220)	0.923		ψ(422)
1.591	1.615	ψ(220)	0.912	0.912	Ag(420)
	1.526			0.882	
1.471	1.479		0.869		ψ(333)
1.437	1.447	Ag(220)		0.854	
1.414	1.421	Ag_2O(311)	2.839	0.839	Ag(422)
	1.389			0.816	
1.358	1.365	Ag_2O(222)		0.811	
1.302	1.303	ψ(222)		0.805	
	1.279		0.800	0.800	ψ(440)
	1.264		0.768	0.785	Ag(333)
1.228	1.231	Ag(311)		0.783	
	1.207				
1.176	1.182	Ag(222), Ag_2O(400)			

Note: No absorption correction has been applied to the data.

was identical to that for the rf oxide coat described above. The product contained ψ phase or phases, silver, and silver oxide (Ag_2O).

The metallographic examination of the set of rf oxidized wires indicated no major differences in the structure of the oxide film present on the different samples. The examination did indicate the presence of one phase adjacent to the wire and a second phase on the surface, the two being separated by a boundary. The oxide film was also found to contain numerous islands of massive silver of varying size. The appearance of the metallographs at the massive silver-oxide surface boundary suggests that the oxidation proceeds by an intergranular corrosion process.

To obtain further information on the characteristics of the two-phase oxide system, electron diffraction photographs were prepared of silver wires oxidized to the second order yellow-red color. The thickness of this oxide coat was comparable to that used in the preparation of massive cathode photosurfaces. The electron diffraction interplanar spacings as well as corresponding x-ray diffraction data are presented in Table XI. The ψ phase lines constitute only a few of the total of all ψ phase lines. It is also of interest that a ψ phase line appears in some experiments at $d/n = 2.66$. It has been omitted from the table because it is not consistently observed. Since the electron beam, in the electron diffraction experiments, does not penetrate very deeply into the sample it is anticipated that only the surface phase will be detected. It seems clear from Table XI that the electron diffraction lines can best be interpreted as arising from the ψ phase. It is to be further noted that x-ray diffraction photographs of the electron diffraction wire samples were similar to those obtained previously and indicated the presence of Ag_2O in the film. This is consistent with the electron diffraction data since x-rays penetrate the entire sample. These results suggest that Ag_2O is the phase in contact with the silver wire, while the surface consists of a higher valence state silver oxide. The fact that the AgO pattern could not be related to the electron diffraction pattern suggests that the higher oxide is actually Ag_2O_3.

Tiapkina and Dankov[23] have reported that the glow-discharge oxide is Ag_2O, on the basis of electron

TABLE XI. INTERPLANAR SPACING DATA

Electron Diffraction RF Oxidized Wire d/n	I	X-Ray Diffraction Data (d/n)	Ag	Ag_2O	AgO
3.03	(10)	3.03			
2.66	(5)	2.62		2.73	2.74
		2.41			2.59
2.32	(10)	2.27	2.36	2.36	2.38
1.99	(5)	1.97	2.04		
1.42	(8)	1.42	1.44	1.42	1.42
1.23	(8)	1.26	1.23	1.23	1.20
0.995	(4)	1.009	1.02	0.963	0.997
0.925	(4)	0.929			0.928

diffraction photographs of a silver film on a celluloid substrate which was oxidized in a glow discharge. The electron-diffraction photographs obtained by them exhibited a high background due to diffuse scattering and the lines were rather weak. This is not in agreement with our results either on silver wire or on thin films (see Section 4.33). It is possible that they actually decomposed the higher oxidents Ag_2O by electron bombardment, or more probably the Ag_2O was formed by the reaction of the higher oxide with the supporting film.

4.3 Products of Thin Film Oxidation.

4.31 Ozone oxidation of silver wedges.

The study of oxidation of thin silver films was undertaken because of difficulties encountered in the study of semitransparent photocathodes. A primary objective of the study was the identification of the solid phases present in the oxidized film. In such a study it is important to perform the oxidation in a variety of ways so that the proportion of solid phases is altered. Otherwise it may not be possible to discover how many phases are present, especially under such conditions that solid phases are encountered which have not been previously studied. For this reason ozone oxidation was studied along with both rf and dc glow discharge oxidations. Moreover, a wide variety of conditions for ozone oxidation were investigated. Among the variables are the following:

1. The rate of evaporation of silver.
2. The thickness of the silver film.
3. The temperature of oxidation.

Earlier experiments (Section 4.2) had already established that the products of oxidation of massive silver by ozone and rf discharge were the same, so the results were expected to be pertinent also to the glow discharge process. The investigation of ozone oxidation was particularly extensive because the technique for x-ray investigation of thin films was developed at this point. In the following subsections

the results of the investigation are briefly reviewed. Detailed data for the various phases of the investigation are given in Progress Report No. 3[24].

4.311 Experimental. The silver wedges were prepared on 1x3-inch microscope slides as described in Sec. 2.22. The percentage light transmission as a function of wavelength for each silver film so produced was measured using the Beckman DU spectro-photometer and a 1P25 phototube. The silver film slides were placed in the pyrex tube furnace and oxidized in ozone under the different conditions shown in Table XII. After oxidation, the transmission curves were determined and the slides examined microscopically at 15, 45, 90, and 440X. X-ray powder photographs were then prepared for oxide samples removed from selected portions of the slides as indicated in Table XII. In describing the slides the 0 (zero) position corresponds to the thickest portion of the silver film. The percent transmission values at 700 mμ versus position on the film (which is a measure of film thickness) are given in Figs. 10, 11, and 12. The x-ray diffraction data (d/n and I) for the thicker portions of the wedges are given in Table XIII, for the intermediate regions in Table XIV, and for the thinner regions in Table XV.

The first and most obvious observation is that the films contain crystals of sufficient size to produce an x-ray diffraction line spectrum, and this is true even in the region for which the light transmission of the silver film before oxidation is 50%. It is therefore sensible to apply the results of phase equilibrium studies on macroscopic systems to the oxidized film wherever such application is useful. In anticipation of the results of Sections 4.32 and 4.33 it may also be stated that similar results are obtained on oxidation by rf and dc glow discharge.

4.312 Preliminary summary of general results. In discussing the results it is useful to contrast the appearance of ozone oxidized films with films oxidized in a dc glow discharge (see Section 4.33) and also to bear in mind a few general observations. In the first

TABLE XII. OZONE OXIDATION OF SILVER WEDGES

Silver Film Sample	Code No.	Ag Evap. Time (Min.)	Oxidation Conditions Temp °C	Oxidation Conditions Time (Hours)	O_3	X-ray Data Film	X-ray Data Sample Region (cm)
A	1761-185 VII	240	28	11	Dry	1760-77-9	0-0.9
						-10	0.9-1.3
						-11	1.5-2.0
						-12	2.0-3.5
B	1761-187 VIII	25	28	10	Dry	1760-82-1	0-1
						-2	2.0-3.0
						-3	3.5-4.5
C*	1761-183 IV	15	100	7	Dry	1760-76-1	0-1
						-2	1-2
						-3	2.5-3.5
						-4	4-5
D	1761-183 V	15	100	10	Dry	1760-76-5	0-1
						-6	1-2
						-7	---
						-8	3.5-4.5
E	1761-187 X	25	140	4	Wet	1760-83-7	0-1
						-8	2-3
						-9	3.5-4.5
F	1761-187 XIII	25	140	4	Dry	1760-93-6	2-3
						-7	6-7
G	1761-187 XI	25	160	3.5	Wet	1760-84-10	0-1
						1760-93-1	2-3
						-2	5-6
H	1761-187 IX	25	170	5.5	Dry	1760-83-4	0-1
						-5	2-3
						-6	4-5
I	1761-187 XII	25	200	2.5	Dry	1760-93-3	1.5-2.0
						-4	3.5-4.5
						-5	6.0-7.0
J	1927-14-1	0.5	28	11	Dry	----------	

*Prior to oxidation, film preheated to 150°C, then cooled to 100°C for oxidation.

TABLE XIII. INTERPLANAR SPACINGS DATA FOR OZONE OXIDIZED FILMS (Thick Sections)

Capital letters A, B, C... identify the specimen (see Table XII)
The d/n values are in angstroms, followed by relative intensity (I)

A d/n(I)	B d/n(I)	C d/n(I)	D d/n(I)	E d/n(I)	F d/n(I)	G d/n(I)	H d/n(I)	I d/n(I)
3.36(25)	3.37(12)	3.35(10)	3.36(20)	3.36(12)	3.39(5)	3.36(6)	3.35(10)	3.39(7)
3.18(25)	3.19(10)	3.19(10)	3.19(20)	3.19(12)	3.21(5)	3.19(6)	3.18(10)	3.21(7)
3.02(3)	3.05(2)	3.03(1)	3.01(1)	3.02(2)	3.04(4)	3.03(2)	3.02(7)	3.05(2)
		2.89(1)		2.87(2)	2.92(2)	2.91(1)	2.90(2)	2.90(1)
2.73(100)	2.73(100)	2.72(100)	2.72(100)	2.75(100)	2.73(100)	2.74(100)	2.73(100)	2.74(100)
2.65(4)	2.66(2)		2.63(3)	2.62(20)	2.66(1)	2.62(2)		
2.51(8)	2.49(5)	2.49(3)	2.49(10)	2.51(6)	2.51(2)	2.48(1)	2.51(2)	2.51(4)
2.43(30)	2.42(30)	2.41(30)	2.42(30)	2.41(75)	2.42(30)	2.41(50)	2.41(50)	2.42(35)
2.36(30)	2.35(8)	2.34(1)	2.36(30)	2.34(2)	2.35(3)	2.36(2)	2.35(2)	
2.29(10)	2.29(15)	2.29(15)	2.28(10)	2.28(35)	2.28(18)	2.28(25)	2.27(30)	2.28(25)
	2.21(1)	2.22(1)						2.20(1)
		2.13(1)		2.12(1)				
			2.04(5)					
1.96(2)	1.96(1)						1.96(1)	1.96(1)
				1.84(1)	1.85(1)	1.84(1)	1.83(2)	
		1.74(1)		1.74(4)		1.73(1)		
1.71(5)	1.71(10)	1.71(8)	1.71(10)	1.70(20)	1.71(15)	1.71(20)	1.71(27)	1.71(20)
							1.67(1)	
1.66(30)	1.66(25)	1.66(20)	1.66(20)	1.66(25)	1.66(25)	1.66(30)	1.66(35)	1.66(30)
1.62(2)	1.62(1)			1.62(12)		1.62(1)	1.60(2)	1.62(1)

TABLE XIII. (Continued)

A d/n(I)	B d/n(I)	C d/n(I)	D d/n(I)	E d/n(I)	F d/n(I)	G d/n(I)	H d/n(I)	I d/n(I)
				1.52(1)	1.52(1)	1.52(1)		
				1.47(6)		1.47(1)		
1.45(15)	1.45(20)	1.45(25)	1.45(18)	1.45(40)	1.45(25)	1.45(40)	1.45(35)	1.45(35)
1.42(10)	1.42(2)	1.42(1)	1.42(6)	1.41(2)	1.42(1)	1.41(1)	1.41(1)	1.42(1)
1.39(8)	1.39(8)	1.39(7)	1.39(6)	1.39(20)	1.39(14)	1.39(20)	1.39(50)	1.39(20)
1.37(8)	1.37(8)	1.37(8)	1.37(5)	1.37(12)	1.37(15)	1.37(20)	1.37(50)	1.37(20)
				1.35(1)				
				1.31(4)		1.31(1)		
	1.25(1)					1.22(1)	1.22(1)	1.24(1)
1.22(2)	1.22(2)	1.21(1)		1.21(8)	1.21(4)	1.21(8)	1.21(10)	1.21(6)
							1.20(1)	
			1.18(2)	1.18(1)		1.18(1)		
		1.14(1)		1.14(2)	1.14(2)	1.14(4)	1.14(2)	1.14(3)
	1.11(2)			1.12(2)				
1.11(2)	1.10(2)	1.11(2)	1.11(2)	1.11(10)	1.11(6)	1.11(10)	1.11(8)	1.11(7)
1.08(8)	1.08(10)	1.08(10)	1.08(8)	1.08(12)	1.08(18)	1.08(22)	1.08(23)	1.08(22)
1.07(1)		1.07(1)		1.07(12)	1.07(5)	1.07(8)	1.07(7)	1.07(6)
1.05(1)				1.05(2)				1.05(1)
				1.04(2)				
	1.03(1)	1.03(2)	1.03(1)	1.03(4)	1.03(6)	1.03(10)	1.03(8)	1.03(7)
				1.00(2)		1.00(1)		1.00(1)

TABLE XIII. (Continued)

A d/n(I)	B d/n(I)	C d/n(I)	D d/n(I)	E d/n(I)	F d/n(I)	G d/n(I)	H d/n(I)	I d/n(I)
				.990(1)				.989(1)
.981(4)	.983(5)	.978(4)	.979(3)	.979(10)	.978(10)	.979(15)	.979(10)	.979(15)
.959(1)	.953(2)	.949(1)		.950(3)	.951(6)	.950(9)	.950(6)	.950(7)
				.940(3)				
.931(4)	.931(6)	.928(5)	.931(1)	.929(12)	.930(10)	.935(15)	.930(12)	.929(15)
.914(2)	.916(4)	.913(1)	.916(8)	.913(5)	.913(6)	.913(10)	.914(6)	.914(8)
				.897(1)				.892(1)
.883(1)	.884(4)	.883(2)	.887(1)	.883(5)	.882(7)	.883(10)	.883(7)	.883(10)
		.885(1)	.858(1)	.856(1)	.856(2)	.856(3)	.856(5)	.855(3)
	.844(1)			.842(1)				
.831(1)	.832(2)	.829(1)	.834(2)	.833(5)	.831(5)	.830(10)	.833(8)	.831(10)
.817(3)	.818(3)	.816(2)	.817(1)	.816(6)	.817(8)	.817(15)	.816(15)	.817(15)
							.806(2)	
.806(3)	.806(4)	.805(3)	.804(2)	.805(8)	.806(10)	.805(16)	.805(18)	.805(17)
					.802(3)	.800(8)	.800(5)	.801(7)
					.785(15)	.785(20)	.785(20)	.785(22)
.784(3)		.784(4)	.785(5)	.784(10)	.784(14)	.784(20)	.784(20)	.784(22)

TABLE XIV. INTERPLANAR SPACINGS DATA FOR OZONE OXIDIZED FILMS (Intermediate Thickness)

Capital letters A, B, C... identify the specimen (see Table XII)
The d/n values are in angstroms, followed by relative intensity (I)

A d/n(I)	B d/n(I)	C d/n(I)	D d/n(I)	E d/n(I)	F d/n(I)	G d/n(I)	H d/n(I)	I d/n(I)
3.38(20)	3.37(30)	3.39(10)	3.33(20)	3.36(10)	3.39(5)	3.39(15)	3.36(13)	3.38(7)
3.20(20)	3.20(30)	3.19(10)	3.19(20)	3.18(10)	3.21(5)	3.21(15)	3.19(13)	3.21(7)
3.04(4)	3.02(10)	3.01(1)	3.00(3)	3.02(3)	3.04(4)	3.08(2)	3.15(3)	3.04(3)
2.80(4)	2.93(10)				2.92(2)	2.90(1)	2.94(1)	2.91(2)
2.73(100)	2.73(100)	2.72(100)	2.74(100)	2.73(100)	2.73(100)	2.73(100)	2.75(100)	2.75(100)
2.64(3)	2.64(5)	2.64(1)	2.63(5)	2.63(8)	2.66(1)	2.64(3)	2.64(1)	2.67(2)
2.50(20)	2.49(15)	2.49(1)	2.50(10)	2.48(1)	2.51(2)	2.51(10)	2.50(4)	2.51(3)
	2.42(10)		2.42(10)	2.42(20)	2.42(30)	2.42(40)	2.42(40)	2.42(50)
2.36(50)		2.36(30)		2.36(9)				
	2.36(20)		2.35(10)		2.35(3)	2.35(2)	2.36(2)	2.36(4)
	2.30(8)	2.30(1)	2.28(6)	2.29(10)	2.28(18)	2.29(20)	2.28(20)	2.29(35)
	2.22(4)		2.20(3)				2.21(2)	
2.05(10)		2.05(3)		2.04(1)		2.04(1)		2.05(3)
1.96(10)		1.97(2)	1.96(5)					
		1.88(1)		1.88(1)	1.85(1)	1.88(1)		1.86(2)
						1.76(1)		
	1.71(5)	1.71(1)	1.70(2)	1.71(5)	1.71(15)	1.71(12)	1.71(15)	1.71(20)
1.67(17)	1.67(13)	1.66(6)	1.66(10)	1.66(25)	1.66(25)	1.66(35)	1.66(25)	1.66(45
1.60(4)			1.62(2)			1.61(1)	1.61(1)	1.61(2)
			1.53(1)	1.52(1)	1.52(1)			1.54(1)

TABLE XIV. (Continued)

A d/n(I)	B d/n(I)	C d/n(I)	D d/n(I)	E d/n(I)	F d/n(I)	G d/n(I)	H d/n(I)	I d/n(I)
	1.47(2)							
1.44(20)	1.45(13)	1.45(8)	1.45(6)	1.45(25)	1.45(25)	1.45(40)	1.45(30)	1.45(50)
1.42(3)	1.42(2)		1.42(4)	1.42(1)	1.42(1)	1.42(1)	1.42(1)	1.42(2)
1.39(1)	1.39(3)		1.39(2)	1.39(3)	1.39(14)	1.39(13)	1.39(13)	1.39(20)
1.36(1)	1.37(2)		1.36(1)	1.37(4)	1.37(15)	1.37(13)	1.37(13)	1.37(20)
			1.27(1)					
1.23(25)	1.23(10)	1.23(8)	1.24(1)	1.24 Blur	1.21(4)	1.24(1)	1.21(4)	1.23(3)
						1.21(1)	1.20(1)	1.21(5)
1.18(4)	1.18(2)	1.18(1)		1.18 Blur				1.18(1)
1.14(1)					1.14(2)	1.14(1)	1.14(2)	1.14(2)
				1.11(2)	1.11(6)	1.11(4)	1.11(6)	1.11(8)
1.08(1)		1.08(1)		1.08(5)	1.08(18)	1.08(15)	1.08(12)	1.08(25)
				1.07(2)	1.07(5)	1.07(4)	1.07(5)	1.07(5)
1.02(1)				1.03(2)	1.03(6)	1.03(4)	1.03(5)	1.03(7)
.983(1)	.980(3)	.974(1)		.980(3)	.978(10)	.978(6)	.981(10)	.978(15)
					.951(6)	.951(3)	.952(5)	.951(7)
.942(3)	.936(2)							.938(1)
.923(8)		.924(2)	.930(2)	.931(3)	.930(10)	.928(6)	.932(10)	.929(20)
	.917(3)			.915(2)	.913(6)	.914(3)	.916(5)	.914(8)
					.882(7)	.883(4)	.884(5)	.883(8)

TABLE XIV. (Continued)

A d/n(I)	B d/n(I)	C d/n(I)	D d/n(I)	E d/n(I)	F d/n(I)	G d/n(I)	H d/n(I)	I d/n(I)
								.869(1)
					.856(2)	.855(1)	.857(2)	.856(3)
.836(4)	.834(2)			.830(2)	.831(5)		.831(6)	.831(6)
			.827(2)			.825(3)		
				.817(2)	.817(8)	.817(4)	.817(8)	.817(10)
	.805(1)		.806(1)	.805(4)	.806(10)	.805(4)	.806(8)	.806(15)
					.802(3)		.802(4)	.801(5)
.787(7)	.786(3)	.786(2)						
				.785(4)	.785(15)	.785(5)	.786(10)	.786(20)
					.784(15)			.785(20)

TABLE XV. INTERPLANAR SPACINGS DATA FOR OZONE OXIDIZED FILMS (Thin Sections)

Capital letters A, B, C... identify the specimen (see Table XII)
The d/n values are in angstroms, followed by relative intensity (I)

A d/n(I)	B d/n(I)	C d/n(I)	D d/n(I)	E d/n(I)	F d/n(I)	G d/n(I)	H d/n(I)	I d/n(I)
3.36(20)	3.37(60)	3.37(25)	3.36(40)	3.38(30)	3.38(15)	3.38(25)	3.38(15)	3.36(6)
3.20(20)	3.20(70)	3.19(25)	3.18(40)	3.19(30)	3.21(15)	3.20(25)	3.18(15)	3.21(6)
	3.00(8)	2.98(2)	3.02(2)	3.04(7)	3.02(2)	3.04(3)	3.02(4)	3.02(2)
	2.93(8)			2.91(7)			2.90(2)	
2.75(50)	2.73(100)	2.74(100)	2.73(100)	2.73(100)	2.75(40)	2.77(45)	2.74(100)	2.77(25)
2.65(2)	2.64(3)	2.63(2)	2.68(3)	2.62(10)	2.62(3)	2.64(2)	2.66(2)	2.65(3)
2.51(10)	2.49(50)	2.49(25)	2.50(10)	2.49(30)	2.49(10)	2.51(10)	2.49(8)	2.51(3)
							2.42(30)	
2.36(100)	2.36(100)	2.36(50)	2.36(90)	2.37(30)	2.37(100)	2.36(100)	2.36(2)	2.37(100)
			2.19(2)	2.29(2)			2.29(15)	2.22(1)
	2.10(3)	2.07(2)						
2.04(20)	2.04(15)	2.04(15)	2.05(20)	2.05(4)	2.05(35)	2.05(35)		2.05(35)
1.96(8)		1.97(10)	1.96(6)		1.98(2)	1.97(8)		1.97(3)
		1.82(1)			1.89(2)	1.88(1)		1.88(4)
							1.71(12)	
1.67(2)		1.67(2)	1.68(2)	1.67(2)	1.68(1)	1.68(2)	1.66(26)	1.68(3)
1.60(2)		1.60(2)	1.60(2)		1.61(1)	1.60(2)		1.61(3)
		1.49(1)	1.51(1)	1.52(1)		1.54(1)		
1.44(20)	1.45(20)	1.45(20)	1.44(20)	1.45(10)	1.45(30)	1.45(40)	1.45(28)	1.45(30)
1.39(1)				1.39(1)			1.39(12)	

TABLE XV. (Continued)

A d/n(I)	B d/n(I)	C d/n(I)	D d/n(I)	E d/n(I)	F d/n(I)	G d/n(I)	H d/n(I)	I d/n(I)
							1.37(12)	
1.27(1)			1.28(1)					
1.23(25)	1.23(30)	1.23(25)	1.23(30)	1.23(8)	1.23(40)	1.23(50)	1.21(3)	1.23(40)
			1.21(1)					
1.18(8)	1.18(5)	1.18(7)	1.18(5)	1.18(4)	1.18(8)	1.18(10)		1.18(10)
1.14(1)			1.14(1)			1.14(1)	1.14(1)	
							1.11(5)	1.11(3)
	1.09(1)						1.08(15)	
							1.07(6)	
							1.04(5)	
1.02(1)					1.02(1)	1.02(2)		
			.987(1)			.983(1)		
							.979(10)	
							.951(5)	
.941(10)	.940(3)	.939(8)	.940(5)		.941(10)	.938(15)		.939(15)
							.930(10)	
.917(12)	.918(7)	.916(10)	.917(6)	.917(2)	.916(15)	.915(20)	.914(4)	.915(20)
							.886(5)	
							.856(1)	
		.841(1)						

TABLE XV. (Continued)

A d/n(I)	B d/n(I)	C d/n(I)	D d/n(I)	E d/n(I)	F d/n(I)	G d/n(I)	H d/n(I)	I d/n(I)
.836(11)	.833(3)	.835(5)	.836(5)		.835(10)	.834(12)	.832(4) .817(7) .806(7)	.834(15)
.787(12)	.787(5)	.786(8)	.787(4)		.787(15)	.787(13)	.785(8)	.787(17)

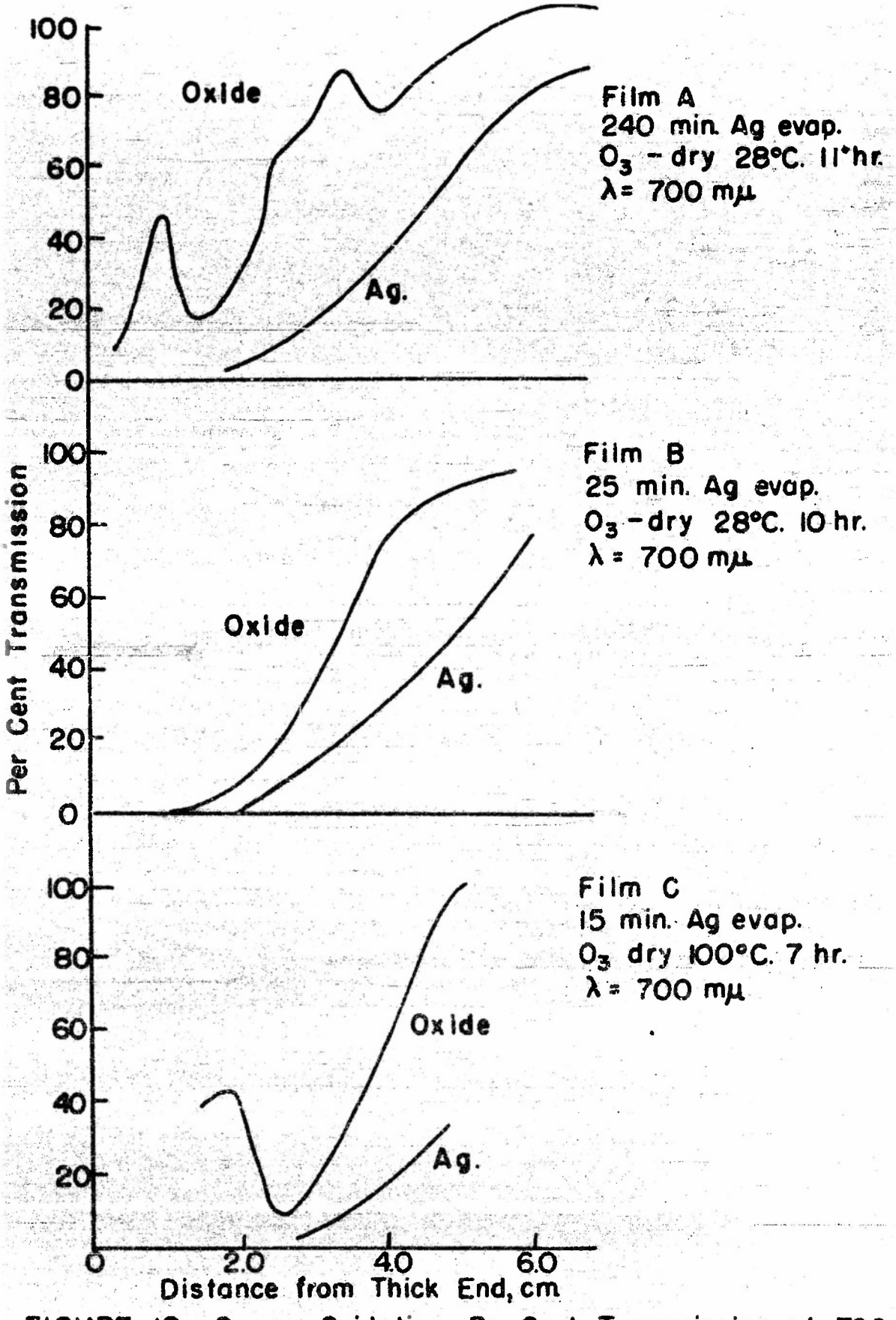

FIGURE 10. Ozone Oxidation Per Cent Transmission at 700 mμ Versus Film Thickness, Films A, B, and C.

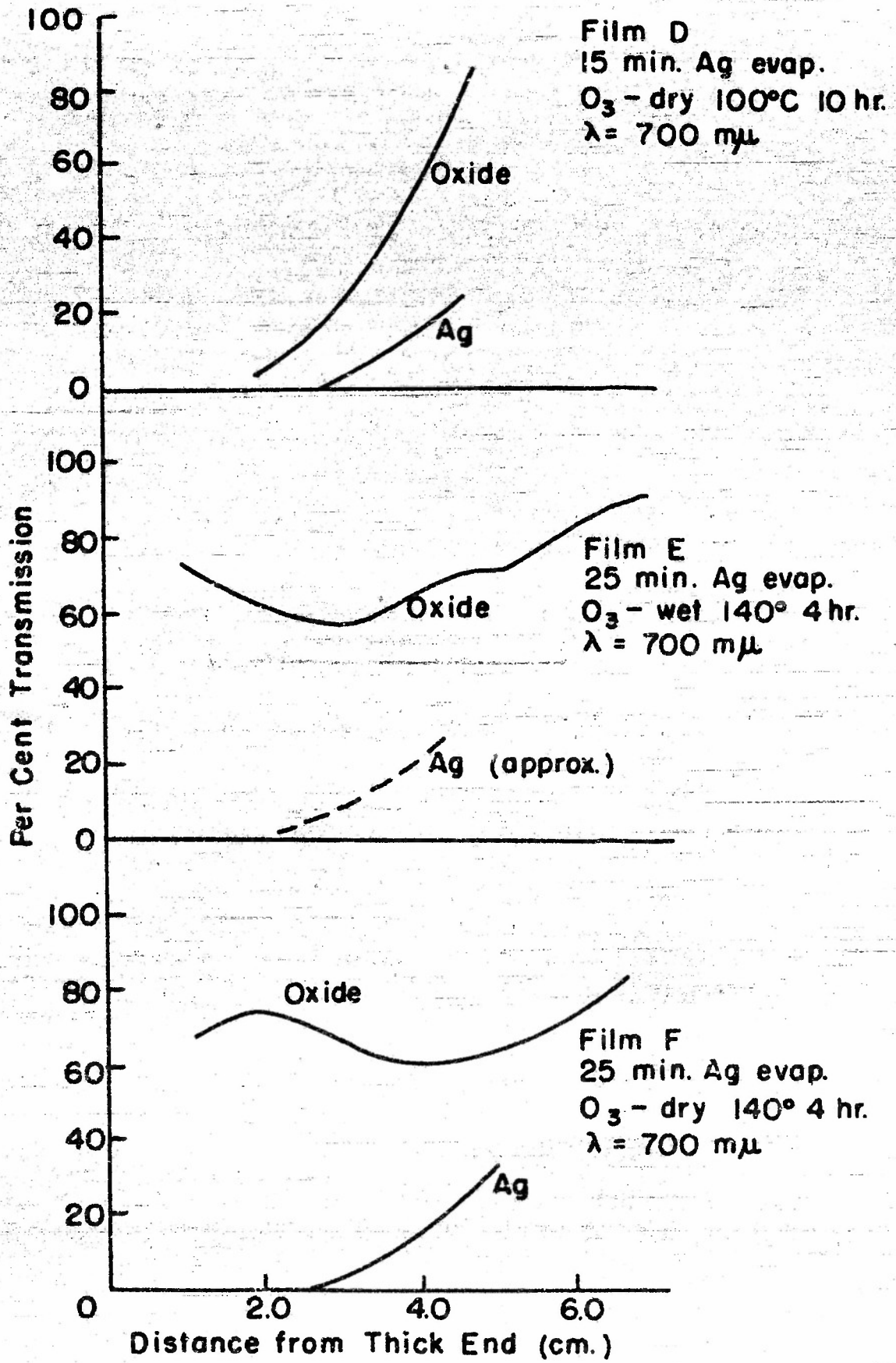

FIGURE 11. Per Cent Transmission at 700 mμ Versus Film Thickness, Films D, E, and F.

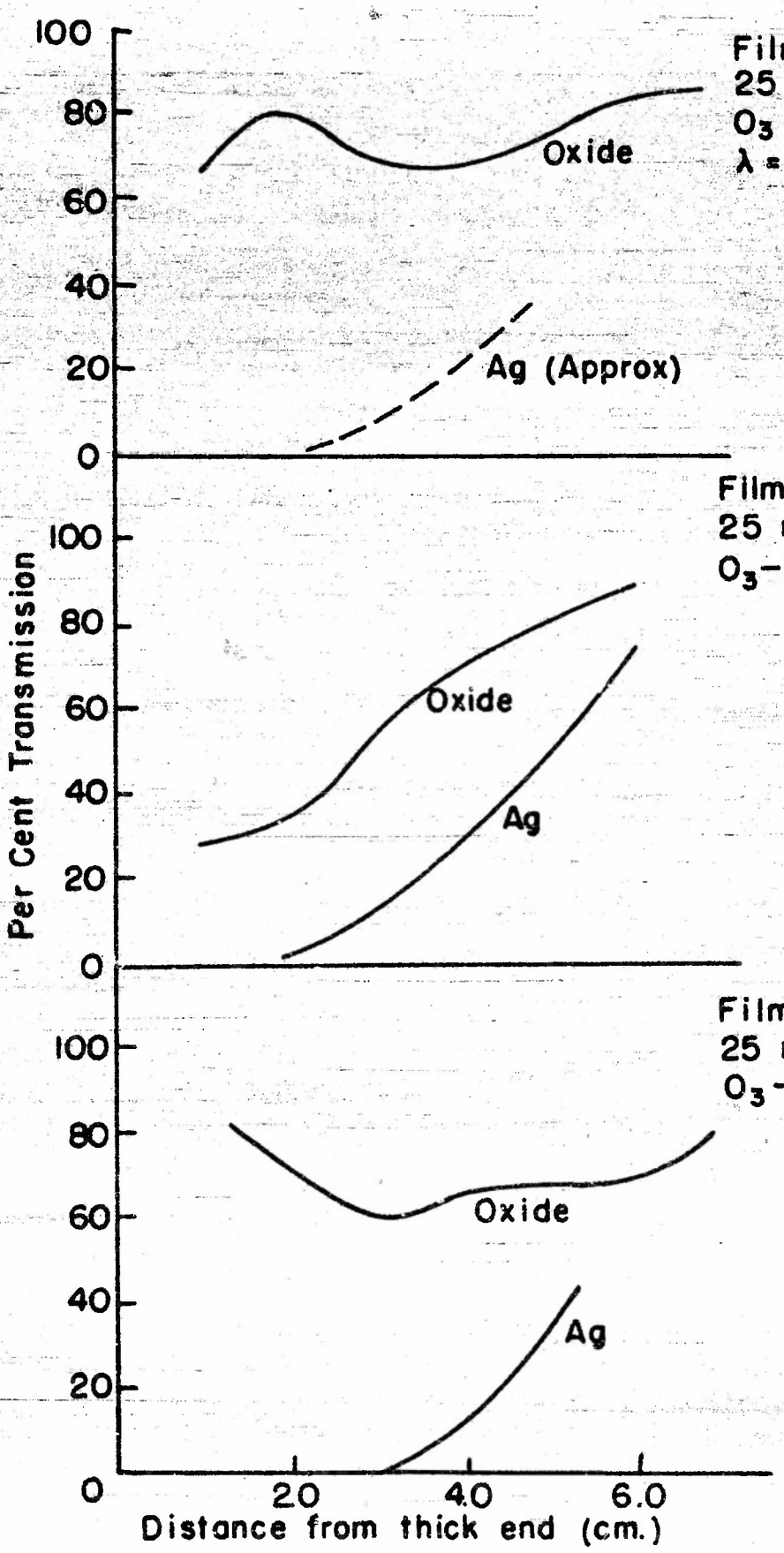

FIGURE 12 Per Cent Transmission at 700 mμ Versus Film Thickness, Films G, H, and I.

place, there is a marked difference in crystallite size and size distribution between films oxidized in ozone and in the glow discharge. In the case of films oxidized by the dc glow discharge, the crystallites are too small to be observable with an optical microscope even at 440X. On the other hand, rather coarse crystallites are produced in ozone oxidation which are easily seen at 440X and in some cases even at 90X. In the second place, in passing from the thin to the thick end of a film of graded thickness which has been oxidized by ozone, a very marked change occurs in the crystallite size and size distribution. Film thickness is, therefore, not a simple variable. Instead, very complex changes in particle size and particle size distribution take place within the same film in passing from a region of one thickness to a region with another thickness. These changes may even be periodic and thus give the appearance of interference fringes on superficial examination. Film A, for example, had such an appearance while film B did not. It is possible that such changes may also occur in films oxidized by dc glow discharge, but since the crystallites produced are too small to be seen in microscopic examination this point has not been established. In the third place, despite the differences in crystallite size, films of the same thickness tend to contain the same solid phases even though the conditions of preparation are different. This is apparently demonstrated by x-ray examination of the ozone oxidized films of equal thickness. The same x-ray lines tend to appear on each film, thus indicating the presence of the same solid phases. The exceptional cases are pointed out in the subsequent discussion. The above statement does not apply to the comparison of the thin and thick sections of the films. Instead, some of the solid phases are not the same in the thin and thick sections of ozone oxidized films. This point is discussed at length in the following text.

In order to illustrate how much two films can differ in appearance and in optical properties without much change in x-ray diffraction pattern it is worthwhile to consider films A and B in more detail. The preparation procedures for these two films differ chiefly in the rate of silver evaporation (see Table XII). Film B was deposited at ten times the rate used for A. Before oxidation no particle structure could be

resolved in microscopic examination at 440X and the transmission curves for the two films are very similar (see Figs. 10A and 10B). After oxidation, however, the two films were very different in appearance. This is indicated to some degree by the transmission curves (Figs. 10A and 10B). These figures do not, however, adequately convey the observed appearances. The films were spectacularly different in appearance. Film A was striated, the striations following lines of equal thickness in the manner expected for interference fringes. Film B had no such striations. The striations in film A are undoubtedly connected with variations in particle size (see Appendix II). Despite the markedly different appearance of the two films there is very little difference in their x-ray powder diffraction patterns (see Tables XIII, XIV, and XV). Where differences in x-ray powder patterns occur the lines are weak enough so that slight differences in line breadth might well account for the presence or absence of the lines. On the whole, the solid phases present seem to be the same in the two cases. This very strongly suggests that the difference between the two films is largely attributable to particle size and size distribution.

The above observations indicate that the optical properties of a film depend markedly on the method of preparation and hence will be difficult to reproduce. On the other hand, the x-ray diffraction data are much less sensitive to variations in the method of preparation although some dependence on film thickness is found, as is pointed out in the next section.

Microscopic examinations of the oxidized films have been made. A detailed description of each is given in Appendix II. For the purposes of the present section it is sufficient to say that large particles tend in general to be formed at the thick end of a film. A granular oxide is formed in the thick section consisting of black grains roughly sperical in shape and separated by voids comparable in size to the particle diameter. Otherwise the particle structure (as revealed by microscopic examination) varies considerably from one film to another (see Appendix II). Some further information on particle size is obtained from x-ray line breadths as discussed in the next section.

4.313 X-ray diffraction results. The oxide x-ray diffraction data for the thick sections of the wedges are given in Table XIII, for the intermedeate sections in Table XIV, and for the thin sections in Table XV. In considering the data it is important to note that lines assigned an intensity of 2 were very weak, while those assigned 1 were just perceptible. Consequently, for these lines there may be an appreciable error in the measurement of the interplanar spacing. In addition, the accuracy of the interplanar spacings and relative intensity estimates decreases rapidly as the line breadth increases, because of the diffuseness of the line as well as the increase in the background scattering. Furthermore, the relative intensities for the lines with interplanar spacings greater than 2.80A may be appreciably low because of the high background blackening present in this region of the diffraction photograph.

Several general characteristics of the ozone oxidation are evident from a visual examination of the films. For a given wedge the increase in the diffraction line breadth with decreasing thickness of the wedge is indicative of decreasing crystallite size. With increasing temperature of oxidation there is a marked increase in the sharpness of the diffraction lines indicating an increase in crystallite size. The photographs for the granular oxide formed in the thick section at high temperatures contain very sharp diffraction lines. This is well illustrated by the fact that the Cu $K\alpha_1$ and $K\alpha_2$ reflections of 0.7850 and 0.7840A are very well resolved.

It was assumed a priori that the silver in the thin section of the film would be most completely oxidized. An examination of the data clearly demonstrates that, for the wedges examined, the reverse was true, since the silver line at $d/n = 2.04$ is relatively more intense in the thin sections than in the thick. The ease of ozone oxidation of the silver decreases with decreasing wedge thickness. The microscopic examination of the wedge J (Table XII), 3-sec silver evaporation, suggests that the ease of silver oxidation by ozone increases with fast rates of silver deposition. X-ray data for this wedge are not available.

Some progress can be made in analysis of the results as follows. Consider first the thick section of film I, Table XIII. Since the line at $d/n = 2.04$ is absent, it follows that metallic silver is absent. Since the line at 2.36 is also missing it follows that

Ag_2O is missing. There is no line at 2.59, which indicates that AgO is absent. The whole x-ray diffraction pattern is therefore due to one or more substances other than the above. If the system is a two-phase mixture, then the strongest lines must be due to the preponderant phase. These lines are 2.74(100), 2.42(35), 2.28(25), 1.71(20), 1.66(30), 1.45(35), 1.39(20), 1.37(20). Here all lines with intensities above 10 and $d/n > 1.25$ have been listed. This argument would in itself be very weak. It is greatly reinforced, however, when we examine the thin sections (Table XV). We first discuss all films of Table XV exsept H. Of the lines listed above, 2.42, 2.28, 1.66, 1.39 and 1.37 are either absent or appear with very low intensities. Lines at 2.74 and 1.45 do, however, appear. That at 1.45 can be accounted for since the 2.04 line is present, which indicates metallic silver. But metallic silver also has a line at 1.45 whose intensity is equal to that at 2.04. This is precisely the situation in Table XV and hence the 1.45 line in Table XV is due to silver whereas in Table XIII it was due to something else. This leaves the 2.74 line to be accounted for. This cannot be due to Ag_2O because this substance has a strong line at 1.66, but the films of Table XV have very weak lines, or none at all, in this position. This line cannot be due to AgO because there is no line at 2.59. The closest are at 2.61 - 2.62 and even these are in general weak. The line at 2.74 in Table XV must therefore be due to another phase. These results tend strongly to confirm the view that all of the strong lines for film I of Table XIII are due to a single solid phase, which we may designate as the Ψ_1 phase, and this solid possesses one diffraction line at 1.45 which coincides with a silver line and another line at 2.74 which coincides with a line from a second solid phase, Ψ_2, which occurs in the thin sections of the films. Further confirmation for this view is obtained by considering film H of Table XV. This is the only film which contains a line at 2.42 or anywhere in the vicinity. If, as seems certain, this corresponds to the 2.41 line discussed above, then the same phase (Ψ_1) as in Table XIII is indicated and this line should be accompanied by others at 2.74, 2.28, 1.71, 1.66, 1.45, 1.39 and 1.37. Inspection of column H shows that this is indeed true and the relative intensities agree with those listed earlier. This constitutes very strong evidence in favor of the initial hypothesis.

The existance of a solid phase ψ_1, which gives rise to a group of diffraction lines, with the 2.41 line particularly prominent, seems to be firmly established and these lines are the most intense in films E, F, G, H, I of Table XIII. There remains the question of whether the weak lines at 3.36, 3.20, 3.00 etc. arise from the same phase ψ_1 or from a second phase ψ_2. The latter alternative, a new solid phase ψ_2, seems to be the correct one. This is indicated by the fact that the lines 3.36, 3.20, 3.00 etc. also appear in the thin sections of the films (Table XV except film H) even though the absence of a line at 2.41 indicates that ψ_1 is missing. In fact, the majority of the diffraction lines of Table XV (except H) can be accounted for on the basis of a solid phase ψ_2 and metallic silver.

As previously pointed out, Ag_2O and AgO are either absent or present in small proportion in most of the films of Table XV. Assuming only ψ_2 and silver to be present, the lines characteristic of ψ_2 can be obtained and rough intensities assigned. This follows because the intensities of the silver lines relative to 2.04 are known (Table VI) and the silver contributions can be subtracted out. When this is done and the relative intensities referred to the 2.74 line as 100 are calculated, the results of Table XVI are obtained. The ψ_1 lines are also included in Table XVI for comparison. The intensities for the ψ_1 lines are obtained by considering films E, F, G, H, I of Table XIII and are rough estimates. There is considerable doubt as to the relative intensities of the 2.51, 1.97, 1.67 and 1.60 lines of the ψ_2 phase. The results can be considered little better than rough guesses. The 2.36 line intensity in Table XV is somewhat peculiar and the results are difficult to interpret. because the films contain silver, which has a line at 2.36. In samples F, G, I the 2.36 line seems due almost entirely to silver, judging from its intensity relative to the silver lines at 2.04, 1.45 and 1.25. This is not the case, however, for films A, B, D, where the 2.36 line is much too intense to be due to silver. There seems at first sight a possibility that samples A, B, D (Table XV) may contain Ag_2O, which has an intense line at 2.36, but further consideration makes this seem unlikely for the following reason. Ag_2O also has a line at 1.42 which does not appear on films A, B, D. The line broadening in thin films, previously mentioned,

TABLE XVI. DIFFRACTION LINES FOR SOLID PHASES φ_1 AND φ_2

φ_1		φ_2	
d/n	I	d/n	I
2.74	(100)	3.36	(40)
2.41	(40)	3.20	(40)
2.27	(25)	3.02	(10)
1.71	(20)	2.74	(100)
1.66	(30)	2.51	(20)
1.45	(30)	2.36	(10-100)?
1.39	(30)	1.97	(10)
1.37	(30)	1.67	(5)
		1.60	(5)

makes it difficult to resolve a line at 1.42 from the silver line at 1.45, but resolution must be possible in film D since two lines at 1.21 and 1.23 are resolved in this case even though they are separated less than 1.42 and 1.45 and, moreover, they are expected to be broader. Under these conditions it seems unlikely that the variable intensity of the 2.36 line is due to varying amounts of Ag_2O. The variation is at present unexplained. We have, however, included the 2.36 line in Table XVI and indicated the range of intensity variation after correction for the contribution of metallic silver. A line at d/n = 2.61 occurs in several cases. The intensity of this line is so variable with respect to the remaining lines of Ψ_2 in all of the Tables XIII, XIV, XV that it has not been included in Table XVI as a Ψ_2 line. Since only one line is involved we cannot tell whether a solid phase is indicated or whether something else (i.e. solid solution formation) might account for its behavior. The discrepancy between 2.61 and the nearest AgO line at 2.59 is consistently obtained and seems too large to indicate the presence of AgO, especially since the remaining line positions and intensities are not in good agreement with those to be expected for AgO.

In summary it seems to be established that a solid characterized by the Ψ_2 lines of Table XVI exists, although we cannot be sure that the lines are characteristic of a single phase. The lines characteristic of the Ψ_1 phase seem better established.

One item remains which is worth mentioning. It was thought at one time that the thick sections of the films oxidized at the highest temperatures (films E, F, G, H, I of Table XIII) might correspond to a pure phase which was the most highly oxidized silver oxide obtainable by these methods. If this were the case, then the weak lines at 3.36, 3.21 and 3.02 might be considered as superlattice lines of phase Ψ_1. In order, however, to account for the absence of the Ψ_1 lines in the thin film sections in this way it is necessary to suppose that the Ψ_1 and Ψ_2 phases have three lines which coincide at these positions, and this seems to be pushing coincidence a bit too far. The interpretation of the preceeding paragraphs seems to be more probable and is tentatively adopted for this report. Further

information which bears on the assigment of these lines is discussed in Sections 4.3 and 4.4.

Having now obtained some information as to the x-ray diffraction lines which characterize the various solid phases, it is worthwhile to return briefly to the consideration of the results. It is useful to discuss the thick and thin sections separately.

Consider first the thick sections. It has already been pointed out that metallic silver is either absent or present in very small proportion as indicated by the absence or weakness of the 2.04 line. The oxide Ag_2O is also present in only trace amounts in films E, F, G, H, I. This is indicated by the low intensity of the 2.36 line in these films. It is further confirmed by the low intensity of the 1.42 line. In films oxidized at the lower temperatures (A, B, C, D), only trace amounts of Ag_2O are present in B and C as indicated by the very weak line at 1.42. Films A and D contain more Ag_2O as indicated by higher intensity of the 1.42 line. To summarize, film A contains an amount of Ag_2O comparable with that obtained in the oxidation of massive silver, D contains less Ag_2O, and all other films contain very much less Ag_2O. Both ψ_1 and ψ_2 are present in all films, ψ_1 being predominant. The ratio of ψ_1 to ψ_2 is highest in B, C, E, F, G, H, I.

Consider next the thin sections. Silver is present in all films except H, as indicated by a diffraction line at 2.04. From the intensity of the 2.04 line it appears that films F, G, I contain the largest amounts of silver, films A, B, C, D contain roughly half as much, film E contains only a trace of silver, while film H contains too little for the 2.04 line to be detectable. The proportion of Ag_2O must be small since this substance has a diffraction line at 1.66 while the thin sections of the films have either a very weak line in this position or none at all. The 1.42 line is absent in all cases. The latter observation would be conclusive except for one factor. X-ray lines for the thin sections tend to be broader than for the thick sections, and the question arises as to whether resolution is sufficient to resolve the silver line at 1.45 from the oxide line at 1.42. In films C, D, and H the resolution is certainly high enough because in C the lines at 2.04 and 2.07 are resolved, in D 1.23

and 1.21 are resolved while in H 1.39 and 1.37 are resolved. It seems likely that resolution is sufficient in all cases, although conclusive evidence is not available from the diffraction spectra themselves. It seems justifiable to conclude that Ag_2O, if present, is in too small proportion to be detected. The diffraction lines at 1.66 must be due to some other substance. It has previously been pointed out that phase ψ_2 is present in the thin sections of all films while film H is unique in that ψ_1 is present only in this film.

One salient fact which arises from the foregoing experiments is the decisive influence of silver film thickness. By far the most significant and consistent differences in chemical composition arise between the thick and the thin sections of the films. Other variations in processing conditions failed to produce much change in the nature of the solid phases (except for film H which seems more like an accident than a consequence of variation in processing). These remarks apply only to the chemical composition of the films. The particle size (as determined by microscopic examination) and optical properties, on the other hand, are quite sensitive to changes in processing conditions, including film thickness.

In speaking of "thickness" some qualification seems necessary. Many experiments by other investigators have shown that silver films containing different amounts of silver per unit area may differ in other ways than in linear extension. Microstructures of very different kinds frequently arise. In passing from the thick to the thin section of a film of graded thickness the microstructure of the film undoubtedly changes, and this alteration in microstructure may be, in fact, the real reason for the difference in behavior. Weight per unit area might well be a more useful quantity than "thickness" for characterizing the films, although we have not made use of this terminology.

It is now of interest to contrast the oxidation products obtained for evaporated silver films with those obtained in the oxidation of massive silver (Section 4.2). In the oxidation of massive silver (silver wires) diffraction lines due to Ag, Ag_2O, ψ_2, ψ_1, are all obtained and it has been established that the order of occurance of the solid phases is

that given, except that the order of Ψ_2, Ψ_1, is unknown. Among the oxidation products of the thick sections of evaporated silver films Ag is missing and Ag_2O is present only in trace amounts except in films A and D. The thin sections of evaporated silver films contain Ag and Ψ_2 after oxidation except for film H, which contains Ψ_1, Ψ_2.

The final problem is to find the reasons for the rather unusual behavior described above. In this undertaking the results obtained by Sennet and Scott[5] in the study of silver films is of considerable assistance. In order to establish a connection between our experiments and theirs we consider the film thickness involved. To obtain the thicknesses we first consider the percentage transmission for each of the thin sections of the silver films before oxidation. The x-ray diffraction data for the oxidation products obtained from these sections are given in Table XV. Using the transmission data, the thickness of each thin section is estimated from the data of Sennet and Scott[5], allowance being made for evaporation time. These estimates, which are only approximate, appear in column five of Table XIIA. Then knowing the positions from which the various samples were taken and using the geometrical dimensions which prevailed during evaporation (Section 2), the thickness values for the thick and intermediate regions were computed. These results are given in columns three and four of Table XIIA. These results, although approximate, are sufficient for our purposes. Note that no sample was taken from the thick section of sample F. The diffraction pattern for this sample is the same in both Tables XIII and XIV. We now proceed to consider some of the results of Sennet and Scott[5] in more detail.

It was observed by Sennet and Scott that below a certain thickness, the "critical thickness", evaporated silver films consisted of very small particles (sometimes only a few hundreths of a micron in diameter) which were not in contact. That is, the particles rested on the substrate in relative isolation. At the critical thickness they touch each other and above that thickness the particles merge, although perceptible voids remain in some cases up to twice the critical thickness or beyond. Ultimately, of course, the films acquire a solid appearance. Of the films in Table XIIA six were evaporated in 25 minutes, two in 15 minutes, and one in 240 minutes.

TABLE XIIA. APPROXIMATE SILVER FILM THICKNESSES OF THE X-RAY SAMPLE REGIONS. Ozone Oxidation.

Film	Evap. Time (Min.)	Thickness (A) of Various Sections		
		Thick	Intermediate	Thin
A	240	930	270	130
B	25	1200	210	90
C	15	1500	190	90
D	15	2300	680	170
E	25	1500	260	110
F	25	—	350	60
G	25	1750	300	70
H	25	1200	200	70
I	25	530	125	50

A series of photographs is given in Sennet and Scott's paper of films evaporated in 20 minutes. From an inspection of those photographs and a consideration of the position of maximum radiation absorption, it seems reasonable to place the critical thickness at about 200A for such films. This is only a rough estimate. At 175A the particles are still well separated; at 220A some merging, usually in pairs, is evident, although close contact is certainly not established. No data are given for films evaporated in 240 minutes. Judging, however, from photographs given for a 75 minute evaporation and taking account of the trend, it seems likely that contact is not established below 400A. These estimates are sufficient for our present purposes.

Now considering the film thicknesses given in Table XIIA it becomes clear at once that all of the thin sections have thicknesses below the critical so that we are dealing with very small silver grains which are not in contact with each other. Residual silver is found in these thin sections (except film H), and hence it is established that large numbers of small, isolated, silver grains are hard to oxidize. The thick sections, on the other hand, considerably exceed the critical value in thickness, and these films contain no silver except for film I which has a trace. This establishes that closepacked small silver grains are easy to oxidize. In the intermediate sections films A and I have thicknesses less than the critical, and both contain silver. Films D, F, G, on the other hand, have thicknesses definitely greater than the critical. D and F have no detectable amount of silver while G has a barely perceptible amount (the line at d/n = 2.04 has intensity 1). Films B, C, and H are so close to the critical thickness that we cannot classify them. One contains silver and the other two do not. The correlation obtained between isolation of silver grains and the appearance of residual silver is very good indeed. There can be but little doubt that failure to oxidize silver follows from the fact that the grains are not in contact. When contact is established, oxidation is complete.

These observations very strongly suggest that nucleation is an important step in the ozone oxidation of silver. If it is necessary to form a nucleus from which a silver oxide crystal can grow before oxidation

can occur, and if the nucleation rate is low, then the above observations become understandable at once. In a film consisting of a very large number of small silver grains isolated from each other, at least one nucleus must develop on each grain before oxidation can take place. If the nucleation rate is low, then on some grains nuclei do not form soon enough and they remain unoxidized. Since the grains are so small, about 0.01 micron or 100A in diameter, oxidation proceeds rapidly, once a nucleus is formed, because there is not enough material to form a thick oxide layer to limit oxidation rate by diffusion. In thicker films, however, the grains, although small, are in close contact. Fewer nuclei are required because a crystal growing from a nucleus can spread to adjacent grains and grow indefinitely although perhaps with numerous imperfections. It is therefore plausible that a thick film can be oxidized completely while a thin film is not, because the oxidation rate for the latter is limited by the nucleation rate whereas the former is limited only by the rate of diffusion through the intervening oxide layer which forms. Further evidence which supports the nucleation hypothesis is the observation (Section 4.2) that ozone oxidation of silver wires frequently starts at a point from which the oxide grows over a considerable area before halting. Oxide then forms again at a new point and grows until ultimately the wire is covered. This strongly suggests that a nucleus is formed at each such point. It suggests in addition that the nucleation rate is low, for if many nuclei formed simultaneously and were uniformly distributed, the oxidation would seem uniform.

It seems desirable at this point to discuss in somewhat more detail what is meant by a nucleus and to differentiate between two types of nucleation. It has been emphasized previously that x-ray diffraction by powder samples scraped from thin films leads to a line spectrum. This proves that the oxidation products have an atomic arrangement which is well enough ordered to form a diffraction grating. A nucleus constitutes a small group of atoms sufficiently well ordered to serve as the center from which a crystal can grow. The nucleus is not necessarily perfectly ordered. According to recent theories of growth rates of crystals, slight imperfections (dislocations) increase the growth rate. Moreover, crystals of a foreign substance may serve as nuclei even though the crystal structure differs from

that of the solid to be formed provided only that it conforms closely enough so as to intiate crystallization. It is useful to distinguish between nucleation which is spontaneous (i.e. the chance formation of a sufficiently well-ordered arrangement of a few atoms to induce crystal growth) and that which is promoted by the presence of a template of some kind which makes particularly easy the first formation of a regularly ordered atomic arrangement of silver and oxygen atoms characteristic of the solid oxide under consideration. Such a template might be provided by a foreign crystal as discussed above, or by one or more crystal faces of a silver grain whose atomic arrangement conforms to that of the oxide, or it might be provided by a disordered or distorted silver grain. No definite conclusions concerning the mechanism of nucleation can be given at present. In the above discussion we have in mind an element of chance in both cases. A nucleus is regarded as formed only when the subsequent growth becomes certain. A template may increase the chance of forming a nucleus without itself being a nucleus because the mere presence of the template does not assure that crystal growth occurs from that instant onward but only that at some subsequent time crystal growth will be initiated and will proceed thereafter, the probability of iniation being greater than in the absence of the template. Activation of the oxidizing agent as in a discharge, might well increase the rate of spontaneous nucleation to such a degree that nucleation was no longer the rate determining step. This is a matter to be considered further (Section 4.33) in connection with the glow discharge oxidation. If nucleation is promoted by a template, then the nucleation rate might well be sensitive to small amounts of impurity which could either increase the rate by providing new or more favorable templates, or reduce the rate by unfavorably altering the existing templates.

The above discussion should make clear what we mean by a nucleus and also why the hypothesis of nucleation has been tentatively adopted. There still remains, however, the problem of accounting for the oxidation products. It has been pointed out that Ψ_2 and Ag are the solid phases found in the thin sections except for film H. Phase Ψ_1 is found only in film H. On the other hand, both Ψ_1 and Ψ_2 occur in the thick

sections along with traces of Ag_2O. Silver is usually absent from the thick sections. Since ψ_1 is found in one section of the film, it follows that ozone is a strong enough oxidizing agent to produce the phase. Absence of silver is not essential to ψ_1 production since ψ_1 is produced in the oxidation of silver wire (Section 4.2) and excess silver always remains in those experiments. On examining Tables XIII, XIV, XV we find a consistent tendency for ψ_1 to be absent from those samples which contain the highest proportion of silver and to be present in those samples which have the lowest proportion of silver. If our previous hypothesis concerning nucleation is correct, then the presence of unoxidized silver in a film indicates that silver particles were not in contact before oxidation. This immediately suggests that ψ_2 grains are still isolated to some degree after oxidation, and the failure to oxidize further to ψ_1 is again due to the slow nucleation rate in the oxidation of ψ_2 to ψ_1. On the other hand, oxidation is faster in those sections of the films for which packing is closer and spreading to adjacent grains is possible. The fact that high proportions of ψ_1 tend to accompany low proportions of residual silver then arises because low silver content indicates, in these particular experiments, close packing of grains and the required nucleation rate is thereby reduced. In silver wires, on the other hand, grains are always close packed, and silver content measures only the extent of oxidation and does not serve as an indicator of grain contact. Unfortunately, the above view of grain isolation is not well supported by microscopic examination of oxidized films. At 400X with an optical microscope particles are observed, and these particles must be of considerably larger size than 0.1 micron. X-ray investigation, on the other hand, reveals line broadening such as would be expected of particles smaller than are observed microscopically so that the observed particles are probably clusters. We do not know how extensive the clustering is and hence the above hypothesis is not definitely disproven. On the other hand neither is it established. The question must remain open for the present since no further experimental results are at hand to test it, and neither is any plausible alternative explanation of the results.

The distribution of Ag_2O in the products is also

of interest. This substance tends to appear in higher proportion in the thick sections. Even there the proportion is small in most cases. The oxidation of silver wire showed that partial, but deep, oxidations in which the supply of silver is not exhausted lead to the formation of a layer of Ag_2O between unoxidized silver and the higher oxides ψ_1, ψ_2. The presumption is strong that unoxidized silver provides a source of silver atoms which diffuse through the layer at a sufficient rate to react with excess oxidizing agent and thus prevent the further oxidation of Ag_2O. It is a known fact that ozone can oxidize monovalent silver to the divalent or trivalent state (Section 4.4). When, therefore, the supply of silver is exhausted, further oxidation of Ag_2O to ψ_1, ψ_2 is to be expected. In the thin sections of silver films the small ($\sim$100A) silver particles oxidize rapidly to completion once a nucleus is formed. Hence Ag_2O, if formed at all, is rapidly oxidized further. In the thick sections the supply of silver is greater so that, even though the supply is exhausted, complete oxidation of Ag_2O does not take place within the time of experiment. In the oxidation of a large silver grain it seems highly likely that at some intermediate stage the grain consists of a core of silver with Ag_2O surrounding it and an additional layer of ψ_1 or ψ_2 (or both) surrounding the whole. Whether even very small grains pass through such a stage, is unknown. No definite indication of Ag_2O has been found in the study of films, thin enough to consist of isolated grains, oxidized by ozone, rf, or glow discharge. To summarize, the low Ag_2O content of oxidized thick silver films in comparison to partially oxidized wire is due to exhaustion of the silver supply in the former case but not in the latter. In the very thin sections of silver films the coexistence of ψ_2 and Ag without Ag_2O is possible because the intimate contact necessary for the diffusion of silver is not established.

4.32. RF oxidation of evaporated silver films.

As a result of the difficulties encountered in oxidizing silver films from 50 to 90% transmission during the preparation of semitransparent cathodes a special tube, PT27, was constructed. At the time the experiment was performed we were under the erroneous

impression that failure to reach 90% transmission was due to incomplete oxidation. Because of this impression an effort was made to oxidize the film as completely as possible. The x-ray diffraction results are therefore of some interest as an example of a heavily oxidized silver film.

In tube PT27 the cathode consisted of a 1x3inch microscope slide with a chemically deposited platinum film boundary surface and an evaporated silver wedge deposited over the surface. The slide was mounted in nickel clips which were attached to the nickel-tungsten lead-in wire through the pyrex tube envelope. The anode was a nickel-tungsten lead-in wire.

The tube was sealed to the vacuum system and outgassed at 250-280°C for 1.5 hours. After introducing oxygen to $P_{O_2} = 0.861$ mm Hg, the slide was repeatedly oxidized with the glow discharge produced from a repeatedly charged high-voltage condenser. During this high-voltage glow oxidation the film appeared to be oxidizing only at discrete points on the surface rather than uniformly over the surface. The final oxygen pressure was 0.833 mm Hg with only a small change having occurred between the 150th and 350th condenser discharge. An aluminum foil sleeve was then placed around the central section of the tube and was connected to the rf oscillator. The first rf discharge reduced the pressure from 0.833 to 0.650 mm Hg, the second from 0.650 to 0,605 mm Hg, and the third from 0.605 to 0.564 mm Hg. During this process there was an increase in the transmission of the surface, the 39% region increasing to approximately 60% transmission. The tube was then sealed off the vacuum system, the tube envelope fractured and the slide removed. The film contained approximately 26 micrograms of oxygen per square centimeter.

Microscopic examination of the slide at 15, 45, 90, and 440X showed a distinct variation in the structure of the oxide film along the wedge. In the 0-1 region the surface consisted of a very nodular black oxide film resting on a substrate of unoxidized silver. In the region 1-2 the oxide was aggregated and the transmission was greater than in the 2-3 or 1-2 region. From 2-3 the film changed to a semi-transparent continuous film of a blue-green color, which changed to pale red at 4, and a yellow-pink at 5.

Accompanying the color changes there is a continuous increase in the transmittance of the film. By reflected light (air-oxide interface) the 5 cm region was red, changed to blue at 4, yellow at 3, to blue at 2, and black between 2 and 0. Microscopic examination of the oxide film between 2 and 5 at 440X showed a continuous film with occasional islands of aggregated black oxide.

To establish the composition of the film, x-ray powder samples of the oxide were removed from the 2.5 - 3.5 region, and the 4.0 - 5.0 region. The diffraction data are presented in Table XVII. From the diffraction data it is apparent that the silver was practically completely oxidized in the region from 2.5 through 5.0. Thus it was established that, in the early experiments on the preparation of transparent cathodes, the silver was practically completely oxidized and the experimental difficulties encountered in oxidizing to 90% transmission could not be due to the incomplete oxidation of the silver. In Table XVII the interplanar spacing data for the AgO oxide and the ozone granular oxide of the thick section of film E (Table XIII) are compared with the data for PT27. It is obvious that the line positions and intensities for film E and PT27 are in close agreement. The same solid phases are obviously present in the two cases. It must be noted, however, that film E is not typical of silver films oxidized at high temperatures. Inspection of Table XIII shows that the 2.62 line is much weaker in films F, G, H, I than in E. We have already concluded that F, G, H, I contain two phases, φ_1 and φ_2, the former being present in much greater proportion. This suggests that E contains still another phase as indicated by the strong 2.62 line. There is a further possibility that this additional phase is AgO. However, the line positions are not in as good agreement as we believe the data justify, especially in view of the sharp x-ray lines involved. Because only one x-ray diffraction line is involved we prefer, for the present, to leave open both of these questions. That is, we do not claim that an additional phase is conclusively established nor that the questionable phase is AgO. We do claim, however, that the products of rf oxidation are the same as for ozone oxidation of film E, and are generally similar to those obtained in the ozone

TABLE XVII. INTERPLANAR SPACING DATA FOR RF OXIDE, TUBE PT27

The d/n values are in angstroms, followed by relative intensity (I)

PT27 Region 2-3 d/n(I)	PT27 Region 3-4 d/n(I)	AgO d/n(I)	Sample E Table XIII d/n(I)
3.35(25)	3.36(25)		3.36(12)
3.19(25)	3.18(25)		3.19(12)
3.06(10)	3.05(10)		3.02(2)
			2.87(2)
2.77(100)	2.76(100)	2.74(100)	2.75(100)
2.61(25)	2.63(30)	2.59(27)	2.62(20)
2.50(3)	2.50(5)		2.51(6)
2.41(50)	2.42(40)	2.38(83)	2.41(75)
			2.34(2)
2.28(25)	2.28(30)	2.25(33)	2.28(35)
			2.12(1)
1.96(1)			
1.87(1)			1.84(1)
1.74(10)	1.74(10)	1.73(15)	1.74(4)
1.70(20)			1.70(20)
		1.69(50)	
1.68(15)	1.68(8)	1.66(17)	1.66(25)
1.62(20)	1.62(15)	1.61(35)	1.62(12)
			1.52(1)
1.48(15)	1.48(10)	1.47(31)	1.47(6)
1.45(20)	1.45(15)	1.45(58)	1.45(40
		1.42(14)	
1.41(15)	1.41(10)	1.41(14)	1.41(2)
1.39(20)	1.39(15)	1.38(58)	1.39(20)
1.35(5)	1.35(2)	1.35(12)	1.37(12)
			1.35(1)
1.31(10)	1.31(1)	1.31(17)	1.31(4)
1.24(1)			
1.21(10)	1.21(5)	1.20(23)	1.21(8)
			1.18(1)

TABLE XVII. (Continued)

PT 27 Region 2-3 d/n(I)	PT 27 Region 3-4 d/n(I)	AgO d/n(I)	Sample E Table XII d/n(I)
1.14(1)	1.14(1)	1.14(5)	1.14(2)
1.12(2)	1.12(2)	1.12(17)	1.12(20)
1.10(10)	1.10(4)	1.10(31)	1.10(10)
1.09(3)		1.09(15)	1.08(12)
1.07(8)	1.07(4)	1.06(25)	1.07(12)
1.05(8)	1.05(1)	1.05(12)	1.05(2)
1.04(3)		1.04(12)	1.04(2)
1.02(8)	1.02(1)	1.01(14)	1.03(4)
		.997(6)	1.00(2)
		.987(10)	.990(2)
		.980(5)	.979(10)
		.971(1)	
.950(1)	.953(2)	.953(4)	.950(3)
.945(5)		.941(29)	
.932(5)	.931(3)	.929(29)	.929(12)
		.923(10)	
.914(2)	.914(1)	.910(10)	.913(5)
		.896(8)	.896(1)
.884(1)		.883(21)	.833(5)
		.872(5)	
		.866(6)	
			.856(1)
		.849(23	
		.838(12)	.842(1)
		.830(15)	.883(5)
.821(2)		.821(31)	
			.816(6)
		.814(4)	
.812(2)		.811(31)	
		.810(13)	
			.805(8)
		.804(50)	

oxidation of films F, G, H, I except for a possible additional phase. Both φ_1 and φ_2 are certainly present in the rf oxidized silver film.

A microscopic examination of a heavily rf oxidized silver film of graded thickness has also been made. The oxidized film was striated in a manner suggestive, on superficial examination, of interference colors. These colors are probably due, however, to the distribution of small particles in the film (see Appendix III).

4.33. Direct current glow discharge oxidation of silver wedges.

For the glow-discharge oxidation study the evaporated silver wedge tube design discussed in Section 2.1 was used. With this tube design it is possible to deposit a silver wedge of varying thickness. Hence the effect of varying silver thickness on the oxidation could be studied.

A series of six wedge-type tubes were prepared in which the change in the percentage transmission (S-4 surface and white light) of the 50% transmission region during the glow discharge was investigated. The data on the tube preparation are given in Table XVIII. In the oxidation of tube 1927-14-1 the discharge was maintained for 6 minutes in order to verify that, with 360 volts across the tube and 8-10 ma current, the cathode was completely covered by the glow discharge. When tube 1927-15-2 was oxidized the transmission appeared to pass through a maximum and consequently the remainder of the oxidations were performed by just flashing the high voltage on and off using 1 to 2 second discharges. The percent transmission versus total discharge time for the last four tubes prepared is shown in Fig. 14. The results for tube 1927-15-3 have already been used in Section 3.5 to illustrate the dependence of light transmission on extent of oxidation. The x-ray diffraction data for the samples indicated in Table XVIII are presented in Table XIX.

The transmission curves in Fig. 14 clearly demonstrate that in oxidation the transmission of the

TABLE XVIII. GLOW DISCHARGE OXIDATION OF SILVER WEDGES

Tube No.	Ag Evap. Time (sec)	P_{O_2} Init. (mm)	P_{O_2} Final (mm)	Ox. Time (sec)	No. of Discharges	Init. %T	Final %T	X-ray Photo	X-ray Sample Ag %T
1927-14-1	300	0.878	0.718	360	1	50	77	1760-94-1	~40-60
								-2	>60
								-3	~20
1927-15-2	30	0.858	0.792	~30	2	50	69	1760-94-4	40-60
								-5	>60
								-6	6-40
1927-15-3	30	0.610	0.573	~20	10	50	67	---	
1927-16-4	15	0.860	0.846	14.6	7	50	72	1760-94-7	40-60
								-8	10-40
								-9	60-90
1927-16-5	15	0.660	---	9.9	9	53	90	1760-94-10	40-60
								-11	10-40
								-12	60-90
1927-16-6	15	0.511	---	16.7	5	43	91	---	

Tubes initially degassed 1 hour at 300°C.
P final $<1 \times 10^{-6}$ mm Hg.
Oxidations performed using 360 volts across the tube and an 8-10 ma tube current.

TABLE XIX. INTERPLANAR SPACING DATA FOR HIGH VOLTAGE DC GLOW DISCHARGE OXIDIZED SILVER WEDGES

The d/n values are in angstroms, followed by relative intensity (I

Tube 1927-14-1			Tube 1927-15-1		
40-60%T Black d/n(I)	>60%T Black d/n(I)	~20%T Black d/n(I)	40-60%T Black d/n(I)	>60%T Black d/n(I)	6-40%T Black d/n(I)
3.40(40)	3.38(30)	3.39(30)	3.38(30)	3.40(30)	3.40(25)
3.21(50)	3.21(50)	3.20(40)	3.21(50)	3.20(40)	3.21(40)
3.01(5)	2.99(5)	2.98(5)	2.99(10)	2.91(10)	3.00(5)
2.77(100)	2.78(100)	2.76(100)	2.76(100)	2.76(100)	2.76(100)
2.67(1)		2.64(5)			
2.51(5)	2.53(10)	2.51(10)	2.53(2)	2.54(15)	2.51(10)
		2.43(4)			
2.36(40)	2.36(40)	2.37(10)	2.36(8)	2.36(10)	2.36(40)
2.22(10)	2.21(5)	2.23(5)	2.20(5)		2.24(2)
				2.11(12)	
2.05(8)	2.04(4)	2.05(5)	2.08(5)		2.05(10)
1.96(45)	1.97(50)	1.97(20)	1.96(25)	1.96(25)	1.97(20)
	1.84(1)		1.81(10)	1.82(4)	
	1.74(1)				
1.68(20)	1.68(20)	1.68(10)	1.67(15).	1.68(6)	1.68(8)
1.60(20)	1.61(20)	1.61(10)	1.60(10)	1.60(5)	1.61(3)
1.45(20)	1.45(8)	1.45(12)		1.44(4)	1.45(20)
1.39(8)	1.39(5)	1.39(5)		1.38(3)	1.37(3)
		1.28(4)			1.28(1)
1.24(15)	1.24(15)		1.24(10)	1.24(10)	1.24(25)
1.226(5)	1.228(5)	1.23(15)			
1.19(8)		1.181(4)			1.19(8)
1.14(10)	1.14(10)	1.13(5)	Broad Lines	1.136(8)	1.14(3)
	1.07(2)				
	.981(2)				
					.939(5)
	.924(1)				
.912(2)		.915(5)			.916(6)
	.879(1)				
.836(2)	.838(1)				.835(4)
.786(1)					.786(4)

TABLE XIX. (Continued)

Tube 1927-16-4			Tube 1927-16-5		
40-60%T Yellow d/n(I)	10-40%T Black d/n(I)	>60%T Black d/n(I)	40-60%T Yellow d/n(I)	10-40%T Yellow d/n(I)	>60%T Yellow d/n(I)
3.43(40)	3.39(25)	3.39(30)	3.42(30)	3.39(30)	3.41(20)
3.21(40)	3.21(25)	3.20(30)	3.21(30)	3.19(40)	3.20(40)
2.98(5)	2.96(5)	2.96(8)	3.01(5)	3.01(5)	3.02(5)
2.75(80)	2.76(100)	2.75(100)	2.76(100)	2.75(80)	2.28(100)
				2.68(10)	2.57(1)
	2.48(10)		2.50(20)		
		2.43(1)			
2.36(100)	2.36(50)	2.35(50)	2.36(40)	2.36(100)	2.36(40)
2.25(5)	2.22(5)	2.22(1)	2.21(2)	2.22(10)	
2.08(2)					
2.06(10)	2.05(20)	2.04(5)	2.07(6)	2.04(25)	2.04(5)
1.97(8)	1.97(20)	1.96(15)	1.96(20)	1.96(20)	1.96(20)
	1.67(10)	1.68(10)	1.67(7)	1.67(5)	1.67(8)
		1.64(12)			
1.60(5)	1.61(5)		1.61(10)	1.61(5)	1.61(10)
1.45(15)	1.45(20)	1.45(15)	1.45(15)	1.45(30)	1.45(15)
		1.397(2)			1.396(2)
1.24(20)	1.24(25)	1.24(17)	1.24(16)	1.24(35)	1.24(20)
1.21(5)					
	1.19(8)	1.18(5)	1.19(4)	1.18(20)	1.17(5)
			1.14(1)	1.134(5)	1.136(4)
	1.01(1)				
.938(6)	.940(5)	.938(4)	.939(2)	.940(20)	.941(2)
.914(6)	.916(8)	.917(4)	.917(4)	.917(25)	.917(2)
.834(5)	.835(8)		.837(1)	.835(20)	
.786(4)	.786(8)		.786(1)	.786(20)	

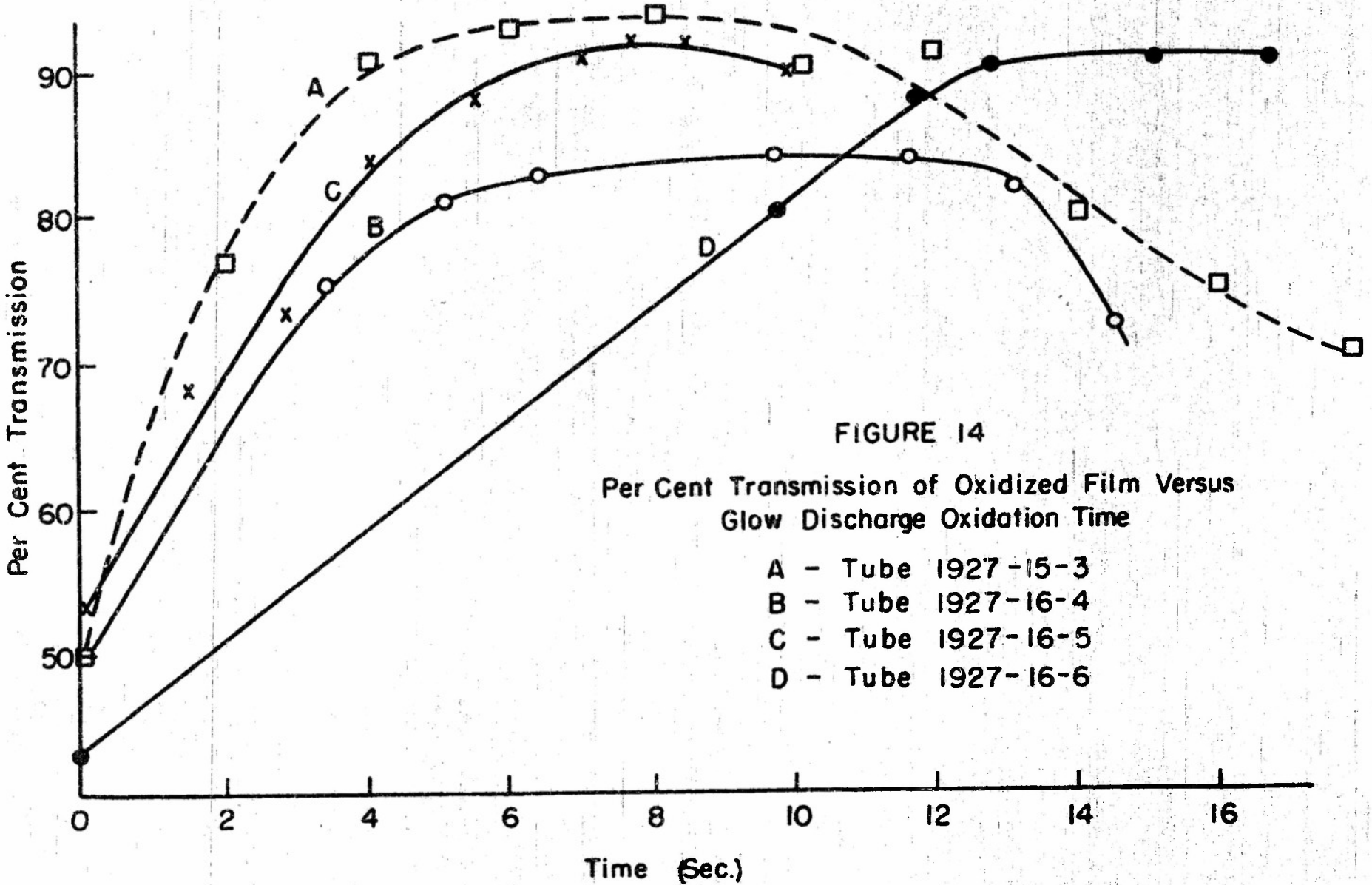

FIGURE 14

Per Cent Transmission of Oxidized Film Versus Glow Discharge Oxidation Time

A - Tube 1927-15-3
B - Tube 1927-16-4
C - Tube 1927-16-5
D - Tube 1927-16-6

film increases to a maximum and then decreases. This observation accounts for the difficulties previously encountered in oxidizing to 90% transmission. The oxidation methods previously used were so rapid that the maximum was passed without recognizing its presence.

In the preparation of the oxide samples for the x-ray diffraction powder specimens, several interesting observations were made. When the film for the powder specimen from the first four tubes was scraped, the oxide was observed to be black when aggregated, easily removed, and easily pulverized. The oxide in the 90% transmission tubes, when the tube was scraped, tended to peel and had a continuous film-like structure, a yellow semitransparent appearance, and was not easily pulverized for loading into the capillary. After being pulverized the oxide was black. A powder photograph of the yellow oxide was prepared immediately after filling the capillary, and a second was made three weeks later. The first photograph indicated that the silver particle size in the sample was very small, probably appreciably less than 100A, since no silver lines were observable with interplanar spacings less than 2.04. The second photograph, which involved doubling of the exposure time, showed sharp silver diffraction lines indicating that the silver crystals had grown in size. It would be of interest to investigate this phenomen using focusing x-ray cameras with which it would be feasible to study the actual surface film. Considering the results quoted in the previous section on the formation of transparent yellow sections in the rf discharge oxidation of a silver wedge, it is evident that the formation of the yellow transparent oxide film involves a fairly complex process. Actually the amount of oxygen per unit area for a 90% transmission tube is of the order of magnitude required for the formation of the first-order yellow color on the massive cathode tube.

From the x-ray diffraction photographs it is evident that a crystalline oxide phase is formed during the oxidation process. It is also evident from the diffraction line at d/n = 2.04A that residual silver is present in the surface, and that a high transmission does not imply complete oxidation of silver. Silver is present in both the thick and thin sections of the film. This is in contrast to the results for ozone

oxidized films where metallic silver was found mainly in the thin sections. There is no real contradiction of the results of Section 4.31, however, as is pointed out later.

Prior to considering in detail the x-ray data of Table XIX it is to be noted that the interplanar spacing and intensity data for these samples are subject to greater error than for the thick oxide films of Section 4.31, because of the line broadening associated with small crystallite size.

The nature of the solid phases produced on dc glow discharge oxidation can best be indicated by comparison with ozone oxidized films. In Table XX the x-ray powder diffraction pattern for film D of Table XV is compared with that for a 40 - 60% transmission silver film which has been oxidized to 90% in a dc glow discharge (see Table XIX). The diffraction patterns are in fairly good agreement. The chief points of difference are (1) at high values of d/n the line positions do not accurately agree, (2) several weak lines in the ozone oxidized film are absent from the other film, (3) the lines at 1.67 and 1.61 are more intense in the glow discharge oxidized film, and (4) in the glow-discharge oxidized film the lines at 1.45 and 1.24 have higher intensities relative to the line at 2.07 than would be expected for metallic silver. The first of these discrepancies is probably due to high background at high d/n and to line broadening. If we examine Table XIX we see that some variability in line position is found. The discrepancy is probably not serious. The second discrepancy must be minor since the lines are so weak. The greater line broadening in the glow-discharge oxidized samples makes it difficult to observe the weakest lines. The third discrepancy is unexplained. Comparing Tables XV and XX we find a consistent tendency for the 1.67 and 1.61 lines in Table XV to be weaker than in Table XIX. The two lines tend to have equal intensities in both cases, however. We cannot be sure whether an additional phase is indicated or whether the intensity scales are somewhat different in the two cases because of differences in line breadth. The fourth discrepancy seems to be of general occurrence (see Table XX) and indicates that another phase may be contributing to the lines at 1.45 and 1.24 (and also to 2.36). Again the results are not quite conclusive.

TABLE XX. COMPARISON OF OZONE AND GLOW DISCHARGE OXIDIZED SILVER FILMS

The d/n values are in angstroms, followed by relative intensity (I)

Ozone Film D Table XV d/n(I)		DC Glow Discharge Tube 1927-16-5 40-60% Transmission d/n(I)	
3.36(40)		3.42(30)	
3.18(40)		3.21(30)	
3.02(2)		3.01(5)	
2.73(100)		2.76(100)	
2.68(3)		---	
2.50(10)		2.50(20)	
2.36(90)	Ag	2.36(90)	Ag
2.19(2)		2.21(2)	
2.05(20)	Ag	2.07(6)	Ag
1.96(6)		1.96(20)	
1.68(2)		1.67(7)	
1.60(2)		1.61(10)	
1.51(1)		---	
1.44(20)	Ag	1.45(15)	Ag
1.28(1)		---	
1.23(30)	Ag	1.24(16)	Ag
1.21(1)		---	
1.18(5)		1.19(4)	
1.14(1)		1.14(1)	
.987(1)		---	
.940(5)		.939(2)	
.917(6)		.917(4)	
.836(5)		.837(1)	
.787(4)		.786(1)	

Despite these uncertainties there can be no doubt as to the similarity between oxidation products obtained in the two cases, and we conclude that in glow-discharge oxidation solid phases Ψ_2 and Ag occur. There is also a possibility, not definitely proven, that the Ψ_2 lines are due either to more than one phase or to a solid phase of variable composition. The whole difference in powder diffraction patterns is one of intensity and this is not large, especially considering that the intensities are visual estimates and the lines have different breadths. Beyond this we cannot go at present.

There is some doubt as to whether Ag_2O is present or not. It seems highly unlikely that any large proportion of Ag_2O is present, but a small amount might remain undetected. As has been pointed out previously the Ag_2O line at d/n = 1.42 probably constitutes the best test of whether Ag_2O is present. The neighboring silver line at d/n = 1.44 is, however, very close and we have always to consider the question of whether reduced resolution due to line broadening might prevent resolution of the two. In the case of the regions with 40-60 and >60% transmission of tube 1927-14-1 (first and second columns of Table XIX), resolution is clearly high enough since a line pair at 1.24, 1.226 is resolved in the first case and a pair at 1.24, 1.228 is resolved in the second case. In neither case is any line at 1.42 found and hence Ag_2O is either missing entirely or present in very small proportion. The remaining samples of Table XIX do not have a line at d/n = 1.42, but at the same time adequate proof of high resolution is not contained within the data and hence we cannot unambiguously conclude that Ag_2O is absent. At present we can only say that there is no evidence for any large proportion of Ag_2O.

From the volume of the system (1 liter) and the pressure change on oxidation the amount of oxygen in each film can be calculated. The film area is subject to error because the thin section boundary is not clearly marked. The estimated area is approximately 35 cm^2. Using these data the weight of oxygen per unit area in each film is as given in the following table.

Tube No.	μg Oxygen/cm^2	% Transmission
1927-14-1	7.7	77
1927-15-2	3.2	69
1927-15-3	1.9	67
1927-16-4	0.2	72

The percent transmission is that after oxidation and is measured at the point for which the silver film transmission before oxidation was 50%. In the case of tube 1927-15-3 the initial oxygen pressure was 0.610 mm and the pressure when the transmission first reached 91% (at the point for which initial transmission was 50%) was 0.600. From these data the film contained 0.49 μg/cm^2 of oxygen at 91% transmission. This is comparable with the amount of oxygen required to oxidize a silver sheet to the first order yellow. The amount of oxygen required to reach 90% transmission is probably not accurately reproducible. Tube 1927-16-4 is unusual in that 90% transmission was never reached (see Fig. 14).

From the data of Sennet and Scott[5] it follows that a silver film with 50% transmission, which is evaporated as for example in tube 1927-14-1, has a thickness somewhat less than 100A. A 100A silver film contains 0.9×10^{-7} gram atoms/cm^2, if close packing is assumed. Tube 1927-14-1 contains 4.9×10^{-7} gram atoms of oxygen or about five oxygen atoms for each silver atom in the region for which the initial silver film transmission was 50%. As pointed out previously the estimates of cathode area are subject to considerable error because the boundary at the thin section is not clearly marked. In addition, the silver evaporator is sealed in and some oxidation of the bead and the silver intercepted on the shield is to be expected. Nevertheless, the ratio of 5 to 1 for oxygen to silver atoms exceeds by considerably more than any reasonable experimental error the 3 to 2 ratio for the most highly oxidized silver compound reported in the literature. Despite the fact that the average amount of oxygen taken up considerably exceeds that required to oxidize silver completely to the trivalent state, metallic silver still remains in the section of oxidized film which had 40 - 60% transmission before oxidation (see Table XIX). In fact, metallic silver is also found in the still thinner section for which the initial transmission was greater than 60% (see Table XIX). These results can be accounted for only on the basis of the assumption that the thicker sections of the silver film take up more oxygen than the thin sections.

The same situation prevails for tube 1927-15-2 but not necessarily for 1927-15-3 or 1927-16-4 since oxygen take-up in the latter cases is small. It should be pointed out that film sections were contained in the tubes which were considerably thicker than any from which the samples of Table XIX were taken.

It has previously been pointed out that the samples of Table XIX oxidized in a dc glow discharge contain silver in both the thick and thin sections, whereas the ozone oxidized samples of Tables XIII, XIV, XV contain silver in the thin sections but not in the thick sections. We might expect differences merely because the oxidation methods are different. Nevertheless, oxidation of silver wires by ozone and by rf glow discharge has been found to lead to the same oxidation products (Section 4.2) so it becomes of interest to inquire more carefully into possible reasons for the difference other than oxidation method. More careful consideration shows that all of the samples of Table XIX come from film sections which are "thin" in comparison with the ozone oxidized samples of Section 4.31. Consider, for example, the thickest sample from tube 1927-14-1 of Table XIX. The transmission was approximately 20%. The thin section of ozone oxidized film D was scraped from the section 3.5 to 4.5 cm from the thick end, and from Fig. 11 it follows that the percentage transmission at 700 mu was less than 20%. The evaporation times, 6 minutes for tube 1927-14-1 compared to 15 minutes for film D, do not differ enough to materially alter the fact that even the thick section of tube 1927-14-1 is comparable in thickness with the thin section of film D. It is highly likely that even the thick section of the former tube has a thickness below the critical value at which silver grain contact is established. In the remaining tubes the evaporation time is much smaller (see Table XVIII). The results of Sennet and Scott[3] show that critical thickness goes down with decreased evaporation time although it is about 100A even for a 2-sec evaporation. The thickness of the intermediate and thin sections of Table XIX are unquestionably below the critical, and at least some portion of the area scraped in sampling the thick section also has thickness below the critical. Even the thickest portion of the thick section is just on the verge of the critical thickness.

It seems very reasonable, therefore, to compare all the samples of Table XIX to the thin sections of the ozone oxidised samples of Table XV. It has already been pointed out that the x-ray diffraction spectra are very similar, the chief differences being in intensity, and it is not sure that the differences are significant. On the whole there is a striking similarity between the products of oxidation with ozone and with the glow discharge, not only for massive silver but for thin silver films. Again we find that film thickness is the decisive factor in determining the oxidation products. We do not mean to imply that the oxidising agent in the glow discharge is actually ozone. There is no evidence for this view. It is possible that some ozone is produced in the low pressure glow discharge, but the steady state partial pressure must be small since, with inert electrodes, the pressure change on operating the discharge is very small.

It seems clear that oxidation brought about in the glow discharge by positive ion bombardment will be less in thin than in thick films because of electrical isolation in the former. Oxidation brought about by electrically neutral species can also be smaller. This is demonstrated by the ozone oxidations of Section 4,31, and quite possibly the same situation may prevail in oxidation by neutral species in glow discharges even though the oxidizing species are not the same in the two cases, provided that nucleation is the rate determining step in thin films. The evidence thus far quoted does not distinguish between the two alternatives. It is, in fact, possible that both positive ions and neutral species contribute to oxidation.

There is some evidence which points to nucleation rate as an important factor in glow discharge oxidation. The highly nonuniform oxidations obtained with certain evaporated silver films has been pointed out in Section 3. The films referred to had thicknesses of 10,000A, much greater than the films to Table XIX. It seems certain that particle contact is established in such thick films and that current distribution in the base metal cannot account for the nonuniformity. Moreover, visual observation indicated complete cathode coverage by the glow in oxidation of these samples. This observation is of course, only qualitative and does not insure accurate uniformity of current density over the cathode. At the time the experiments were performed, however, we found it hard to reconcile the nonuniform

oxidation with the idea of nonuniform current density in view of the appearance of the discharge. It has also been pointed out in Section 4.2 that nonuniform oxidation of silver wire by rf glow discharge has been observed which is very similar to that observed in ozone oxidation. This observation is again consistent with nucleation. Finally, the observation in Section 4.32 that oxidation beginning at points, and not spreading far, was observed in oxidation of a silver film of graded thickness by repeated discharge of a condenser is also suggestive of a nucleation mechanism.

The hypothesis of a low nucleation rate seems to us to be plausible in view of all the evidence. In the case of the glow-discharge oxidation of thin films we cannot exclude, however, the possibility that electrical isolation is responsible for the failure to nucleate. Very thin insulating layers of some impurity may also be a factor. At present both of these must be lumped with other factors as possible causes for what we have called a "low nucleation rate". In other words we have nothing to offer as a mechanism by which nucleation is promoted or retarded.

4.34. Silver films oxidized by commercial process.

In addition to the tubes described in the preceding section, x-ray diffraction patterns have been prepared of the oxidized surface formed by the rf oxidation, using a commercial process, of evaporated silver from 30% to approximately the maximum transmission.* In the diffraction pattern the lines shown in Table XXI were observed.

TABLE XXI. INTERPLANAR SPACING DATA FOR COMMERCIALLY RF OXIDIZED SILVER FILM.

d/n	(I)		d/n	(I)	
3.40	(10)		1.68	(2)	
3.21	(10)		1.61	(2)	
3.00	(5)		1.45	(20)	-Ag+ X
2.75	(100)	Broad	1.23	(20)	-Ag+ X
2.66	(100)	Band	1.19	(5)	-Ag
2.36	(80)	-Ag+ X	0.938	(4)	-Ag
2.05	(15)	-Ag	0.915	(4)	-Ag
1.97	(5)		0.833	(2)	-Ag
1.89	(1)		0.785	(2)	-Ag

*We are indebted to R.G. Stoudenheimer of the RCA Victor Division of RCA for these partially processed tubes.

The transparent oxide film in these tubes exhibited the yellow color previously observed; however, on scraping a black oxide aggregate rather than a peel was obtained. The x-ray diffraction photographs clearly demonstrated the presence of unoxidized silver, thus confirming the previous observation that a 90% transmission film contains unoxidized silver. In the photographs the intense line 2.74A consisted of a broad line with two apparent intensity maxima corresponding to 2.75A and 2.66A. The silver diffraction lines at 2.36, 1.45, and 1.23A were rather intense and it appears likely that other phases are contributing to these lines. The low intensity of the 1.68A line relative to the 1.45A line suggests that appreciable Ag_2O is not present. It is also significant that, in contrast to the previous 90% transmission tubes, the 3.40 and 3.21A lines have a relatively low intensity compared to the 2.75A line. It is possible that some oxide decomposition may have occurred in the evacuated tube during the period of approximately one month between fabrication and x-ray powder sampling. It is also of some interest that the 1.68 and 1.61 lines have intensities which agree well with those observed in ozone oxidation (see Table XXI). Otherwise there seems to be no essential difference between this tube and the glow-discharge oxidized films of the previous section.

4.4 Chemical Nature of the Oxidation Products.

From the foregoing investigation it seems to be established that two solid silver oxides, not Ag_2O nor AgO, are formed in the oxidation of silver by ozone, rf and dc glow discharge. A complete structure determination does not seem feasible on the basis of these data. Some progress toward an understanding of the general chemical nature of the products can nevertheless be made by utilizing the chemical information which is available on the oxidation states of silver. This information is very briefly reviewed below and the connection with the present work is indicated.

4.41 Properties of di- and trivalent silver compounds.

The oxidation state for silver is the normal one in silver compounds and is so well known that further discussion seems unnecessary. It seems to be established, however, that silver has oxidation states of +2 and +3 in certain less well-known substances. We shall be particularly concerned with these higher oxidation states in what follows.

The early literature on the higher oxidation states of silver is somewhat confusing as is indicated by reviews on the subject[18,25]. During the course of a number of more recent investigations, however, the situation has been considerably clarified. In 1926 Yost[17] studied the initial black silver oxide precipitate formed on reaction of ammonium persulfate with a silver salt. The precipitate is a powerful oxidizing agent, the oxidation number being compatible with the existence of trivalent silver. Further investigation on this subject by Carmen[26] during the course of another investigation, showed that on standing the oxidation number of the black precipitate decreased to that expected for divalent silver. This indicated a reaction between trivalent silver and monovalent silver to produce divalent silver. Later investigations showed that pure AgO could be prepared by treating potassium persulfate solutions with silver nitrate. The method of de Boer and Van Ormand[27] was used in preparing the AgO sample whose powder diffraction pattern is given in Table VIII. As stated in Section 4.1 the substance obtained is too strong an oxidizing agent to be a peroxide.

The production of trivalent silver in aqueous solutions by means of ozone oxidation has been extensively studied by A.A. Noyes and collaborators[18,19,20,21,22]. By means of kinetic studies it was shown that production of a hydrolyzed trivalent silver ion (AgO^+) is the first step in the oxidation in aqueous solution. The trivalent silver is then rapidly reduced to divalent silver by reaction with monovalent silver. The oxidation of metallic silver by ozone has been studied by Jirsa and Jellinek[28] and by Tronstad and Höverstad[29]. The products formed were found to depend markedly on the conditions of oxidation including the moisture content of ozone[29]. Both trivalent and divalent silver, in the form of oxides, could be produced. An x-ray study of complex salts[30]

has provided evidence for the existence of divalent silver in the solid state.

The divalent and trivalent oxidation states for silver seem well established and the corresponding oxides AgO and Ag_2O_3 are to be expected. It has previously been pointed out in Section 4.1 that an x-ray powder diffraction pattern has been obtained for the former but not for the latter in a pure form. It is not possible, therefore, to identify Ag_2O_3 among the oxidation products by means of x-ray diffraction methods. Some additional information can be obtained, however, by means of a qualitative chemical study which is described below.

4.42 Chemical properties of silver oxide produced in the dc glow discharge.

It has not been feasible to undertake a detailed chemical analysis of the oxide formed during the glow-discharge oxidation of silver; however, several qualitative experiments have been performed.

A few milligrams of the black high-voltage glow discharge oxide was prepared by repeated oxidation of a silver sheet and brushing off the loose surface oxide. This oxide dessolved in 1δN H_2So_4 to give a deep brown solution. The acid solution gave no test for H_2O_2 using a titanium sulfate solution. The solid added to a dilute acid solution oxidized I^- to I_2, and Mn^{++} to MnO_4^-. In addition, the suspension of the solid in water slowly reacts with the evolution of a gas. If the solution is acidified with dilute sulfuric acid there is an initial vigorous gas evolution which is followed by a slow, steady rate of gas evolution.

The chemical properties of the oxide described above are consistent with the assumption that the oxide formed in the glow-discharge oxidation contains silver in a valence state higher than +1. It is also of interest that when slightly oxidized thin evaporated silver films are rinsed with concentrated sulfuric acid, a reaction occurs during which a brown coloration is observed at the reaction zone. Thus silver in valence state higher than +1 is present even in thin oxidized silver surfaces.

In the first of the experiments described above the silver sheet was not completely oxidized. It is to be expected, therefore, that the oxidation products are as described in Section 4.2 for silver wire. From the x-ray powder diffraction data of Table X and the discussion of Section 4.1 it appears that Ag_2O, φ_1, and φ_2 are the phases present. AgO if present at all must be in small amounts. The oxidizing power of the oxide must then be due to φ_1, φ_2 or both. From the chemical behavior of thin films and the known fact that thin films oxidized in the dc glow discharge contain mainly φ_2 and Ag, it appears that φ_2 is a strong oxidizing agent. This is farther confirmed by the behavior of oxide formed in the incomplete oxidation of silver sheet although in this case φ_1 is also present. No conclusive direct evidence is found that φ_1 is a strong oxidizing agent. It seems highly likely that φ_1 is an oxidizing agent, however, because either by ozone oxidation at high temperature or by extreme rf oxidation (Section 4.32) φ_1 is produced. Since these conditions are such as to produce extreme oxidation it seems very likely that φ_1 also contains silver in a valence state higher than +1. Since there is no conclusive evidence for the presence of AgO we are inclined to think that both φ_1 and φ_2 contain silver with valence +3 or higher. Two different crystalline modifications of Ag_2O_3 might be involved, although no definite evidence is available to indicate this. Whatever the precise structures of the solids may be, it certainly seems to be established that the oxides formed are strong oxidizing agents.

4.5 OXIDATION AND PHOTOSURFACE PROPERTIES

During the investigation of the gross composition of the photosurface using radioactive cesium, significant results were obtained relating the oxidation step to the photoelectric and thermionic emission of the photosurface (see report no. 2 of this series). The conditions for the preparation of a good infrared-sensitive surface on a massive silver substrate had been well established at the time the tracer studies were undertaken. Consequently, a tube design for the tracer study of photosurface composition was adopted in which the photosurface was formed on a thick (10,000A) evaporated silver film deposited on a microscope cover glass as substrate.

A priori it was assumed that photocathodes prepared from the thick evaporated silver surface would be similar to those prepared using a massive silver sheet. In the following paragraphs the relationship observed between the silver film characteristics and the photocathode characteristics is discussed. Detailed data for the investigation are presented in the Master's Degree Thesis of W. Haubach[b]. The results are also described in detail in Part II of this final report series.

During the initial stages of the tube fabrication five nonradioactive tubes were prepared on Vacuum system II. The fabrication procedure used for preparing the tubes was as follows:

1. Preliminary cathode oxidation.
2. Degas tube and decompose oxide at 390-400°C for 1-2 hours.
3. Cool tube to room temperature.
4. Oxidize cathode.
5. Heat tube at 190°C for 10 minutes.
6. Add cesium from side tube using Auxilliary furnace to heat cesium, i.e. the side tube.
7. Measure emission during cesium addition using a Galvanometer.
8. Cool cesium at thermionic emission maximum.
9. Cool tube at second emission maximum.
10. Seal tube off vacuum system.
11. Bake tube.

In the measurement of the thermionic emission during cesium addition it was not possible to distinguish between a thermionic emission current and an ohmic conduction current due to the formation of a conducting film on the tube envelope. The five tubes were characterized by the following maximum photocurrent wavelengths and long wavelengths limits respectively: (1) 620 and 950 mμ; (2) 790 and 980 mμ; (3) tube not sensitive; (4) 955 and 1400mμ; (5) 765 and 1100mμ. In the group there was only one tube (4) which could be classified as a good infrared sensitive tube.

Subsequently a number of tubes were prepared by a modified procedure in which it was possible to determine the thermionic and photoelectric emission during cesium addition. This was accomplished by sealing the tube off the vacuum system after firing

the Si-Cs_2CrO_4 pellet and mounting the tube in an oven at 190°C. The Si-Cs_2CrO_4 pellet, which provides metallic cesium after heating with an induction heater, was contained in a side tube connected to the phototube through a fine capillary which limited the rate of effusion of cesium vapor in the phototube. The thermionic emission during the cesium addition (which was slow because of the capillary constriction) was measured by connecting the tube to a vibrating reed amplifier Brown recorder unit. Photoemission was followed by intermittent illumination of the cathode with white light passed through infrared filters, the photocurrent being recorded as a current superimposed on the thermionic emission. The apparatus was so constructed that the variation of the photoelectric and thermionic emission with voltage could readily be determined.

Subsequently a series of eight radioactive cesium tubes were prepared in which the photoelectric emission and thermionic emission during cesium addition were recorded on the Brown recorder. With one exception, these tubes were characterized by the absence of thermionic emission and the presence of a conduction leakage current during the cesium addition. In addition, appreciable infrared sensitivity did not develop during processing of the tubes. The photoresponse curves were characterized by a long wavelength limit of the order of 850 - 1000 mμ and maximum photocurrent responses at 500 to 650 mμ. During the preparation of the tubes numerous processing conditions were varied in an effort to learn the conditions for the production of a good infrared sensitive surface.

Finally, after establishing that the difficulty was not connected with the use of home made Si-Cs_2CrO_4 pellets containing radioactive cesium, it was concluded that the difficulties were associated with the silver base and the oxidation process. In the oxidation of the cathodes difficulties were encountered in forming a uniform oxide film during the glow discharge oxidation. It was found that a repeated oxidation and thermal decomposition process tended to improve the oxidation characteristics but did not appreciably improve the infrared sensitivity.

In the previous experiments the silver base was formed by the evaporation of a 10,000A silver film. It was consequently of interest to prepare thicker silver film surfaces which possibly would behave more like the massive silver cathodes. Cathodes were prepared using thicker silver films and it was found that both integral and infrared sensitivity were markedly improved. During the addition of cesium to these thicker film cathodes, the thermionic and photoelectric emission developed in a manner similar to that observed in the fabrication of massive silver cathodes with good infrared sensitivity. In addition, it was now possible to produce consistently good infrared sensitive tubes having a photoelectric emission maximum between 900 and 950 mμ and long wavelength limits greater than 1200 mμ.

From the experiments it was not evident at this point whether the observed results were due solely to the change in the silver thickness, or whether there was an associated change in the aggregation of silver which influenced the oxidation process. Sennet and Scott[7] have studied the effect of the silver evaporation rate upon the structure of silver films. In their experiments a rate of 90A/sec for a 180A film was considered a fast evaporation rate, and a 21.5A/minute rate for a 430A film a slow rate. Films evaporated at high rates contained particles whose sizes differed markedly from those evaporated at low rates. In both cases particle sizes depended on the amount evaporated. Using these extreme rates as a basis, an evaporated silver cathode was prepared with a silver film half the thickness used in preparing the poor tubes. The evaporation time for this film was approximately ten hours compared to the 15 minutes used in the preparation of the poor tubes. The cathode characteristics during the fabrication of the tube were normal, and a good infrared-sensitive surface was obtained. The photocathode so prepared was semitransparent. Thus good tubes could be prepared by either increasing the silver thickness or by changing the rate of deposition of the silver substrate.

From the experiments quoted above, and

considering the difficulties which have been encountered in the preparation of semitransparent cathodes by evaporating silver films to 50% transmission followed by oxidation to 90% transmission, it appears that the silver film structure and the subsequent oxidation step may exert a profound effect upon the final characteristics of the photo surface. In the poor tubes (i.e. those having low infrared sensitivity) the characteristic absence of appreciable thermionic emission during cesium addition is an interesting fact.

The experiments described above were performed on photocathodes of several thousand angstroms thickness, far beyond the critical thickness at which the merging of silver grains takes place. It would be of interest to have experiments at hand to illustrate the changes which occur as the silver film thickness increases through the critical range. Such experiments have been performed by Morozov and Butslov[34]. They first established, by means of auxiliary measurements on electrical conductivity, that grain contact is established in passing from silver films containing 7 micrograms (μg) of silver per square centimeter to films which contain 14 $\mu g/cm^2$. If the void volume were zero the thickness range would be 70 to 140A. They then prepared photocathodes on silver films of graded thickness which covered the range from 7 to 14 $\mu g/cm^2$ and beyond. The spectral response, measured at a point on the film containing 7 $\mu g/cm^2$ of silver, had a maximum at 450 mμ wavelength and a low infrared sensitivity. At 14 $\mu g/cm^2$ the maximum had shifted to 750 mμ and the infrared sensitivity was greatly increased. A steady gradation occurred in the intermediate range. This establishes that an increase in infrared sinsitivity accompanies the grain merging process. Morozov and Butslov[34] state that beyond 14 $\mu g/cm^2$ no further change in spectral response takes place. In view of the experiments, previously described, on thick silver films we cannot, of course, agree that this is generally the case. This does not mean that the results of Morozov and Butslov are in error. In fact we have repeated their experiment, with less care, and obtained similar results, although the results are

more sensitive to processing conditions than was indicated by them. There are probably two effects. One sets in at small thicknesses and is connected with silver grain merging. The second effect may occur at much larger thicknesses depending on the manner of preparation of the silver base.

We cannot at present go beyond these general statements. Our own experiments, on photocathodes prepared on thick evaporated silver films, conclusively demonstrate that the preparation and oxidation of the silver base have a decisive influence on infrared sensitivity of the finished photocathode. It was recognized from the very beginning of the research that this might be so, but a demonstration was obtained only in the final stages of the investigation. As a result it now appears that still further investigation of the silver evaporation and oxidation would be worthwhile. Some suggestions for further study are described in Section 5.0.

5.0 DISCUSSION OF RESULTS. SUGGESTIONS FOR FURTHER WORK.

The investigation of the silver oxidation step was undertaken partly for the purpose of establishing methods of control in the fabrication of photocathodes and partly in the hope that new process variables would be disclosed which might help to account for the poor reproducibility encountered in the preparation of infrared-sensitive cathodes. The control methods adopted are not very different from those employed in the industrial manufacture of cathodes and have been clearly described in the previous text. In this concluding section, therefore, attention is devoted to the description of those variables which might reasonably affect the finished photocathode. A brief appraisal of the present status of the problem is also included, together with some suggestions for further work.

In considering the possible factors which might influence the finished photocathode it is important to distinguish clearly between these two: (1) the types of solid phases which are produced, and (2) the particle size for each phase.

Attention in the present study, has been devoted almost entirely to the first of these factors. In order to make headway on phase identification it has been necessary to lay aside the question of particle size determination. As a result we have only qualitative information on the sizes of oxidized silver particles. The x-ray diffraction investigation of the products of oxidation reveals in all cases an x-ray diffraction line spectrum. The solids are therefore crystalline and have linear dimensions greater than 100A in all cases. Even this conclusion must, however, be viewed with some caution. Grain growth may occur <u>after</u> the sample has been taken for x-ray analysis. For grain contact is more intimate in the powder sample scraped from a film than in the original film, and considerable periods of time usually elapse before x-ray photographs are completed. Grain growth is undoubtedly possible under these conditions.* This is especially true for thin films oxidized in a dc glow discharge since the particle size is very small in the film before sampling. A case has already been mentioned in which grain growth of silver particles did take place. In ozone oxidized films the particles were already of considerable size before the sample was taken so subsequent grain growth is probably of less importance. Finally it must be emphasized that in the dc glow discharge oxidized films the samples were <u>not heated above room temperature</u>. In preparing a photocathode the oxidized film is heated to a high temperature (ranging from 150°C to 190°C depending on the method of preparation) before adding cesium. This is a step which seems certain to promote grain growth. If the objective is to obtain information on grain size immediately prior to cesium addition then the oxidized film should be preheated. This has not been done in our experiments. Despite the

* It is also possible that grain growth may occur in the original film on standing if the particles are very fine. It is not unusual to observe changes with time of electrical conductivity of thin silver films. Such behavior has been repeatedly reported by other investigators.

uncertainty which arises on account of the above factors there is, nevertheless, considerable information available on particle sizes in silver films since other investigators have studied this question. There is, moreover, considerable evidence which indicates that particle size and size distribution in the original silver film can influence not only the sizes of the silver oxide particles produced but also the oxidation products. Factors (1) and (2) above are, therefore, inter-related in a complicated way. Before returning to further discussion of this point a brief summary of the facts is in order.

As far as the type of solid phase is concerned, the thickness of silver base seems to be a variable of major importance. This shows up very clearly in the ozone oxidation of silver films of graded thickness. It also appears when we contrast the products obtained on the oxidation of silver wires with the dc glow discharge oxidation of thin silver films. In the oxidation of wires the supply of silver is never exhausted, so conditions are similar to those which prevail in the preparation of photocathodes on a massive silver base. It is found that Ag_2O, Ψ_1 and Ψ_2 phases are all formed with Ag_2O next to silver and Ψ_1, Ψ_2 further out. In the case of thin silver films with 50% transmission oxidized in the dc glow discharge to 90% transmission residual silver is found in the oxidized film. There is no evidence for the presence of either Ag_2O or Ψ_1 solid phases, however. Under the conditions which we have used for oxidation there is undoubtedly a difference between the solid phases produced by oxidation of a massive silver base and a 50% transmission silver film. It is not particularly surprising, therefore, that the final photocathodes should be different, although the precise mechanism by which the difference arises as cesium is added to form the photocathode is not known. It has been consistently observed in our preparation of photocathodes that those prepared using a massive silver base have higher infrared sensitivity than those prepared by oxidizing a 50% transmission silver film to 90% transmission. This statement applies whether the thin film oxidation was performed

using an rf glow discharge, an intermittent discharge produced by repeated discharge of a high voltage condenser, or a dc glow discharge. Judging from the commercially manufactured photocathodes which we have tested, both massive and semitransparent, the differences between massive and thin cathodes which we obtain are much greater than are normally encountered in the commercial fabrication. This occurs despite an attempt on our part to follow the commercial procedure. The massive cathodes which we have prepared by carefully controlled methods usually have higher infrared sensitivity than the corresponding commercial product, but the semitransparent cathode has a much lower infrared sensitivity than the commercial cathode. This suggests some difference in our processing method from that used in commercial practice, but thus far we have not found the reason for the difference.

As was emphasized in Section 4.5 the thickness of silver base can affect infrared sensitivity in two ways. The first is connected with silver grain merging and occurs at small thicknesses. The second extends to much greater thicknesses and appears to be of a different character. The effect of evaporation rate suggests that grain <u>size</u> rather than grain <u>contact</u> is a factor in the second case. A slow evaporation is expected to result in larger grains. The fact that high infrared sensitivity is thereby obtained is certainly suggestive. Confirmation is provided by the fact that high infrared sensitivity is invariably obtained in massive cathodes with silver sheet, containing very large grains, as the base.

It is suggested above that both grain <u>contact</u> and grain <u>size</u> in the silver film have an influence on the resulting photocathode. The first of these seems to be established while the second is tentative. We now consider how these two factors affect the oxidation products. It has been amply demonstrated that the nature of the oxidation products changes markedly on passing through the region in which grain contact is established. It is also possible, however, that silver grain size <u>may</u> affect the oxidation products further, even though grain contact is established. This

possibility arises as follows. Investigation of the oxidation of silver wire indicates that oxidation proceeds most rapidly along grain boundaries (see ref. 1). Since evaporated silver films contain much smaller grains than massive silver wire or sheet, which is drawn from the product crystallizing from a melt, it follows that small grains are quickly surrounded and oxidized to completion. During the intermediate stages of oxidation of a given grain several layers probably form. A core of unoxidized silver is expected to be surrounded by a sheath of Ag_2O and further out a sheath of φ_1, φ_2. If the silver supply is exhausted then Ag_2O is also further oxidized to φ_1, φ_2. This tentative picture suggests that the proportion of Ag_2O depends on silver grain size even though grain contact is established. It would be of considerable interest to extend the x-ray investigation to thick evaporated silver films in order to test this point. No new techniques are required for this investigation. The suggestion that silver grain size may control the nature of the oxidation products seems to us worthy of further study. For it is certainly true that two oxidized surfaces which contain chemicals of widely different properties just prior to the addition of cesium cannot with any certainty be expected to contain the same oxides of cesium after processing is finished. This is especially true since Ag_2O is a much weaker oxidizing agent than either φ_1 or φ_2. Moreover, eight different cesium oxides are known so final product is by no means assured.

In the above discussion the nature of the oxidation product has been emphasized. The particle size of the oxidation product just before cesium must also be considered. Here we have so little information that no conclusions can be drawn. In view of the remarkable effect of silver grain isolation on the products of oxidation it certainly seems necessary to investigate the particle size before cesium addition. There seems, however, to be little point to speculation on the probable outcome until experimental data have been accumulated.

In our past thinking we have usually assumed implicitly that impurities arising, e.g. from vacuum pumps or traps, could affect a photocathode because adsorption on or reaction with the surface

brought about a change in work function. This conception assumes that a very small amount of impurity affects the photocathode after it has already been prepared. The nucleation concept, discussed in connection with silver oxidation, leads us to ask, however, whether an equally small amount of impurity might affect the photocathode by acting during the very first step in the preparation, namely the silver evaporation. An impurity might influence the course of subsequent chemical reaction if nucleation is involved. This suggestion opens up some distinctly unpleasant possibilities. It should be possible, however, to experimentally test this point by studying the influence of impurities which might be added to the silver before evaporation, evaporated on to the substrate before silver evaporation, or added in gaseous form to the vacuum chamber in which evaporation takes place. A deliberate program of investigation whose purpose is alteration of the silver base would be of considerable interest. Preheat treatment of the silver base both before and after oxidation would also be of interest and a more systematic study of process variables in the glow discharge oxidation, particularly the pressure, might well be included.

There is apparently no lack of possibilities for investigation. The only question is whether the possibilities show sufficient promise to make the investigation worthwhile. It appears to us that further study of the silver base shows promise. In other cases the situation is not sufficiently clear to permit a definite statement.

APPENDIX I

OXYGEN PRESSURE MEASUREMENT

In the experimental investigation of the preparation of the S-1 photosurface it was necessary to be able to measure rather small differences in pressure in the range from 0.1 to 1.0 mm Hg. The pressure measurements were performed using two micro Pirani gauge tubes designed by Dr. S. Naiditch while working for The Ohio State University Research Foundation. Since the gauge units developed have proven very satisfactory it seemed desirable to describe the two systems in detail. The micro Pirani gauges for vacuum systems I and II are described in the following sections A and B respectively.

A. MICRO PIRANI GAUGE FOR VACUUM SYSTEM I

The construction of the micro Pirani gauge tubes which were used in the pressure measurements is shown in Fig. 15. These gauge tubes are quite stable over long periods of time in the measurement of oxygen pressure in the range 0.1 to 1.0 mm Hg. To reduce the temperature fluctuations of the Pirani tubes they were surrounded by a Dewar after being attached to the vacuum system.

In vacuum system I the pressure was measured using the unbalanced Wheatstone bridge circuit shown in Fig. 16. The procedure followed in the use of this gauge was as follows: The bridge is initially balanced with the 500-ohm Helipot to give no galvanometer deflection with the open Pirani tube at atmospheric pressure and the galvanometer shunt potentiometer in the high sensitivity position. After balancing the bridge, the 100-ohm shunt shifted to the low sensitivity position and the Pirani tube is evacuated. After introducing oxygen to a pressure greater than 0.3 mm Hg the 100-ohm shunt is shifted to the high sensitivity position and the galvanometer deflection used to determine the pressure.

This Pirani gauge was calibrated using an

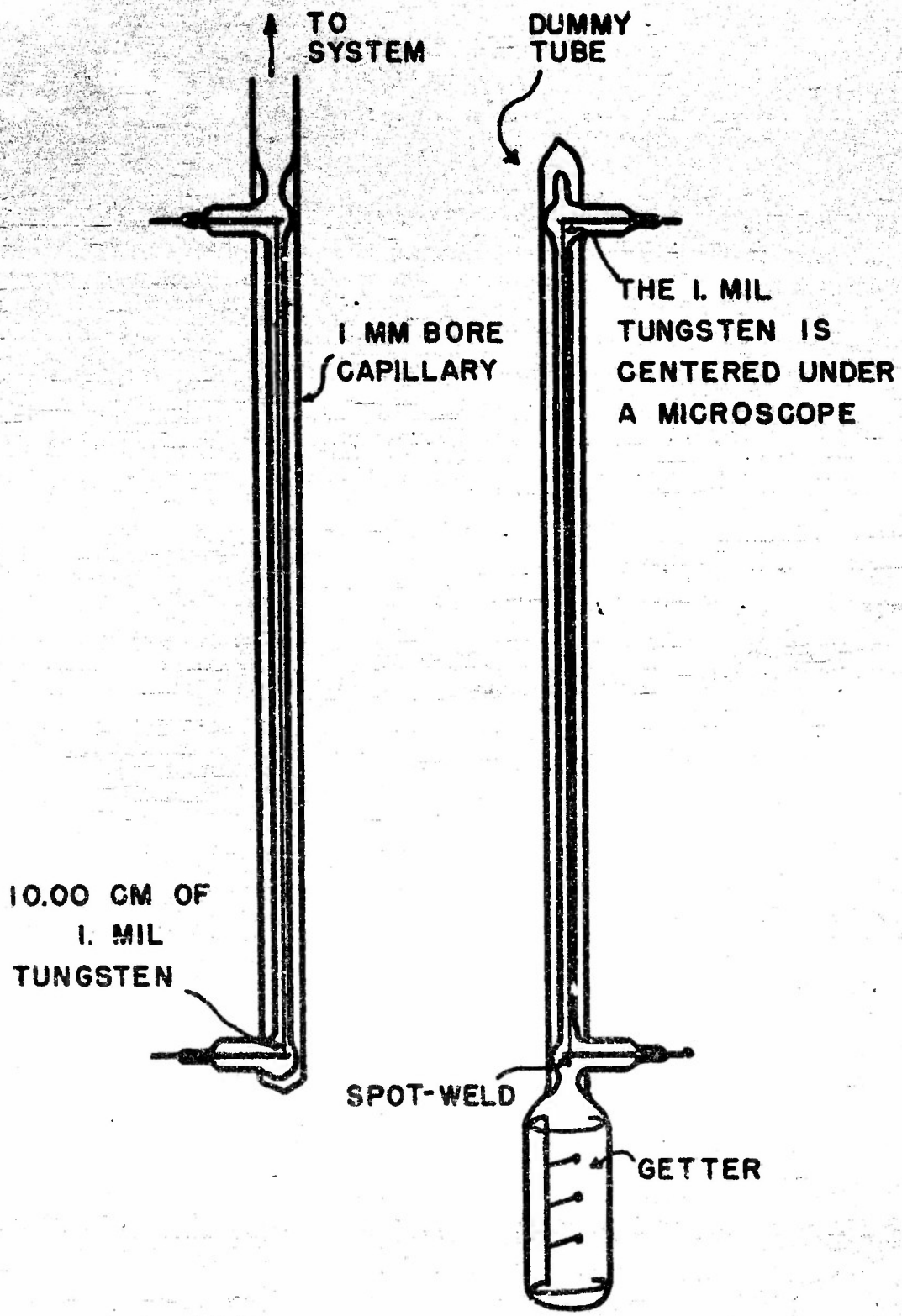

FIG. 15 MICRO PIRANI GAUGE

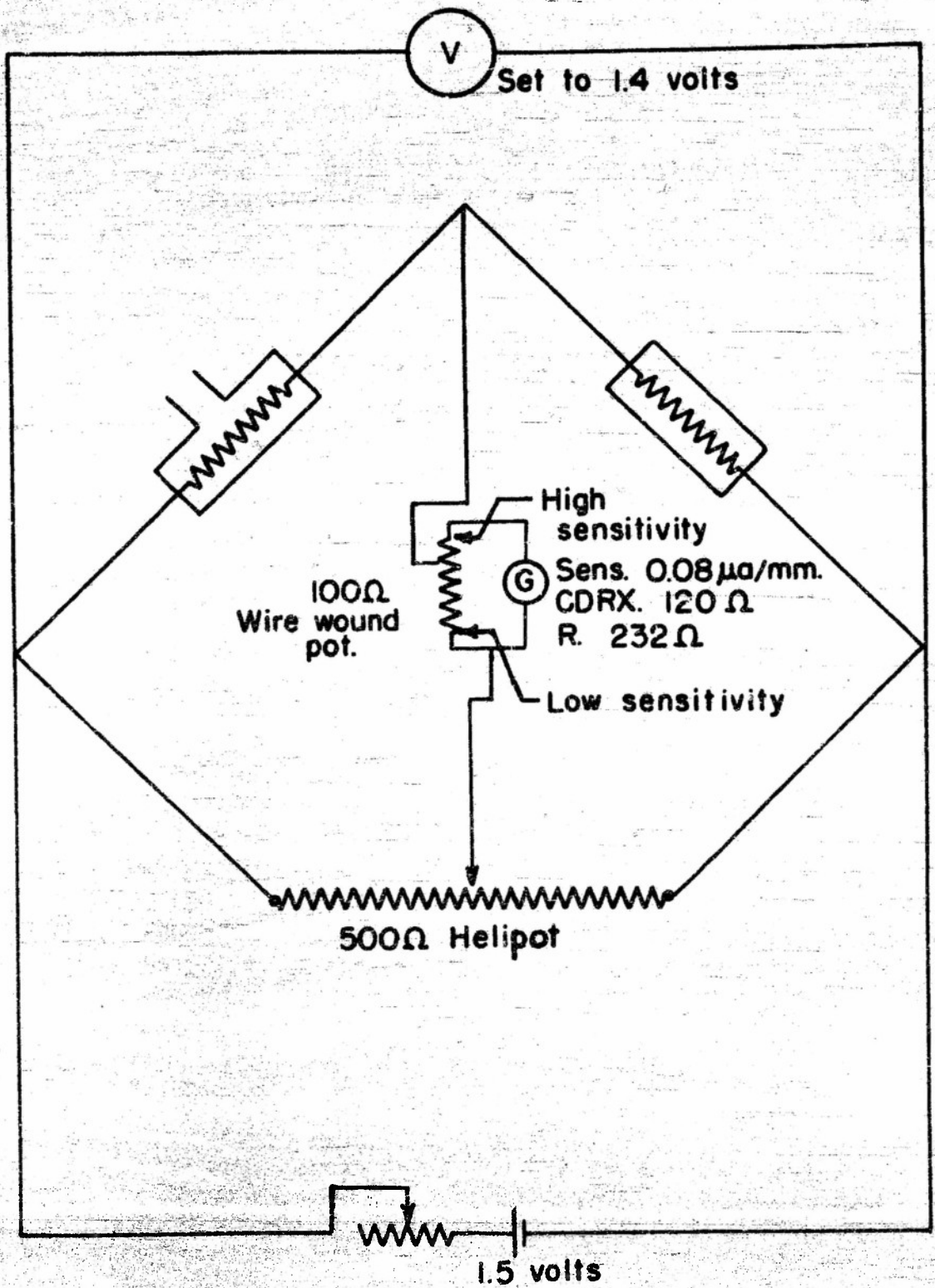

FIGURE 16
Vacuum System I Micropirani Gauge

octoil-S manometer for which 1 mm Hg was equivalent to 14.9 mm of oil. Two sets of calibrations for this gauge are shown in Fig. 17. From the data it is evident that in the period from August 11, 1950 to February 25, 1952 there was no significant change in the calibrations. For the pressure range from 0.3 to 3.0 mm Hg the calibration curve is well represented by the equation

$$S \times P^{0.926} = 23.7$$

where S is the galvanometer deflection in centimeter and P the pressure in mm Hg.

The principal source of error in this gauge unit arises from the method of calibration. It is probable that the absolute pressure could be in error by as much as 0.05 mm Hg. However, the measured quantity of interest is the difference in oxygen pressure, and this should be accurate to approximately 5 microns.

B. MICRO PIRANI GAUGE FOR VACUUM SYSTEM II

For the tracer photosurface composition study it was desirable to measure the oxygen deposited during the oxidation as precisely as possible. Therefore, a more precise system for using the micro Pirani tubes was developed.

The circuit consisted of a balanced Wheatstone bridge circuit as shown in Fig. 18. The variation of the micro Pirani sensitivity with the input voltage to the bridge is shown in Fig. 19. The deviation of the 2.0 volt curve from the family may be due to experimental error. The gauge voltage chosen for routine operation was 3.0 volts. In operation the gauge has a sensitivity of 1.7 cm galvanometer deflection per micron at 1 meter scale distance for the pressure range 0.6 to 0.9 mm Hg, and approximately 6 cm per micron for the range 0.4 to 0.6 mm Hg. In actual operation the galvanometer was used as a null instrument and readings were taken from Helipots in the lower left arm of the bridge as shown in Fig. 18. These readings are used on axes in Fig. 19 and 21.

The sensitivity of the gauge can be increased by placing the tubes in a liquid-air bath but this marked increase did not seem necessary. The gauge was actually calibrated at each tube fabrication, and slight temperature fluctuations had no great effect. The calibration of a fixed ohm point at several temperatures is shown in Fig. 20 and several calibration curves at different temperatures are shown in Fig. 21. The numbers at the points indicate the date and phototube number.

The resistors shown in the bottom-left arm of the bridge in Fig. 18 were Helipots. The 1000-ohm resistance was set every 10 ohms and the 10-ohm Helipot was read to 0.01 ohm but was stable to only 0.1 ohm. The 1000-ohm resistor at the bottom of the bridge could be switched in or out of the circuit to change the range of the gauge. For this work the resistor was always in the circuit.

The gauge was calibrated as follows, referring to Fig. 22 of the vacuum system.

An absolute pressure point was obtained by introducing dry oxygen through the tower into both the manometer and the micro Pirani calibration bulb. For Fig. 22 this means that stopcocks (1, 2, 4, 5) are closed and (3, 6, 7, 8, 9, 10) are open. After adjusting the pressure to 10 - 11 cm Hg the stopcocks (3, 6, 7, 8, 10) are closed. The micro Pirani calibration bulb volume was measured using mercury and was found to be 18.01 ml including stopcock (3).

Stopcocks (1, 4) were opened and the system evacuated. After complete evacuation stopcock (1) was closed. Stopcock (3) was now opened and the 18.01 ml of oxygen at the original pressure (~11 cm Hg) was released into the system which included the approximately 2-liter bulb and the bulb for volume determination, but not the manometer. The actual volume of the two liter bulb was 2075.6 ml. From the initial volume and pressure and the final volume, the final pressure may be calculated. The micro Pirani is read at this point and the calculated pressure is assigned this ohm reading.

Stopcocks (3, 4, 9) are now closed and stopcock (2) is opened, thus evacuating the micro Pirani

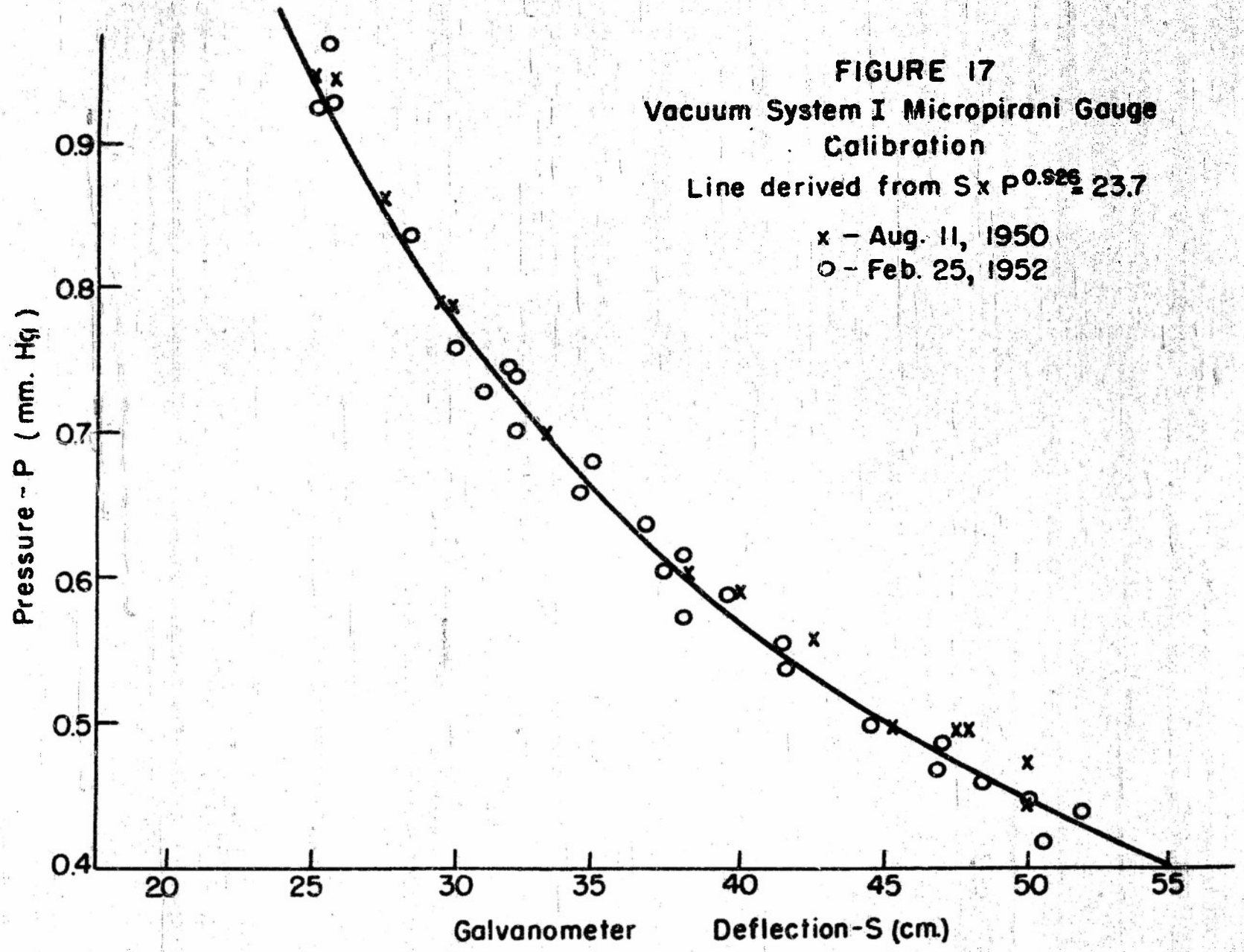

FIGURE 17
Vacuum System I Micropirani Gauge
Calibration
Line derived from $S \times P^{0.926} = 23.7$

x – Aug. 11, 1950
o – Feb. 25, 1952

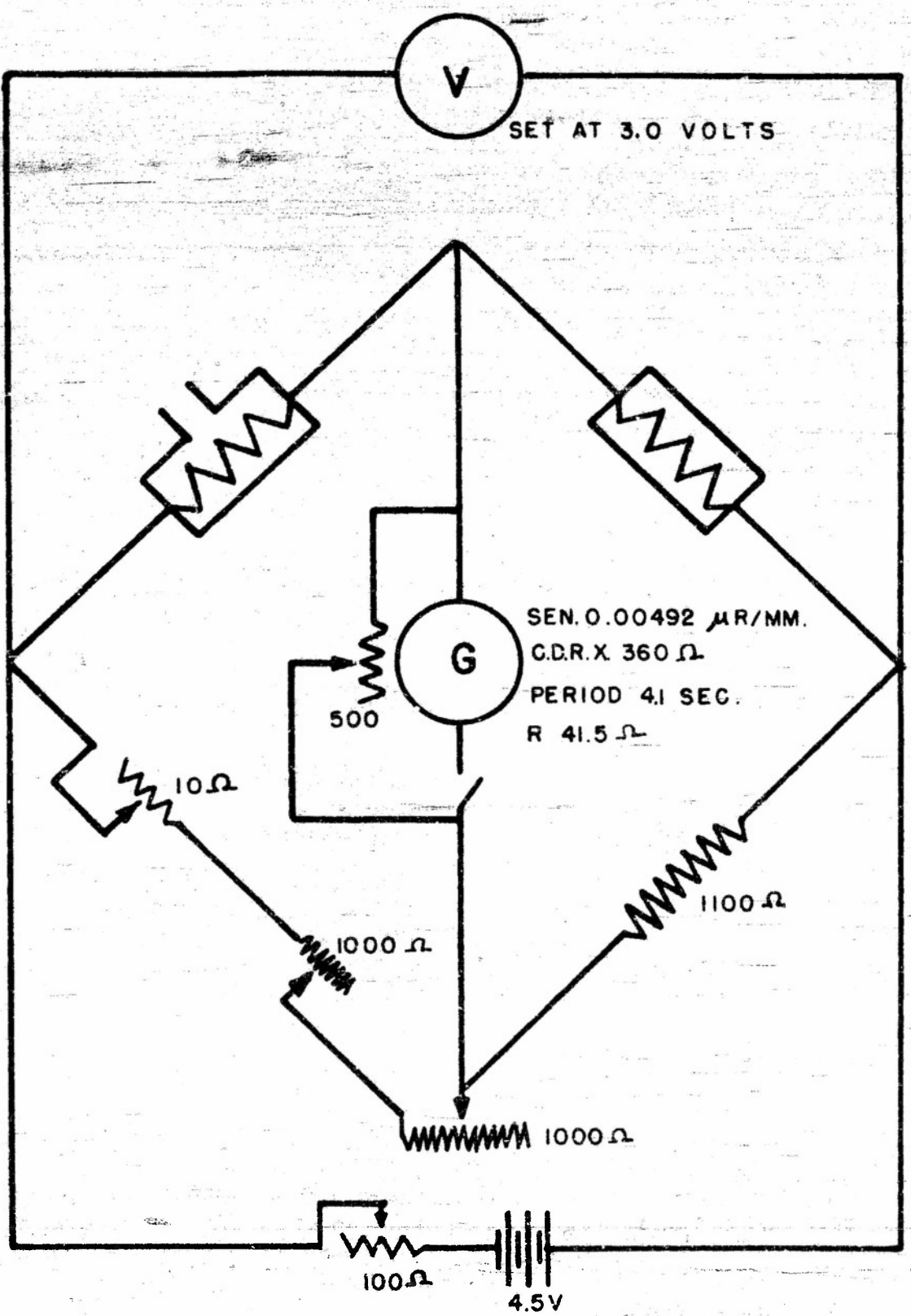

FIG. 18 VACUUM SYSTEM II MICRO PIRANI GAUGE CIRCUIT

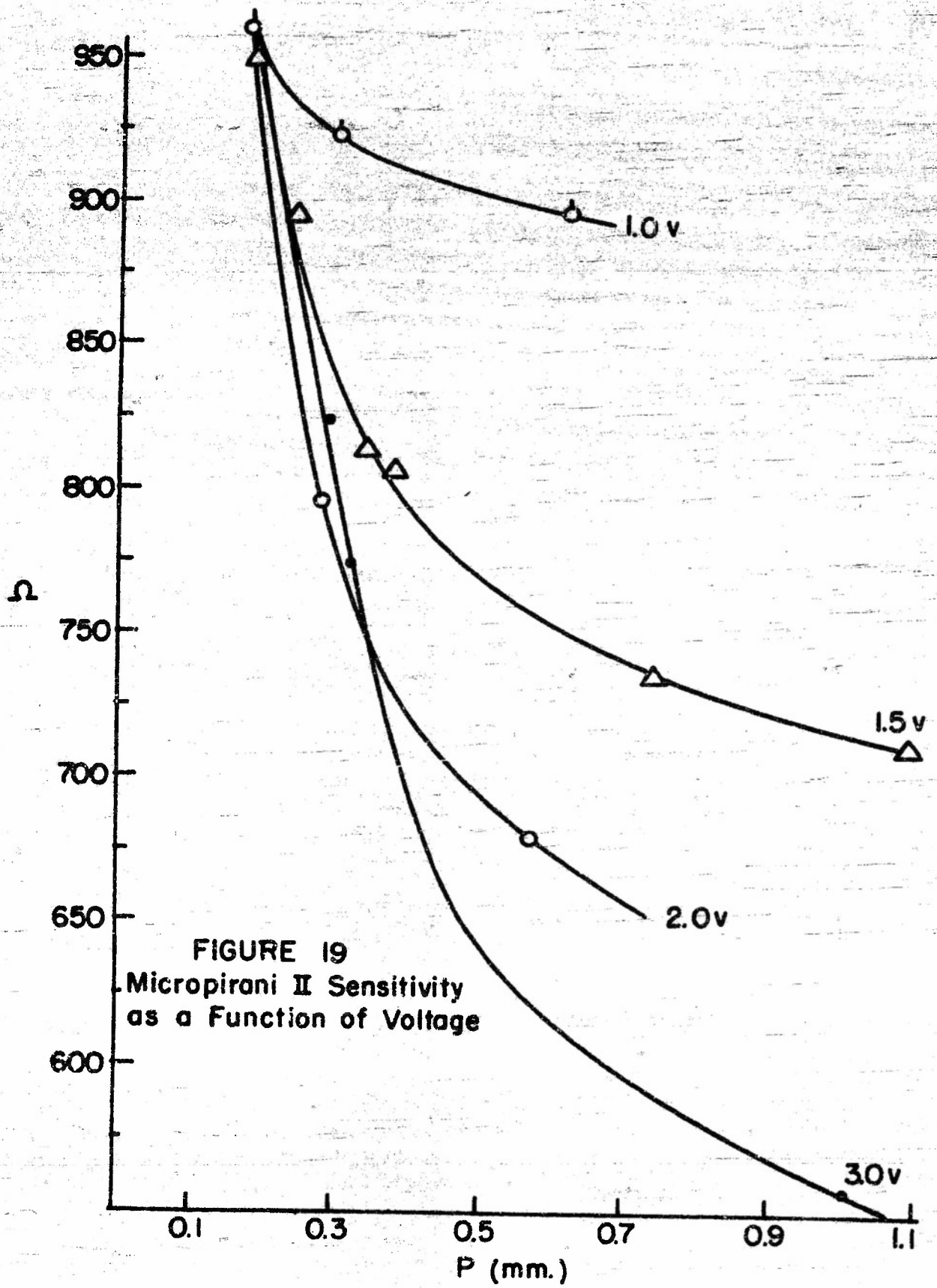

FIGURE 19
Micropirani II Sensitivity
as a Function of Voltage

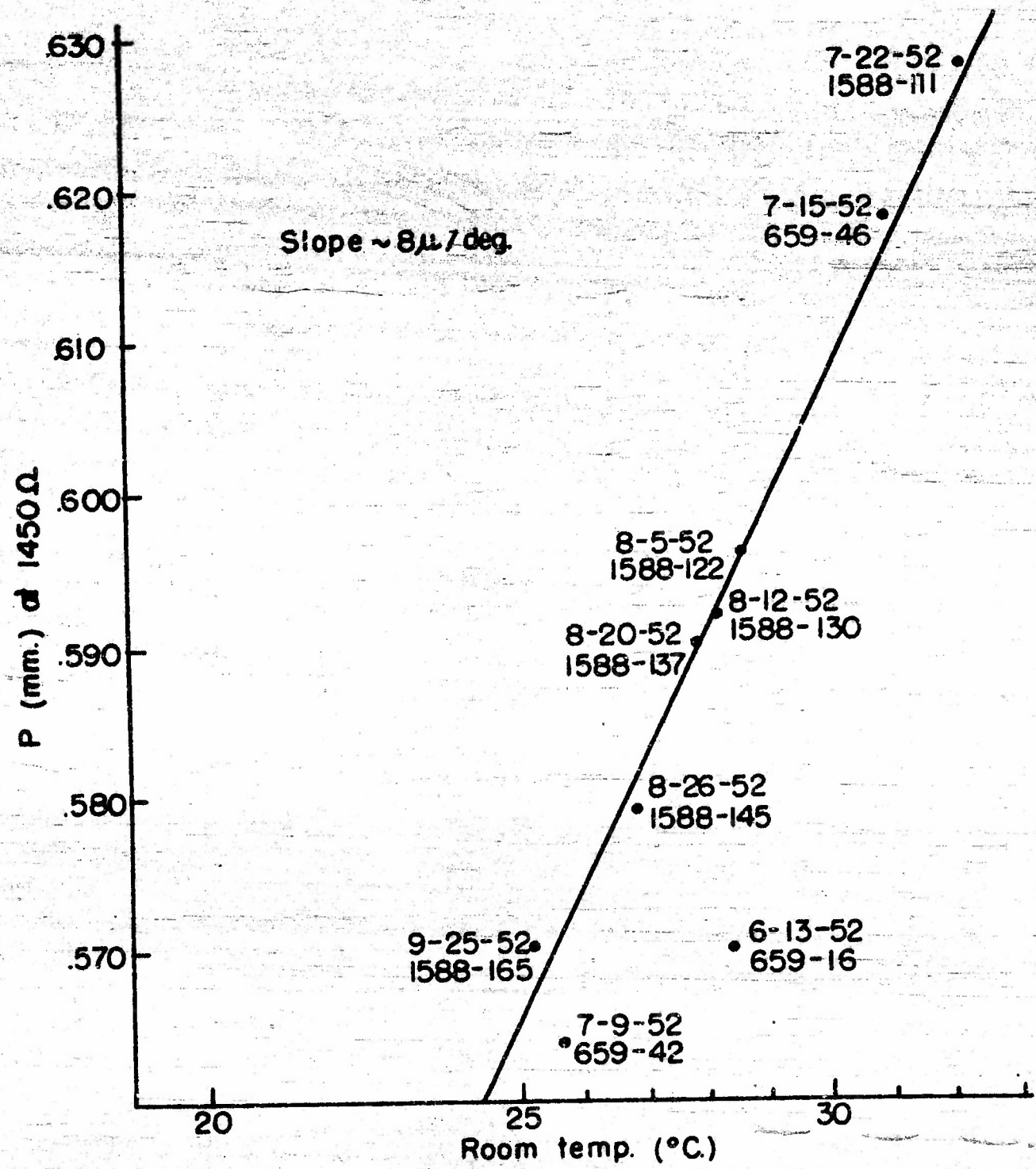

FIGURE 20

Micropirani II Calibrations as a Function of the Ambient Temperature

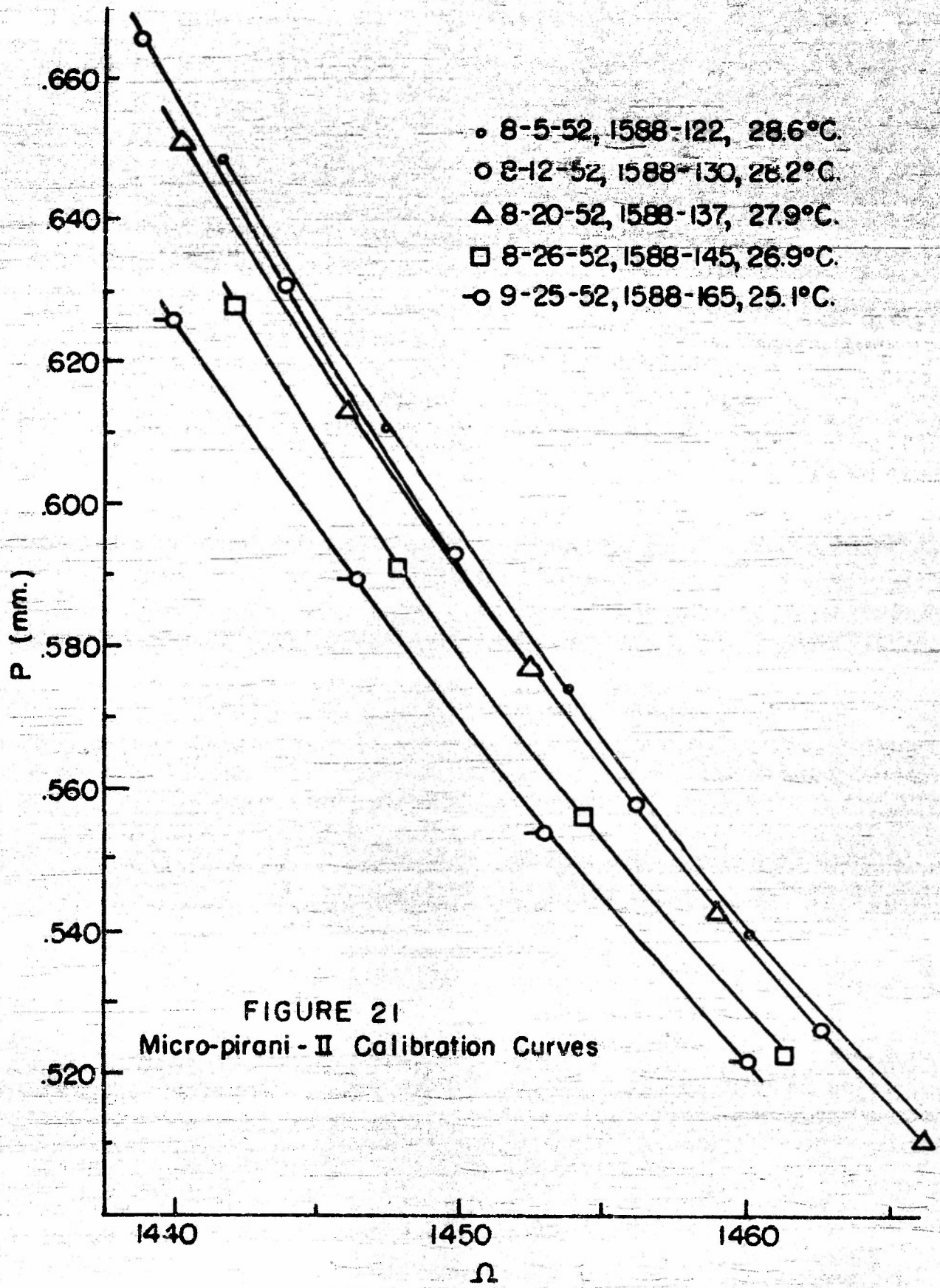

FIGURE 21
Micro-pirani - II Calibration Curves

calibration bulb. After evacuation, stopcock (2) is closed and (3) is opened, allowing oxygen at known volume and pressure to expand into a known volume; hence, the final pressure may be calculated and assigned an ohm reading. Repeating this process provides additional points for the calibration curves. The working graphs had expanded scales as compared to Fig. 21.

APPENDIX II

DESCRIPTION OF MICROSTRUCTURE AND OPTICAL PROPERTIES OF OZONE OXIDIZED FILMS

The results of the microscopic examination of the films may be summarized by describing the variation in microstrucsture of oxide as a function of thickness. In the discussion of the individual samples the terminology "blister oxide" describes a black oxide film which formed as a blister with a continuous microstructure. The "granular oxide" corresponds to black oxide grains which usually have a roughly spherical shape and are separated by voids of appreciable size compared to the particle size. The "continuous film" refers to a structure observed in the thin portion of an oxidized slide and which consisted of an unoxidized silver film more or less bonded to the glass substrate. The small oxide particle which at 440X apparently rested on the continuous film actually may not have made contact with it. The microstructure around an oxide particle on the continuous film could not be resolved at magnifications of 600X or less. Microscopic examination of the silver films before oxidation revealed a continuous silver film having no marked microstructure.

Film A. (240-minute Ag evaporation, 28°C oxidation. Region 0-0.8 consists of a blister oxide on top of small isolated oxide grams. Region 0.8 - 1.3 is a "lace-like" granular oxide with large voids and relatively high transmission. Region 1.2 - 1.6 is a semicontinuous oxide film with rather few voids. Region 2.0 - 7.0 is a continuous film with oxide granules dispersed on the surface. These oxide granules decrease in size and number per unit area with decreasing wedge thickness.

Film B. (25-minute Ag evaporation, 28°C oxidation). Region 0-1 consists of the blister oxide on top of small isolated oxide grains. From 1.0 to 2.5, granular spheroidal-shaped oxide particles with decreasing size as the film thickness decreases, void area small. From 2.5 on, fine particles at 90X with relatively large voids.

From 5.0 to 8.0 the particle size of the oxide grains which rest on a thin silver film is invariant (440X) but the number per unit area decreases as the silver film thickness decreases.

Film C. (15-minute Ag evaporation, 100°C oxidation). Region 0 to 1 consists of the blister oxide on top of a granular oxide with background of minute oxide particles. From 1 to 2 the film consists of small uniform granules with appreciable void volume. At 2.0 the film becomes continuous with small aggregates of oxide present on the surface. From 2.5 to 3.5 there are small isolated islands of black oxide plus a uniform distribution of small grains on top of a silver film. From 4.0 to 8.0 small oxide particles (440X) are distributed on a silver film substrate.

Film D. (15-minute Ag evaporation, 100°C oxidation). The region 0 to 1.0 consists of large (~0.001 mm) spheroidal granules of oxide with a large number of very small particles dispersed between the granules. From 1 to 2 the structure consists of close-packed uniformly sized spherical grains, the sizes of which decrease as the wedge thickness decreases. From 2.5 to 8.0 there is a continuous film substrate for the small (440X) oxide particles. The particles appear to be more closely pakced than in Film C.

Film E. (25-minute Ag evaporation, 140°C oxidation). Region 0 to 1.0 consists of large oxide granules with appreciable void volume. From 1 to 3 the size of the granules decreases with rather large voids relative to the particle size. From 3 to 4 the samll particles are close-packed while beyond 4 the particles are dispersed on a continuous film and have a rather small uniform particle size at 440X.

Film F. (25-minute Ag evaporation, 140°C oxidation). From 0 to 3.0 the film consists of oxide granules which decrease in size as the thickness of the silver decreases. From 3.5 to 8.0 the film appears to consist of a continuous silver film with small (440X) spheroids of oxide resting on a continuous film.

Film G. (25-minute Ag evaporation, 160°C oxidation). Similar to "F" but fine particles on continuous film starts at 4.0.

Film H. (25-minute Ag evaporation, 170°C oxidation). Similar to "G". Fine particles on a continuous film start at 4.0. The particle size uniformly decreases from 0 to 4.0 with a narrow size distribution at each segment across the slide. The void volume 0 to 4.0 is rather small.

Film I. (25-minute Ag evaporation, 200°C oxidation). Granular oxide for the full length of the wedge. The presence of a thin silver film at the thin section could not be definitely established at 440X. The size of the granules decreases regularly as the thickness of the initial silver wedge decreases.

Film J. (0.5-minute Ag evaporation, 28°C oxidation). For the thick silver region of this slide (<5% T) the surface was characterized by the formation of a thin blister oxide which peeled and thus exposed a fresh silver surface to the O_3 which then in turn oxidized and peeled. The adhesion of the oxide to the silver was poor, and after oxidation a thick silver film remained at the thick end. In the intermediate region the oxide structure changed to a granular "lace-like" network of oxide grains. In the thinnest portion of the surface the oxide grains were rather close-packed and very small. There was no evidence of a continuous film, and oxidation appeared to have occurred over the entire surface of the silver film. Depending upon the oxide structure present, there is a systematic variation in the transmission, the "lace-like" regions being the highest, the granular oxide in the thin regions next, and the blister oxide regions are opaque.

The microstructure of the films is correlated with the variation in the transmission of the wedge with wavelength and distance along the wedge. The transmission for the rather coarse granular oxide at the thick portion of the film is independent of the wavelength, the transmission being a measure of the void area. When the coarse grain structure changes to a semicontinuous film with small black oxide granules, the transmission tends to increase with increasing wavelength for the range 600 to

1000mμ. The actual form of the curve depends upon the structure and distribution of the oxide grains on the surface. In the cases where the transmission increases with wavelength for the very granular portion of the film (0 - 2.0 cm) there are very small oxide particles dispersed between the large grains. In the transmission versus thickness curves of Figs. 10, 11, and 12 the maxima and minima in the transmission between 0 and 3.0 are related to the changes in the structure and packing of progressively small-size oxide grains. The optical properties beyond 3.0, however, depend upon the amount and distribution of residual silver as well as the size and distribution of oxide grains.

The transmission data indicate that 50% transmission silver may be ozone oxidized at room temperature and 100°C to give films with 90% transmission. Films oxidized at temperatures above 100°C showed less than 90% transmission at the region originally showing 50% transmission. However, since the variation in the transmission of the film during the oxidation was not studied, it cannot be definitely stated that silver cannot be oxidized from 50 to 90 percent transmission at the higher temperatures.

APPENDIX III

MICROSTRUCTURE OF RF OXIDIZED FILMS

It has been reported by Borsiak and Morgulis[33] That a glow-discharge oxidized silver wedge formed on a glass substrate exhibits several maxima and minima in the reflection coefficient ($\lambda = 800 m\mu$) with increasing thickness of the wedge. Their film exhibited a completely clear interference picture corresponding to lines of equal thickness. To obtain a verification of these results a tube was prepared in which a silver bead was evaporated from a central electrode to give a wedge-shaped cylindrical silver deposit on the tube wall which was thickest opposite the silver bead and thinnest at the remote end of the tube. The silver was deposited in 15 seconds with the pressure in the system less than 2×10^{-6} mm Hg.

After introducing oxygen into the system to $P_{O_2} = 0.705$ mm Hg, grounding the anode, and placing a cylindrical aluminum foil electrode around the tube, the rf generator was turned on and the film oxidized to $P_{O_2} = 0.365$ mm Hg. In the thin film region the silver appeared to have been completely oxidized, but the region near the oxidized Ag - massive Ag boundary showed very brilliant colors by reflected light. More oxygen was introduced to give $P_{O_2} = 0.880$ mm Hg and the film further oxidized to $P_{O_2} = 0.610$ mm Hg. At this point the silver had been oxidized so that the demarcation between oxide - Ag was opposite the Ag bead. After evacuation, the tube was tipped off the vacuum system.

By reflected light the film showed a pattern of circular bands the colors of which varied with the distance from the silver bead level. A schematic diagram of the variation of visual transmittance as a function of wedge thickness is shown in Fig. 13. The colors observed by reflection and transmission at the various numbered points of Fig. 13 are given in Table XXII. No pronounced spectrum was observed by reflection from the air-oxide interface.

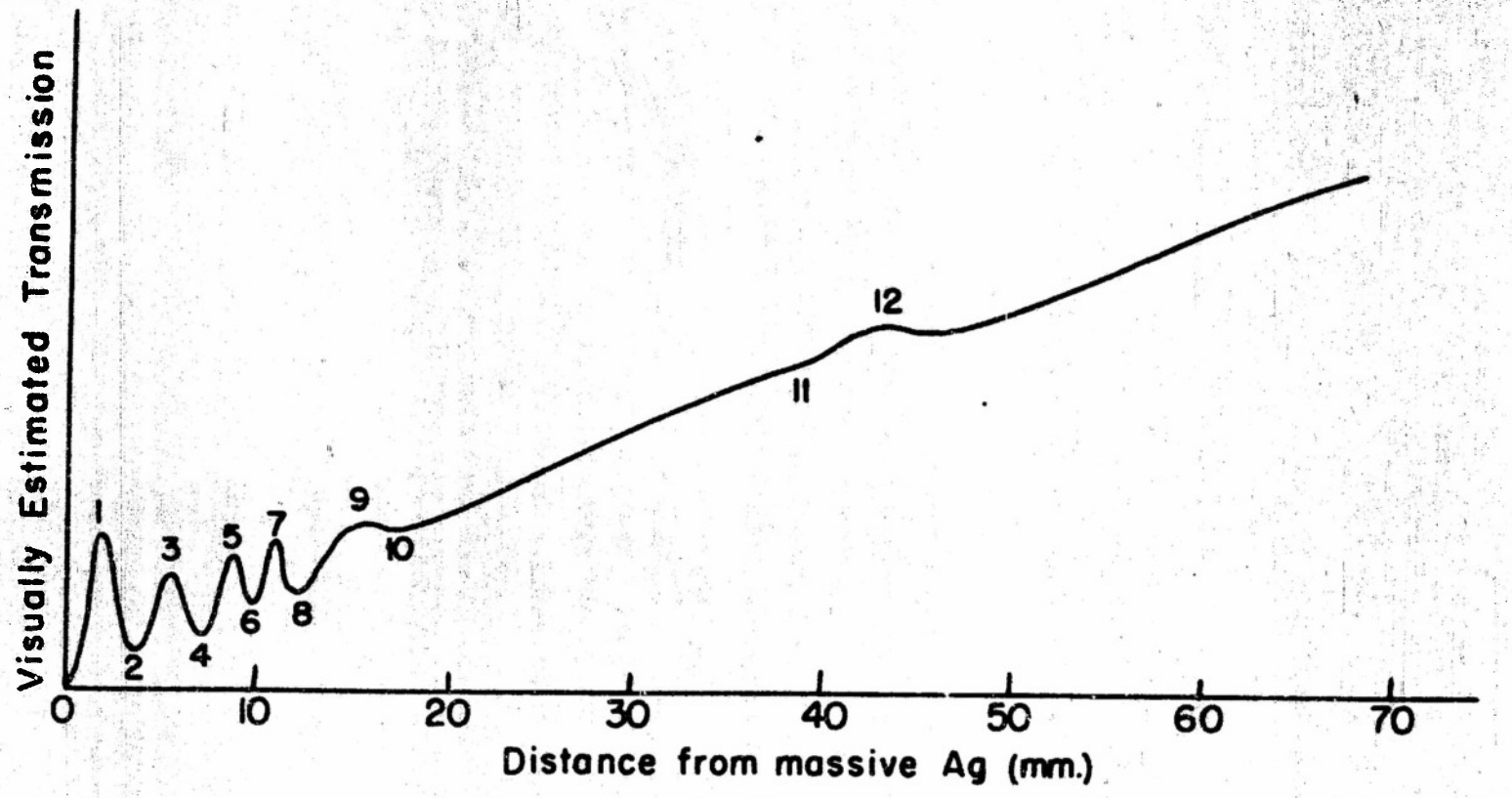

FIGURE 13

Relative Transmission Versus Distance from Massive Unoxidized Silver
(Schematic)

TABLE XXXI. COLORS OBSERVED AT DESIGNATED POINTS OF FIG. 13 FROM RF OXIDIZED SILVER WEDGE

Point Fig. 13	Reflection at Glass-Oxide Interface	Transmitted Light
0	massive Ag	none
1	black	yellow
2	red to yellow	dark brown
3	yellow to green	grayish yellow
4	blue to red	red brown
5	red to orange	yellow green
6	orange	gray green
7	orange to yellow	light green
8	yellow to green	pink
9	green to light blue	light yellow
10	blue to red	pale yellow
11	black	pale green
12	black	blue

Examination of the film at 90X with transmitted light showed that it consisted of a yellow transparent matrix in which were embedded minute particles of some material (possibly Ag). The density of small particles was greatest in the regions of minimum transmission (Fig. 13) and least in the regions of maximum transmission. Careful microscopic examination at 100X of the yellow transparent regions near the massive silver demonstrated that the particles in the yellow matrix are uniformly distributed in depth. The size of the particles decreased in the order of region 2, 4, 6, 8. Individual particles could not be resolved in region 10 and beyond.

Since the colors of the surface are not very dependent upon the angle of incidence of the light, it is probable that the optical properties are related to a light absorption and scattering process. It is indicated in Part II of this report series that the oxide surface formed by oxidation of silver from 50 to 90% transmission exhibits a yellow color. From the data it is evident that the relationship between color changes accompanying the rf oxidation and the thickness of the oxide film is not a simple one. It is possible that the color changes are a measure of the distribution of small particles in the oxide film and not really a measure of the film thickness in the sense of the conventional interpretation of interference colors. Definitely, the optical properties of an rf oxidized film are not simply related to the silver surface structure. An x-ray diffraction characterization of this type of rf oxide surface would undoubtedly provide information of value to the understanding of the oxidation mechanism.

REFERENCES

1. Final Report to Engineer Research and Development Laboratories, Fort Belvoir, Va., Contract N-44-099-673. P.M. Harris and E.N. Lassettre, The Ohio State University Research Foundation, December 31, 1950.

2. Ibid., pp. 48-49

3. L.E. Loeb, Fundamental Processes of Electrical Discharges in Gases. John Wiley and Sons, Inc., New York, 1939. pp. 560-601.

4. Druyvesten and Penning, Revs. Mod. Phys. 12, 88 (1940).

5. R.S. Sennet and G.D. Scott, J. Opt. Soc. Am. 40, 203 (1950).

6. W.J. Haubauch Jr., "Radioactive Tracer Analysis of the Gross Composition of the Ag-O-Cs Infrared Sensitive Photocathode", Master's Thesis, The Ohio State University (1952).

7. Final Technical Report, Part II to the Engineer Research and Development Laboratories, Fort Belvoir, Va., Contract DA-44-009eng 405. This report also contains the material of reference 6 above.

8. G. Switzer, J.M. Axelrod, M.L. Lindberg and E.S. Larsen, Tables of d Spacings for Angle 2θ. U.S. Dep't. of Interior, Geological Survey, Circular 29, August 1948.

9. Ref. 3, p. 578.

10. Ref. 4, p. 131.

11. Ref. 3, p. 566, also Ref. 4, p. 133.

12. Ref. 3, p. 575.

13. V.K. Zworykin and E.G. Ramberg, Photoelectricity, John Wiley and Sons, Inc., London, 1949. 94.

REFERENCES (Continued)

14. W. Hartmann, Z. tech. Physik 5, 111 (1943).

15. V.V. Tiapkina and P.D. Dankov, Doklady Akad. Nauk VSSR, 59, 1313 (1948).

16. Ref. 1, pp. 7 and 15.

17. D.M. Yost, J. Am. Chem. Soc. 48, 159 (1926).

18. A.A. Noyes, J.L. Hoard, K.S. Pitzer, J. Am. Chem. Soc. 57, 1221 (1935).

19. A.A. Noyes, K.S. Pitzer, C.L. Dunn, J. Am. Chem. Soc. 57, 1229 (1935).

20. A.A. Noyes, D. DeVault, C.D. Coryell, T.J. Deahl, J. Am. Chem. Soc. 59, 1326 (1937).

21. A.A. Noyes, C.D. Coryell, F. Stitt, A. Kossiakoff, J. Am. Chem. Soc. 59, 1316 (1937).

22. A.A. Noyes, A. Kossiakoff, J. Am. Chem. Soc. 57, 239 (1935).

23. V.V. Tiapkina and P.D. Dankov, Compt. Rend. Acad. Sci. USSR, 54, 415-18 (1946).

24. Progress Report No. 3 to Engineer Research and Development Laboratories, Fort Belvoir, Va., under Contract DA-44-009eng 405, for the Period Ending Oct. 1, 1951, P.M. Harris and E.N. Lassettre, The Ohio State University Research Foundation.

25. J.W. Mellor, A Comprehensive Treatise on Inorganic and Theoretical Chemistry, Vol. III. Longmans, Green and Co., London. p.383

26. P.C. Carman, Trans. Faraday Soc. 30, 566 (1934).

27. de Boer and Van Ormand, British Patent No. 579, 817.

28. F. Jirsa and F. Jellinek, Z. anorg. Chem. 57, 290 (1926).

REFERENCES (Continued)

29. J. Tronstad and T. Hoverstad, Trans. Faraday Soc. 30, 1114 (1934).

30. G.A. Barbieri, Atti. Accad. Lincei, 13, 882-7 (1931). Cf. Chemical Abstracts 26, 663 (1932).

31. Haakon Braekken, Kgl. Norski. Videnskab Selskab. Fork. 7, 143-6 (1935).

32. R. Faivre, Ann. Chem. 19, 58 (1944).

33. P.G. Borwiak and N.D. Margulis, Doklady Akad. Nauk USSR 61, 625-8 (1948). In Russian. Translated for us by Mrs. Justina Epp.

34. P.M. Morozov and M.M. Butslov, Bull. Acad. Sci. USSR. Ser. Phys. 8, 291 (1944). In Russian. Translated for us by Mrs. Justina Epp.

NOTE: In submitting this report it is understood that all provisions of the contract between The Foundation and the Cooperator and pertaining to publicity of subject matter will be rigidly observed.

Investigator ..... Date .....

Supervisor Edwin M. Lansford Date Sept. 9, 1953

For The Ohio State University Research Foundation

Executive Director Oram C. Wolfert Date 9 Sept. 1953

W.E.H.